Transient thermal effects in extra-high-voltage cable systems

by

D. J. Horrocks, B.Eng.

A Thesis

Submitted for the Degree of

Master of Philosophy

in the University of Southampton

September 1969

ABSTRACT

FACULTY OF ENGINEERING AND APPLIED SCIENCE

ELECTRICAL ENGINEERING

Master of Philosophy

TRANSIENT THERMAL EFFECTS IN EXTRA-HIGH-VOLTAGE CABLE SYSTEMS

by David John Horrocks

The transient response of a heavily loaded, sheath cooled 3 in^2, 400 kV through joint and associated cable to cooling by oscillation of the duct oil is investigated. The development of a digital computer program to analyse the oil oscillation is described. Results are quoted for several flow rates and cycle times. The effects on the ferrule temperature of induced turbulence in the whole joint or in the joint ferrule alone are investigated and discussed. The results obtained indicate that the use of oil oscillation in reducing large temperature differentials in cable systems is worthwhile. The results also show that use of oil oscillation provides a convenient method for uprating a cable system. A generalized digital computer program for the analysis of oil oscillation in general cable systems is developed. The program written in FORTRAN IV is listed and discussed.

Thermal instability in the dielectric of a sheath cooled 3 in^2 400 kV joint and cable is investigated. It is shown that the 3 in^2 cable is stable even under the most extreme fault conditions and failure under fault is likely to be due to charring of insulating papers because of the high temperatures involved rather than to thermal instability.

ACKNOWLEDGEMENTS

I should like to express my thanks to my supervisor, Dr. B. M. Weedy, for his constant encouragement and advice.

I should also like to thank Mr. M. J. Thelwell of C.E.R.L. Leatherhead and the Pirelli-General Cable Co. Ltd. for advice in technical matters.

Finally, my thanks are due to Miss S. L. Parker for her patient and careful typing of this thesis.

* * * * * *

The work was financed by a contract from the Central Electricity Generating Board (Research Laboratories, Leatherhead).

CONTENTS

Symbols used in the text

The following are the principal symbols used in the text:

C_p	specific heat (J/°C cm^3)
E	electrical stress (V/cm)
g	thermal resistivity (°C cm/W)
H,K	thermal conductance (W/°C)
I	load current (A)
q	heat generated at a node (W)
T	temperature (°C)
V	system voltage (V)
δ	dielectric loss angle (rad)
ε_o	8.854×10^{-12} (F/m)
$\varepsilon_o \varepsilon_r$	dielectric constant (F/m)
θ	nodal temperature rise (°C)
θ'	nodal temperature rise after time step, Δt (°C)
ω	oil flow rate (cm^3/s)
Δt	time step (s)

Other symbols are defined in the text as necessary.

CHAPTER 1

INTRODUCTION

The demand for electricity is increasing at a rate of between 6% and 7% per year, which requires a doubling of generating capacity about every 12 years. To meet this demand, more efficient power stations using large machines are needed, with the result that the capacity of a station, constructed at the present time, is 2000 MW, generated by 4 x 500 MW turbo-alternators - sets with outputs greater than 1000 MW being in the design stage. Because of the need for an adequate supply of cooling water and cheap primary power, stations have been built on sea-coasts, estuaries or near coal-fields; these last being mainly in the North and East Midlands. Stations are therefore mostly remote (50-100 miles) from the main load centres so that transmission of power in bulk is necessary. To do this economically, the transmission voltage has tended to increase with the power required so that today in the U.K., bulk transmission is at 400 kV using underground cables or overhead lines with a winter rating of 2200 MVA.

The technical problems associated with insulating and cooling an overhead line are less than with an underground cable of comparable rating. Installation and construction costs are also less for the overhead line system as compared with an underground cable so that, where possible, overhead lines are used for bulk

power transmission. However, an underground system is necessary in built-up areas and in crossing large stretches of water. In areas of 'outstanding natural beauty', there is pressure from Nature Conservancy interests, at both local and national level, for underground systems to be used in preference to overhead lines. However, terminating a 400 kV overhead line system with a Winter rating of 2200 MVA would, at the present stage in cable design, require two cable circuits in parallel and for these to be thermally independent a trench 30 ft wide is required. The case for an improvement in the current carrying capacity of an underground cable system is obvious.

Underground cables consist of one or more copper or aluminium conductors, insulated from each other and earth by a wound, oil-impregnated, paper-tape insulation. To ensure a uniform electric field in the insulation, both the conductor and the outer surface of the insulation are 'shielded' by a wound, metallized paper tape. The insulated conductors are then sheathed with an aluminium or lead sheath. This is the so-called 'solid-type' cable, the main problem with which is the tendency for cavities or 'voids' to form in the dielectric. These voids may be due to faulty manufacture, impregnating compound drainage or, more likely, due to movement during load cycling. This cavitation during load cycling is due to the different coefficients of thermal expansion of the insulating paper, impregnating compound and the conductor and sheath materials; during cycling, the papers move and the sheath expands and these fail to return to their original positions and dimensions on

cooling. Unless the maximum operating temperature and design stress are kept relatively low, ionization in voids which are near the conductor may cause a spark discharge which finds its way first radially through the dielectric and then tracks from gap to gap across the paper surfaces until breakdown of the insulation occurs.

Thus both the maximum operating temperature and design stress are limited by void formation. The relatively low design stress, 4 - 4.5 kV/mm, coupled with the need to keep the cable flexible (limiting the insulation thickness) puts an upper limit on the system operating voltage. Solid-type cable is normally used in systems operating at 33 kV and below. The limitations can be overcome in two ways:

1. by preventing the formation of voids as in, for example, the oil filled cable;
2. by tolerating the presence of voids and subjecting them to gas pressure, as in, for example, the gas-filled cable.

The cable used in the system under consideration is the self-contained, oil-filled type which was originally proposed by Emanueli[1] in the 1920's and is, consequently, sometimes referred to as the Emanueli-type. The construction of these cables is in essence like that of solid-type cables except that the multi-conductor construction is used only rarely for 132 kV systems and never used for higher voltage systems. The electric stress in the

REFERENCES

1 Oil duct
2 Metallized paper screen
3 Core screen
4 Copper woven fabric tape
5 Lead alloy sheath
6 Bedding
7 Reinforcement
8 P.V.C. tapes
9 Rubber tapes
10 Hessian tapes

FIG.1 SELF-CONTAINED OIL-FILLED CABLE

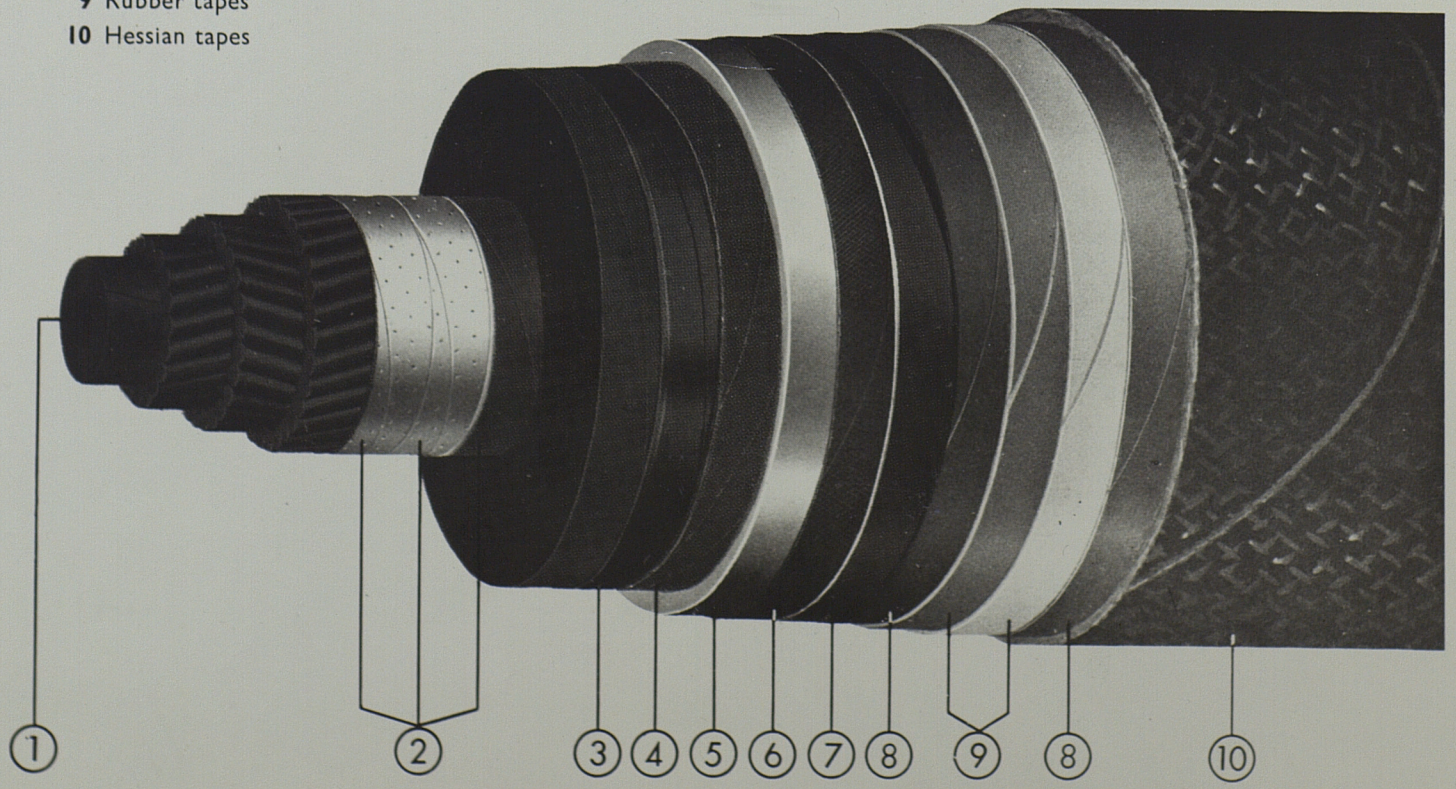

dielectric varies in accordance with the law

$$E = \frac{V}{r \ln \frac{D}{d}} \qquad (1)$$

where D and d are, respectively, the conductor and insulation outer radii, r is the radial distance from the cable centre and V is the system voltage to earth. Because of this stress distribution, the insulation is 'graded', that is thinner tapes, having a higher breakdown strength, are applied near to the conductor, where the stress is highest, than at the insulation outer surface. The construction of the self-contained, oil-filled cable is also different from the solid-type in that the conductor has a hollow core and the sheath, if lead or lead alloy, is reinforced.

The hollow core in the conductor is provided to allow for the longitudinal movement of the low viscosity, insulating oil as it expands or contracts with temperature changes. The oil is maintained within pre-determined pressure limits by means of suitably positioned external 'reservoirs'. A reservoir, or pressure tank, consists of a number of collapsible, gas-tight cells filled with a gas, usually nitrogen, and contained in a tank filled to a pre-determined pressure with cable oil. Each cell comprises two circular, corrugated metal diaphragms sealed together with a cylindrical distance piece between them to give the required volume. The purpose of the reinforcement of the lead sheath is to prevent its distension under the maintained pressure, the increase in volume

of the oil being accommodated in the reservoirs which return the oil to the cable during periods of lighter loading. In this manner, the cable is maintained full of oil under all working conditions.

The construction of an underground EHV cable involves essentially a dielectric problem and requires:

1. high instantaneous dielectric strength - that is 'extreme homogeneity macroscopically';
2. high long term dielectric strength - that is 'no microscopic heterogeneity' which would cause locally dense and destructive energy dissipation;
3. maintenance of 1 and 2 at normal operating temperatures and also at the maximum temperatures likely with normal copper ($I^2 R_{ac}$) and other losses or short-circuits.

There are three main sources of loss in an underground cable. The largest is the loss due to the current flowing in the conductor; this is known as the I^2R or copper loss. There is a dielectric loss in the insulation which is negligible for the lower voltages but becomes significant with system voltages of 275 kV and above and at 400 kV is of the order of 15 W/m per phase. There is also a loss caused by the eddy currents generated by the induced sheath voltages. Sheath losses can be reduced considerably by sheath crossbonding, which is a method of interconnecting the sheaths of the three phases to balance out the induced voltages.

These losses increase with increasing transmitted power and, if the system is to remain secure, they must be dissipated through as low a thermal resistance as possible. However, a low thermal resistance, and hence a low thermal resistivity, implies a low electric resistivity which is not compatible with the need for high dielectric strength. The designer of a buried power cable system is faced with conflicting requirements; the power transmitted must be as great as possible without endangering the security of the system. The limits imposed on the power which can be transmitted by a buried power cable are defined by:

1. the physical properties of the insulation (breakdown strength, loss factor, thermal conductivity);
2. the need to keep cable dimensions to reasonable values, if it is to remain flexible;
3. the thermal characteristics of the cable surroundings;
4. the test specifications.

Equation (1) shows the relationship between phase voltage, cable dimensions and the electric stress in the insulation. The voltage is determined by the system, and the conductor diameter is dependent on the current to be carried so that Equation (1) relates maximum operating stress and insulation diameter. The maximum operating stress is proportional to the breakdown strength of the insulation tapes applied in the immediate vicinity of the conductor and on the static oil pressure for which the cable is designed.

Present day cable practice allows a range of design operating stresses from 10 kV/mm to 19 kV/mm depending on the tape thickness and oil pressure. These values are determined by the test specification (especially the impusle withstand test) and the safety margin allowed between the prescribed test stress and the breakdown strength.

At the highest system voltage at present in use (750 kV in Quebec, Canada), Oudin[2] states that manufacture of an oil-filled cable is possible. Allowing an insulation diameter of 125 mm and a conductor diameter of 46 mm, the maximum operating stress is about 19 kV/mm, which is the upper allowable limit. The 125 mm insulation diameter corresponds to an overall diameter of 150 mm, which is, according to Oudin, the maximum compatible with available production and transport facilities; thus 125 mm may be considered as the optimum insulation diameter. Barnes[3] states that a conductor of 3 in^2 (1840 mm^2) cross-section is the limit compatible with existing manufacturing facilities. This cross-section corresponds to a maximum hollow-core conductor diameter of $2\frac{3}{8}$ in. (approximately 60 mm). Thus a conductor diameter of 60 mm and an insulation diamter of 125 mm may be considered the present optimum cable dimensions.

The maximum current, I, which a buried cable system will carry, is given by the equation

$$I = \left[\frac{\theta - W_d \left(\frac{1}{2} R_1 + R_2 + R_3\right)}{R_{ac} \left(R_1 + R_2 + R_3\right)} \right]^{\frac{1}{2}} \qquad (2)$$

where θ is the maximum steady-state conductor temperature rise, W_d is the dielectric loss and R_1, R_2 and R_3 are the insulation, cable serving and soil thermal resistances respectively.

For system voltages above 275 kV, the dielectric losses cannot be neglected and

$$W_d = 2\pi f\, CV^2 \tan \delta$$

where f is the system frequency and C is the cable capacitance. Since W_d increases as the square of the voltage, it will be seen that the current, and hence the transmittable power, passes through a maximum, which will be at the optimum value of system voltage, and may even become zero.

The influence of the cable surroundings may be illustrated by a consideration of Equation (2). Under normal conditions, the value of R_3 will be equal to, or possibly greater than, the sum of R_1 and R_2 and certainly greater than $(\frac{1}{2} R_1 + R_2)$, even though the soil thermal resistivity is between 20% and 25% that of the insulation. The resistivities of the insulation and serving are fixed so that it will be seen that any improvement in the external thermal conditions will increase the current carrying capacity of the cable system.

Making certain assumptions (see Appendix 2), Equation (3) describing the continuous power transmission capability (P) of a buried cable system may be derived from Equation (2).

$$P = \left[\frac{9E_m d\ V^2}{R_{ac}} \left\{ \frac{2\theta - 2\pi f\ \varepsilon_o \varepsilon_r \tan\delta\ V (Vg_1 + 2Ed\ (ag_2 + bg_3))}{Vg_1 + Ed\ (ag_2 + bg_3)} \right\} \right]^{\frac{1}{2}} \quad (3)$$

Using this equation, curve 1 of Fig. 2 has been obtained, assuming a conductor temperature rise of 65°C, a soil thermal resistivity of 120°C cm/W and the optimum cable dimensions as described above. The curve is seen to peak at a system voltage of about 520 kV and a power of 1100 MVA.

Problems are encountered in practice with buried EHV cables because the surrounding soil tends to dry out due to the dissipated losses. A constant soil thermal resistivity cannot be guaranteed and in such circumstances a 'thermal runaway' condition results and the cable fails, for example, the failure of two 132 kV cable circuits in S.E. London in July 1962[4] where the soil thermal resistivity had increased from 60°C cm/W at installation to 600°C cm/W at failure. The need for an improvement in the heat conduction near to the cable is apparent.

At the present time, three methods are used to improve the external thermal conditions:

1. installation in specially constructed concrete surface troughs filled with a 'stabilized thermal sand';
2. increase and rigorous control of soil thermal conductivity, so increasing the natural heat transfer;
3. forced cooling.

FIG 2: CONTINUOUS TRANSMITTABLE POWER

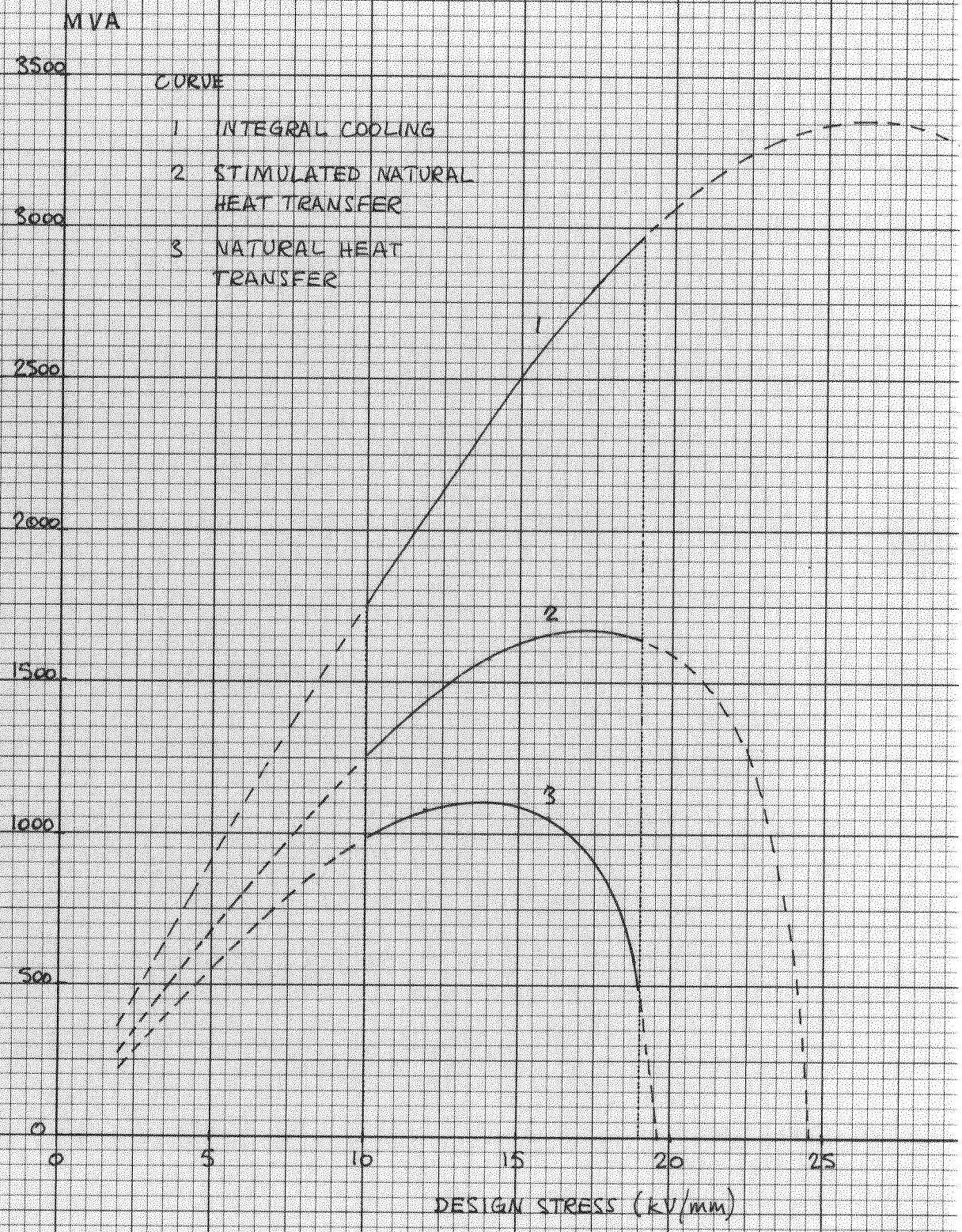

FIG 3: CONTINUOUS TRANSMITTABLE POWER

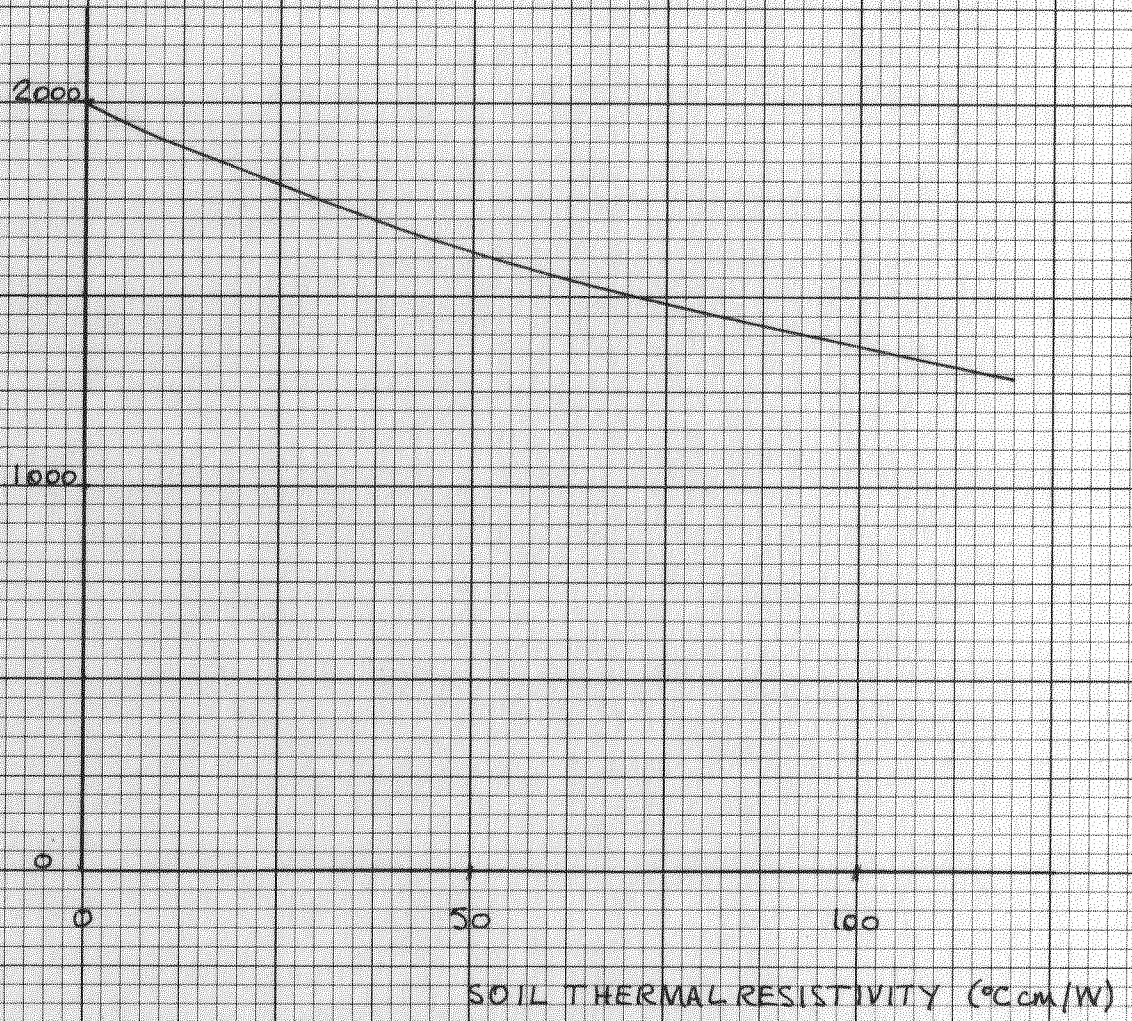

We shall consider methods 2 and 3, since method 1 has, at present, been used in only one installation[5]. Various ways of reducing soil thermal resistivity have been suggested including back-filling the cable trench with oil-loaded sand[6], back-filling with the so-called 'stabilized thermal sand'[7], and the use of water pipes with 'pop-up' nozzles to irrigate the trench area[8]. The normal practice is to use a 'stabilized thermal sand'. Methods of forced cooling fall naturally into two categories (see Fig. 4):

1. Using external water pipes laid in the trench close to the cable circuit[9], thus effectively reducing the soil thermal resistance (Fig. 4(a)).
2. Bringing the coolant into direct contact with the cable sheath. The coolant may be air[10] or water. With water as coolant, two schemes can be employed either laying the cables inside water-filled pipes[11], known as integral cooling, or laying the cables in an open water-filled trough; this latter method has been employed in the Chilling-Fawley crossing of Southampton Water[12].

Curves 2 and 3 of Fig. 2 indicate the increases in transmittable power which are possible, for a given cable, by improving the soil thermal resistivity (soil g = 60°C cm/W, curve 2), or by application of sheath water cooling (soil g = 0°C cm/W, curve 3). It can be seen that the value of transmittable power increases markedly as soil thermal resistivity

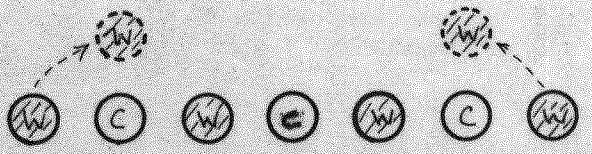

(a) Separate Cooling Pipes

(b) Integral Cooling Pipes

FIG 4 : COOLING PIPE ARRANGEMENTS.

decreases. It is also apparent that the voltage for maximum power transmission increases with decreasing soil thermal resistivity. Fig. 3 shows the effect of reducing soil thermal resistivity on the maximum power transmitted by the cable which was the initial object of this investigation, a 400 kV, 3 in^2 conductor, paper-insulated, self-contained, oil-filled cable. It is possible, using an integrally cooled cable system, to match the full Winter rating of a 400 kV overhead line.

Manufacturing facilities set no limit on the length of cable which can be produced. For example, the lengths of cable manufactured in the U.K. for the English part of the cross-Channel d.c. link were 2800 yards long. However, these lengths could be transferred directly to a ship for transportation by sea; the normal methods of transportation, road and rail, impose a weight, and hence a length, limit on the cable manufacturer. Short manufacturing lengths necessitate the jointing of cables on site. Modern paper cables are manufactured with great care, the paper tapes being applied with a controlled tension by expensive, precision machines in air-conditioned rooms. The whole cable is thoroughly dried before impregnation with degassified high quality oil. In contrast, making the joint on site means that the papers are exposed to the air and applied by hand; the joint is therefore more heavily insulated than the cable and presents a higher thermal resistance to heat flow. Dielectric losses are only marginally

higher but heat dissipation is a much more difficult problem with the joint than with the cable. The temperature of the joint is thus higher than that of the cable, and the ferrule, in particular, is a hot-spot.

The insulation used in modern EHV power cables is a high grade, wood-pulp paper, and to avoid damage to the insulation it is necessary for operating temperatures to be kept below a predetermined maximum. Damage to the insulation due to overheating may result in deterioration of the paper and contribute to the eventual breakdown of the insulation. The manufacturers and the supply industry are agreed that the full load rating of an EHV power cable must be such that the maximum paper temperature does not exceed 85°C. Work performed by Clark[13] and Murphy[14] among others has shown that deterioration of paper at temperatures between 85°C and 100°C is negligible and the possibility of breakdown is slight; between 100°C and 120°C the rate of deterioration increases and breakdown becomes more likely. For temperatures in excess of 120°C, breakdown is almost certain after a limited period of time. Weedy and Perkins[15] have shown that a 400 kV cable, normally buried and rated at 1100 MVA, will run with a joint ferrule temperature in excess of 100°C and a cable conductor temperature of 85°C; thus the joint is seen to be the limiting factor to increase in transmitted power.

For a normally loaded cable, the joint-cable temperature differential may be reduced by increasing the spacing between

joints and thus reducing the joint temperature. In a heavily loaded cable, the copper losses are much greater than the dielectric losses and increasing the cable spacing does not produce so marked an effect on the joint-cable temperature differential. Although the application of external cooling will reduce the temperature over the whole cable and joint system, the joint-cable differential is not significantly affected. Since the cables are installed in pipes and are, therefore, thermally independent of each other, some means, other than increase of joint spacing, must be employed; one such method would be circulation of the oil already present in the conductor.

Several investigators[16, 17] have discussed the advantages of schemes of this type. Reference 16 discusses the design of a cable for use in an oil circulation system and indicates three areas for discussion, as follows:

1. satisfactory manufacture of a cable with a large cross-section conductor having a large central duct;
2. the conditions under which the cable oil can be circulated at relatively high flow rates without hazarding the electrical integrity of the cable system;
3. the provision of an accessory which will provide the required cable oil flow into, and out of, the conductor.

Cables with different conductor constructions have been designed and manufactured satisfactorily. The most economic cable

design is one involving a duct diameter of 50 mm; the increase in overall cable diameter for such a design compared with a cable having the conventional 12 or 16.5 mm duct is relatively small, the large duct cable having a diameter of 130 mm as compared with 114 mm. Oil flow in and out of the conductor can be achieved by incorporating oil flow passages into a stop-joint assembly.

The problems raised by oil circulation include the designing of the oil circulation pump to prevent oil degradation, whether the conductor material will be eroded, whether cavitation and gas evolution will arise. Reference 17 discusses various designs for oil circulation systems. An oil circulation scheme[2] has been in operation in France for several years, although the length involved is short (100 m). The main objections to an oil circulation system of the type discussed are the special cable designs required and the high capital expenditure involved in providing pumping and heat-exchanger equipment.

Kitagawa[18] and others have suggested another method of cooling, the oscillation of the duct-oil. The main advantages of such a scheme are as follows:

1. a cable of conventional design can be used;
2. low oil flow rates can be used, so reducing the conductor erosion problem;
3. the use of pumps is not necessary and the consequent oil contamination problem is avoided;

4. expensive heat exchanger equipment is not required;
5. the method can be applied to existing installations without too much difficulty.

The only additional equipment necessary is a system to enable the adjustment of oil pressure differences between the remote ends of the cable system to be made; provision for cooling the pressure tanks may also be required. Such a system is illustrated in Fig. 5, where the valves could be operated either by time switches or by pressure limit switches.

Many of the thermal problems associated with bulk power transmission can be solved by the use of cooling, both external cooling using water in contact with the sheath or in separate pipes and internal cooling using the duct-oil; one problem, however, remains, the breakdown of the insulation due to thermal instability. The problem has been known for a long time, and it is discussed by Whitehead[19]. The level of the dielectric loss in a cable is dependent directly on the dielectric loss angle which, in turn, is a function of the dielectric temperature. The losses must be dissipated to the surrounding heat sink through the thermal resistance of the insulation and the cable environment, and an equilibrium condition can exist only if all the heat generated in the cable can be dissipated to the cable surroundings. The equilibrium point for a particular cable system is determined by an inspection of the curves of heat generation and dissipation, for the system, plotted against temperature.

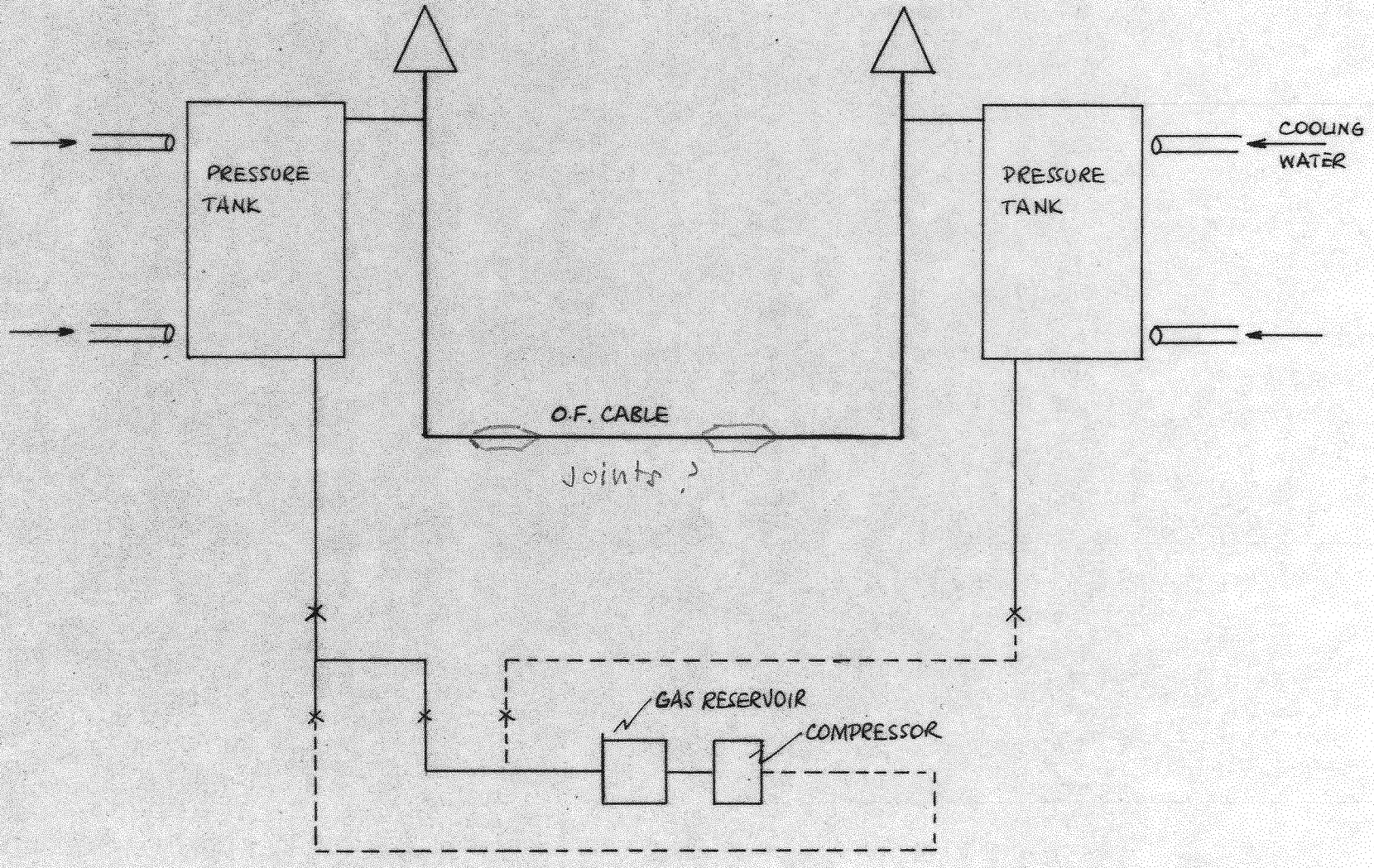

FIG 5 : OIL OSCILLATION SYSTEM

For example, consider the curves shown in Fig. 6 where the curved line represents the total losses, copper (I^2R) and dielectric losses, in the cable, the intersection of the curves at 'A' represents the equilibrium point. There are three ways in which a critical condition can be reached:

1. by increasing the thermal resistance to the heat sink, so reducing the slope of the dissipation line until the line is tangential to the curve (point 'B');
2. by an increase in the ambient temperature so that the dissipation line moves to the right remaining parallel to its first position (point 'C');
3. by an increase in the generated losses so that the curves cross again, as at point 'D'.

The temperatures represented by points 'B', 'C' and 'D' are critical temperatures. Should any one of these three conditions exist, then any temperature increase would mean that more heat is being generated than the system can dissipate and thermal instability would result.

The situations described in 1 and 2 above can be controlled by methods mentioned earlier in this discussion, the use of the stabilized thermal sand or the various methods of internal and external forced cooling. However, a situation is conceivable in which condition 3 would result and such contingencies cannot be guarded against. Instability under condition 3 could arise, for

FIG 6: THERMAL STABILITY DIAGRAM

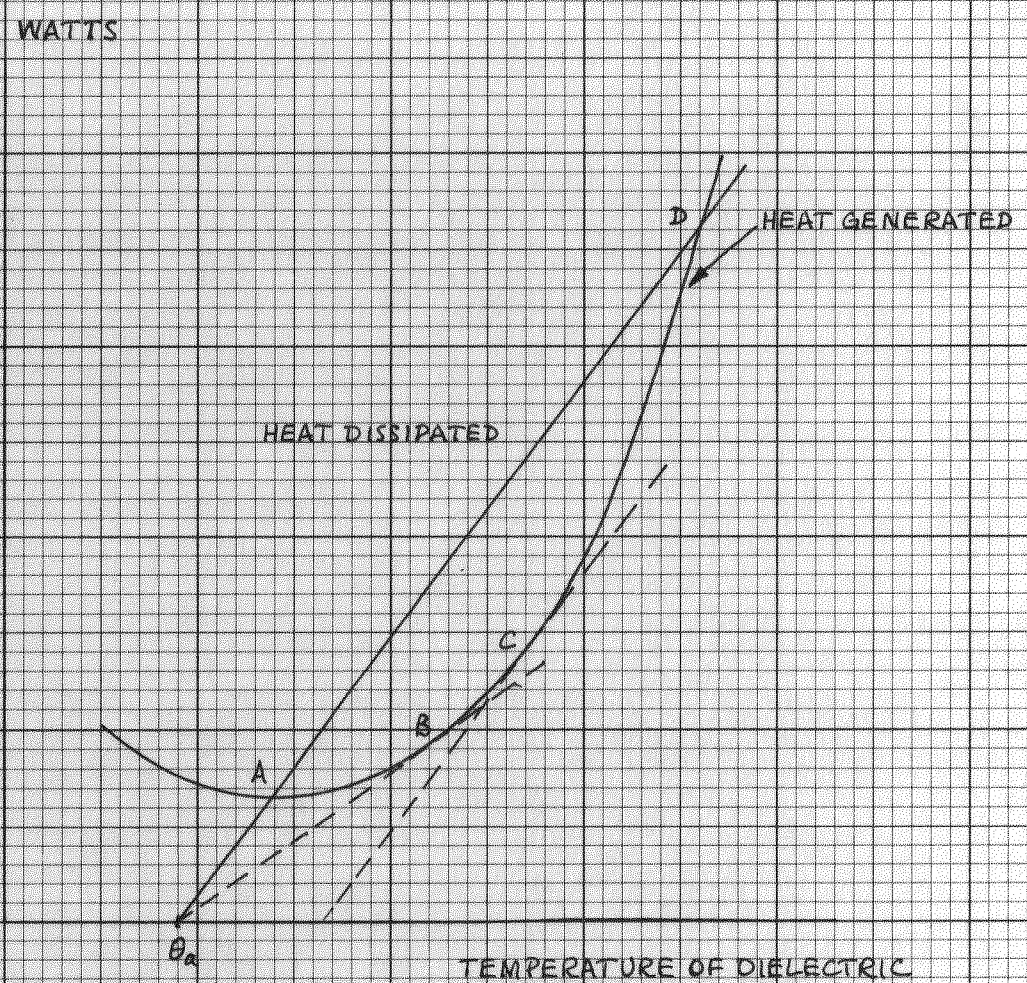

example, either due to the repeated application of a high fault level short-circuit in a system using auto-reclose switch-gear or the presence of sustained fault current higher than the design current but too low for the protection to detect. The problem of thermal instability is, therefore, an important one and the stability of the 400 kV cable and joint typically employed in the transmission system in this country is investigated and discussed.

CHAPTER 2

THEORY AND METHOD OF THE MODEL FOR OIL OSCILLATION

The steady state and transient thermal behaviour of a 400 kV cable and joint has been comprehensively recorded[15,19] and the need for such work is apparent from the results reported. The object of the present investigation is to study the behaviour of 400 kV cables and joints, in particular, and EHV cables and joints, in general, which have local hot-spots reduced by the slow flow of the insulating oil in the conductor duct. Because of the complicated relationship between oil and conductor temperatures, which are both changing in time, the problem is a transient one. The object is, therefore, to determine the time constants of the temperature transients and the 'stable-condition' temperatures (i.e. the conductor and oil temperatures when the system has settled down) and also the optimum velocity and periodic time for the oil coolant.

The problem is difficult to investigate by direct measurement on an actual joint since the insertion of a temperature probe into the joint or cable presents problems because of the high voltage. Measurements at the sheath are of no value since the behaviour of the sheath does not adequately reflect the behaviour of the conductor[20]. Measurements made with load currents circulated at low voltages are of little value because, at the high voltages

under consideration, dielectric losses, which are high and cannot be neglected, are difficult to simulate exactly.

Since the problem cannot be investigated directly, another method must be employed. Consider the elemental volume shown in Fig. 7 and assume that the temperature at each point in the element is changing with time and that the heat generated per unit volume per unit time is q'. The rate of heat generation in the volume is thus

$$q_{gen} = q' \, (dx \, dy \, dz)$$

The rate of heat entering the element along the x-axis is

$$q_{x,in} = (dy \, dz) \, g_x \, \frac{\partial T}{\partial x} \tag{4}$$

Differentiating (4) with respect to x, we obtain the difference between the rates of heat entering and leaving along the x-axis.

$$\Delta q_x = (dy \, dz) \, \frac{\partial}{\partial x} \, (g_x \, \frac{\partial T}{\partial x}) \, dx$$

Similar expressions are obtained for Δq_y and Δq_z.

The rate of heat storage in the element is given by

$$q_{stor} = (dx \, dy \, dz) \, Cp \, \frac{\partial T}{\partial t}$$

The sum of the rate of heat generation in, and the differences in the rates of heat entering and leaving, the element is equal to the rate of heat storage in the element, so that we have

$$Cp \, \frac{\partial T}{\partial t} = \frac{\partial}{\partial x} \, (g_x \, \frac{\partial T}{\partial x}) + \frac{\partial}{\partial y} \, (g_y \, \frac{\partial T}{\partial y}) + \frac{\partial}{\partial z} \, (g_z \, \frac{\partial T}{\partial z}) + q' \tag{5}$$

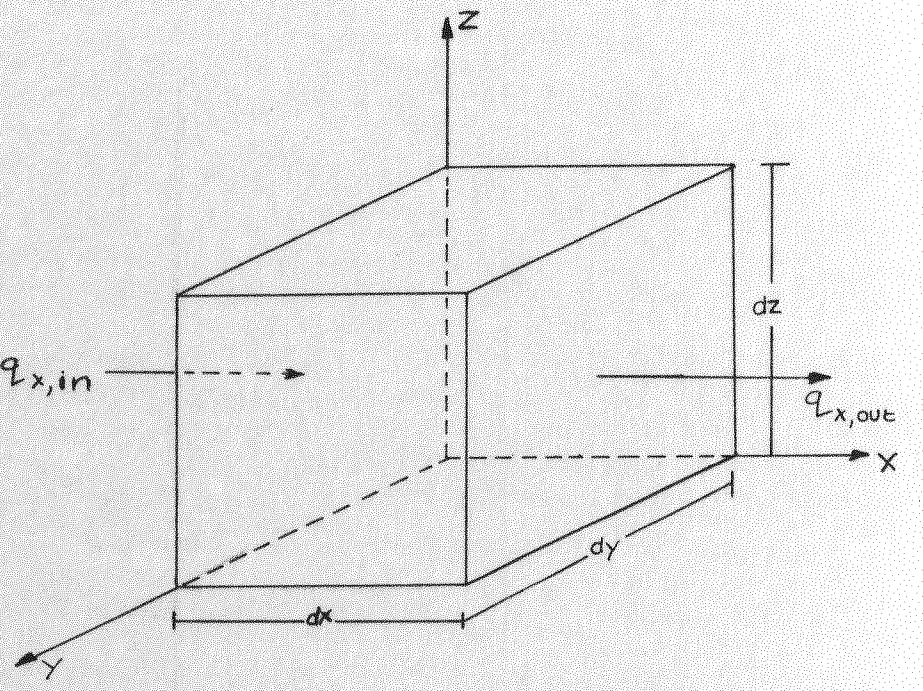

FIG 7 : ELEMENTAL VOLUME

This is the Poisson equation for unsteady-state heat conduction. If thermal conductivity is assumed to be independent of temperature and the material isotropic (as in the case of a buried cable), then Equation (5) becomes

$$\frac{\partial T}{\partial x} = \frac{g}{Cp}\left(\frac{\partial^2 T}{\partial x^2} + \frac{\partial^2 T}{\partial y^2} + \frac{\partial^2 T}{\partial z^2}\right) + \frac{q'}{Cp} \qquad (6)$$

where the term $\frac{g}{Cp}$ is known as the thermal diffusivity.

Although transient heat-transfer problems can be described by Equations (5) and (6), they are, nevertheless, difficult to solve analytically. Complex boundary conditions and the large number of terms in the slowly converging series all help to make the analytical solution of these problems unwieldy. Exact solutions are available in the literature[22], but computation of results is tedious. From the engineering point-of-view, the most practical solutions to transient, heat-transfer problems are obtained using approximate methods. These approximate methods are based on the principle of dividing time into finite intervals, Δt, dividing space into finite volumes ($\Delta x\ \Delta y\ \Delta z$) and assuming that temperatures within these limits vary linearly. Thus, the following approximations are made:

$$\frac{\partial T}{\partial t} = \lim_{\Delta t \to o} \frac{T_{x,t+\Delta t} - T_{x,t}}{\Delta t} \simeq \frac{\Delta T}{\Delta t} \qquad (7)$$

$$\frac{\partial^2 T}{\partial x^2} = \lim_{\Delta x \to o} \frac{T_{x-\Delta x,t} - 2T_{x,t} + T_{x+\Delta x,t}}{(\Delta x)^2} \simeq \frac{\Delta^2 T}{(\Delta x)^2} \qquad (8)$$

and similarly for $\frac{\partial^2 T}{\partial y^2}$ and $\frac{\partial^2 T}{\partial z^2}$. Substituting these values into Equation (6) we obtain:

$$\frac{\Delta T}{\Delta t} = \frac{g}{Cp} \left(\frac{\Delta^2 T}{(\Delta x)^2} + \frac{\Delta^2 T}{(\Delta y)^2} + \frac{\Delta^2 T}{(\Delta z)^2} \right) + \frac{q'}{Cp} \qquad (9)$$

Equation (9) may equally well be expressed in cylindrical or polar co-ordinates and may be used to obtain approximate solutions of heat-transfer problems using either numerical or analog means. In either case, the method requires a lumped-constant representation in which the system is divided into a large number of sub-sections in which the thermal properties of each sub-section are considered as lumped instead of being evenly distributed.

In the case of a three dimensional problem, the system is divided, for example, along the three rectangular axes, resulting in a large number of small cubes. The thermal resistance in the direction of each axis is then calculated for all the cubes. An equivalent network is obtained by taking a node at the centre of each sub-division and connecting adjacent nodes, in the direction of the axes, by thermal resistances equal to the half-sum of the thermal resistances, in the corresponding direction, of the cubes in question. This results, in general, in six branches at each node. The thermal capacitance of each sub-division is calculated and considered to be lumped at the node. The heat, if any, generated in a sub-division is also considered to be concentrated at the corresponding node.

The equivalent thermal network thus obtained may then be solved by:

1. a numerical method, i.e. by determining the heat balance at each node and solving the resulting equations, complex problems being solved using an electronic digital computer;
2. an analog method, i.e. by building an electrical resistance-capacitance network analogous to the thermal one.

The basic design and accuracy of analog networks of this kind has been discussed by Paschkis and Baker[23], but the application to buried cable systems presents special problems which have been discussed by Weedy[24]. The choice between digital and electrical analog methods is largely dependent on the problem to be studied. Neither method gives a continuous temperature distribution, but rather temperatures are given at nodes corresponding to the sub-divisions in the model, although this is not too disadvantageous since nodes can, in general, be positioned where temperature information is required.

A program must be written and developed for the digital computer, but components must be designed and assembled for the analog. A program can be designed so that several segments are developed and debugged at the same time, whereas the design and construction of an analog must, of necessity, be sequential. For

transient solutions, the digital computer does not consider time as a continuous variable as does the electrical analog, but time must be increased in discrete steps and a linear variation must be assumed over these steps. The time step used is chosen as a compromise between the need to keep errors to a minimum and the need to keep computation time, which is expensive, to a minimum.

Electrical analogs can be built to any size required whereas models used for digital computation are limited in size by the core storage available, although this is becoming less critical with the development of large-capacity, high-speed-access disk storage. The over-riding advantage which the digital computer has over the electrical analog is that a program can be written so that it is generally applicable to all classes of problem whereas an electrical analog is necessarily built for the solution of a specific problem. (It should be noted that the limitations discussed here apply to electrical analogs and not to electronic analog computers.) In the specific problem to be investigated, although some results are reported which were obtained using Perkins' electrical analog[20], the complicated problems which result from the incorporation of oil flow in the model shifted the emphasis to digital computation. Also, because the investigation was to be extended to examine EHV joints other than the 400 kV one, it was decided to solve the problem by digital computation and to develop a computer program to do this.

The problem of heat flow in a cable and joint is a three dimensional one which can be reduced to two dimensions by assuming that the conductor and cable sheath (joint shell) are isothermals circumferentially. This assumption, which means that, within the cable, only uniformly radial and longitudinal heat flow need be considered, has been verified by Weedy and Perkins[15] using a finely divided resistance mesh. All calculations are performed for a water-cooled-sheath system so that external thermal conditions are completely specified by the temperature of the cooling water at any particular cross-section. Lis and Thelwell[25] state that, for a water-cooled-sheath system, the water temperature rises from 15°C to 27°C in 4000 m, i.e. 3°C rise in water temperature per 1000 m. In this investigation, because of the lengths involved (less than 1000 m), the sheath temperature is assumed constant, at 20°C, along the length of the cable and joint, thus simplifying the problem. The resistances between, and the capacitances at, the mesh nodes determine node temperatures and time constants.

To provide an adequate representation of the dielectric, it ought to be sub-divided in the manner described earlier in the Chapter. However, to reduce computation time, it is proposed to lump the insulation and conductor thermal capacitances at the conductor and to represent the distributed thermal resistance between the conductor and the reference surface (i.e. the cable sheath or joint shell) by a single lumped resistance. These are valid simplifications since the temperatures to be determined are

those in the conductor and the system time constants at the conductor are small. The complicated resistance-capacitance network, which would, normally, be used to represent the joint and cable, thus, is reduced to the relatively simple ladder network illustrated in Fig. 9. Fig. 8 shows the circuit adopted to represent the heat transfer between conductor and oil.

Losses are injected at the conductor nodes and consist of the sum of the copper loss and half the dielectric loss for the particular section. The copper loss is equal to $I^2 R_{ac}$ where I is the load current and R_{ac} the effective electrical resistance at $85^{\circ}C$ of the conductor in that section; the copper loss is corrected for the temperature dependence of the conductor resistance by multiplying the factor $(1 + \alpha \Delta T)$ where ΔT is the difference between the measured conductor temperature and the $85^{\circ}C$ datum and α is the temperature coefficient of resistance of copper. The dielectric loss for each section is equal to $(2\pi f CV^2 \tan \delta)$, where C is the electrical capacitance of the insulation, V is the voltage between the conductor and earth and tan δ is the insulation power factor (dissipation factor). The dielectric loss is divided, according to the usual convention, equally between the conductor, as mentioned above, and the sheath. It is apparent that the sheath loss has little effect in this water-cooled-sheath system, so that the only heat injection in the program occurs at the conductor.

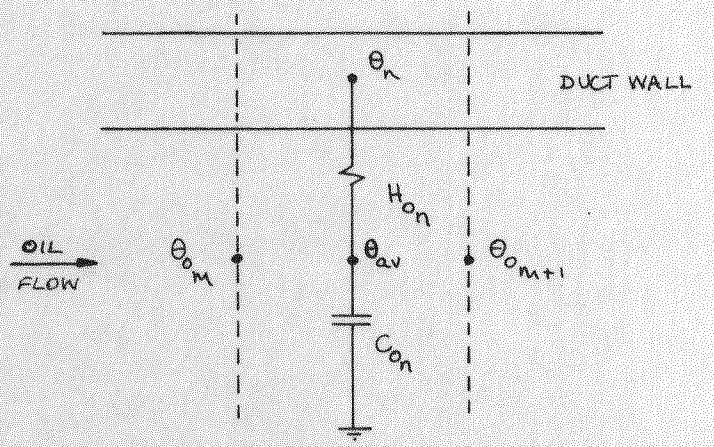

FIG 8: REPRESENTATION OF DUCT

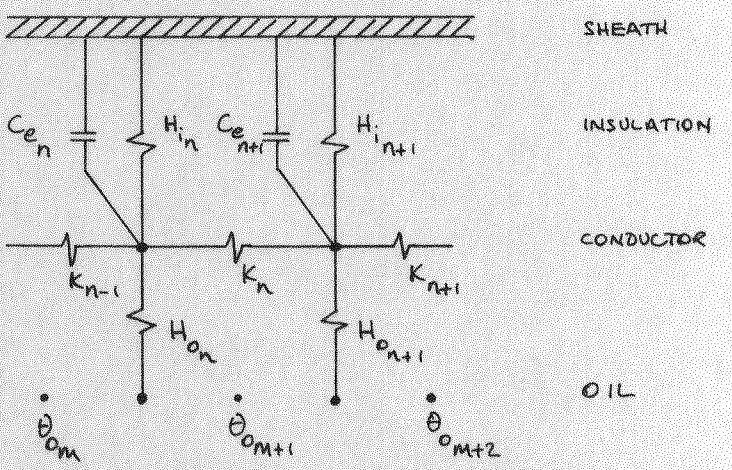

FIG 9: REPRESENTATION OF CABLE INSULATION AND CONDUCTOR

The behaviour of the conductor and duct-oil temperatures is described by Equations (10) and (11), which are developed in Appendix 4. It should be noted that subscript 'n' refers to nodes located in the conductor and 'm' to nodes in the oil; the relationship between 'n' and 'm' is that 'n' is at the centre of the nodal region and 'm' is at the downstream boundary of the region.

$$\theta'_n = \frac{K_n \Delta t}{C_{e_n}} \theta_{n+1} + \frac{K_{n-1} \Delta t}{C_{e_n}} \theta_{n-1} + \left(1 - \frac{\Sigma \Delta t}{C_{e_n}}\right) \theta_n + \frac{H_{o_n} \Delta t}{2C_{e_n}} \left(\theta_{o_m} + \theta_{o_{m+1}}\right) + \frac{q_n \Delta t}{C_{e_n}} \qquad (10)$$

where $\Sigma = K_n + K_{n-1} + 2H_{o_n} + H_{i_n}$

$$\theta'_{o_{m+1}} = \frac{H_{o_n} \Delta t}{C_{o_n}} \theta_n + \frac{(2\omega Cp - H_{o_n}) \Delta t}{2C_{o_n}} + \left(1 - \frac{(2\omega Cp + H_{o_n}) \Delta t}{2C_{o_n}}\right) \theta_{o_{m+1}} \qquad (11)$$

CHAPTER 3

DERIVATION OF, AND LIMITATIONS ON, THE MODEL FOR OIL OSCILLATION

The first part of the investigation is concerned with forced-cooling of EHV cables and joints by oscillation of the conductor duct oil and has two main objectives, namely:

1. determining the transient performance of a forced-cooled 400 kV, 3 in^2 joint;
2. developing a generalized digital computer program with which the transient performances of EHV joints, in general, can be determined.

The problem is tackled in the order indicated above because an electrical analog for the 400 kV, 3 in^2 joint, constructed by Perkins[20], is available; both the joint and its analog are described in Appendix 3. The availability of the analog facilitates the writing of a program to solve the problem of oil oscillation in the 400 kV, 3 in^2 joint, since results obtained digitally can be readily verified using the analog. Once this first program is running satisfactorily, the generalized program will be derived from it. This chapter is concerned with development of the first program and subsequent chapters will deal with the transient performance of the forced-cooled, 400 kV, 3 in^2 joint and the development of the generalized program.

The program solves the equations for conductor and oil temperatures derived in Appendix 4, using the simplified mesh described in Chapter 2. The resistances used in this simplified mesh are the radial thermal resistances between nodes in the conductor and the sheath, the longitudinal thermal resistances between nodes in the conductor and the heat transfer resistances between the nodes in the conductor and the duct oil (Figs. 8 and 9). The insulation and conductor resistances may be calculated using the expressions

$$R_{cond} = \frac{g_c x}{A} \tag{12}$$

$$R_{ins} = \frac{g_i}{2\pi\ell} \ln \left(\frac{r_i}{r_c} \right) \tag{13}$$

where g_c and g_i are the conductor and insulation thermal resistivities, A the conductor cross-section, x the distance between adjacent nodes, ℓ the nodal region length and r_c and r_i the conductor and insulation outer radii. Although Equation (12) is used to determine the conductor thermal resistances, the insulation thermal resistances are measured directly from the analog.

The design of joints results in a gap between the insulation and the joint shell; this gap is filled with the cable insulating oil. The gap existing in the joint used for the first part of the investigation is greater than 2 cm (0.9") so that it is apparent that there will be convection in the oil and the heat transfer

characteristic, consequently, modified. This modification may be considered as due to an effective thermal conductivity, k_e, which is related to the true thermal conductivity, k ($= \frac{1}{R}$), by the expression

$$\frac{k_e}{k} = 0.11\ (a\theta\delta^3)^{.29} \qquad (14)$$

where a is the convection modulus, δ the distance between the joint insulation and the shell and θ is the temperature difference across the gap. The dimensionless group $(a\theta\delta^3)$ is known as the Rayleigh number, N_{Ra}. The modification defined by Equation (14) is allowed for in the first program to agree with the modifications made by Perkins. However, joints are normally designed with much smaller gaps and, because of the doubts which exist concerning the validity of Equation (14), normal design practice is to neglect oil convection and to assume that the dielectric consists entirely of paper. This practice is followed for all the joints subsequently investigated.

The mechanism of heat transfer between the conductor and the duct oil is convective and the calculation of the heat transfer resistance is less straightforward than in the cases of heat transfer through the insulation and along the conductor. The heat transfer at the duct wall to the oil may be described by an equation analogous to Newton's cooling law

$$q = hA\ (\theta_\omega - \theta_o) \qquad (15)$$

where q is the rate of flow of heat across the wall, area A, temperature θ_ω, to the oil, temperature θ_o. The factor of proportionality, h, is called the heat transfer coefficient. Equation (15) may be regarded as a definition of h, although, in practice, the heat transfer coefficient of a flow is defined using the dimensionless group $\frac{hD}{k}$, where k is the oil thermal conductivity and D a characteristic length, in this case the duct diameter. This dimensionless parameter is known as the Nusselt number, N_{Nu}, the physical significance of which can be explained on the basis of the existence of a stationary layer of oil, the boundary layer, adjacent to the duct wall. If we assume that the temperature drop which occurs in this layer is the same as that on which the heat transfer coefficient is based, then the thickness of the layer is $\frac{k}{h}$ and the Nusselt number may be written

$$N_{Nu} = \frac{D}{k/h}$$

and interpreted as the ratio of characteristic length (i.e. duct diameter) to the boundary layer thickness.

Application of the principle of similarity to the problem of heat transfer in forced convection produces a functional relationship between the Nusselt, Reynolds and Prandtl numbers of the flow.

$$N_{Nu} = F\ (N_{Re}, N_{Pr}) \qquad (16)$$

Limitations are imposed on the flow by the pressure available to maintain flow and the limit on the quantity of oil which can be absorbed at the remote end of the system so that the flow regime to be considered is laminar. The nature of the problem is such that oil is first heated and then cooled as it approaches and then leaves the joint ferrule so that allowance must be made for the thermal entrance effect. A thermal entrance effect is always present whenever a fluid is heated or cooled as it flows through a duct. At the position where heating (or cooling) starts, the heat transfer coefficient has a very high initial value and decreases in the direction of the flow until, for the case of constant fluid properties, a constant value is reached. In the case of the joint, there are two thermal entrance effects, one where the oil is entering the hotter joint section and the other at the ferrule where the conductor temperature begins to fall. Sieder and Tate[27], having correlated a large amount of data on heating and cooling viscous liquids, recommend the following empirical expression for the Nusselt number of laminar viscous liquid flow inside horizontal or vertical tubes:

$$N_{Nu} = 1.86 \left(\frac{\mu_b}{\mu_\omega} \right)^{.14} (N_{Re} N_{Pr} \frac{D}{L})^{1/3} \qquad (17)$$

where μ_b is the bulk fluid kinematic viscosity, μ_ω is the fluid kinematic viscosity at the wall and L the distance downstream from the thermal entrance. The factor $\left(\frac{\mu_b}{\mu_\omega} \right)$ in Equation (17) makes

allowance for the variation in properties of the fluid due to the temperature gradient across the tube.

As the distance from the thermal entrance increases and the $\frac{D}{L}$ term becomes progressively smaller, the Nusselt number tends to an asymptotic value, which varies in size dependent on the shape of the duct and the assumptions made about the wall temperature. If the wall temperature is assumed to vary linearly, then it can be shown (Appendix 6) that the asymptotic value of the Nusselt number is 4.36. This is the value assumed for the major part of the results obtained in this investigation. The effect of varying the Nusselt number over the range $N_{Nu} = 2.42$ to $N_{Nu} = 12.1$ is investigated, as is the effect of allowing for the thermal entrance effect using Equation (17).

The determination of the capacitances to be lumped at the conductor presents a different problem since this single, lumped value is required to represent the distributed capacitances of both conductor and insulation. To obtain an equivalent capacitance which would define the transient behaviour of the conductor, the analog described in Appendix 3 is used. The transient temperature rise at each node is measured during the application of a step function load to the energized cable system. A series of 'best-fit' exponential curves is obtained and the time constant at each node determined. Fig. 10 shows both the curve measured on the analog and the 'best-fit' exponential, for the joint ferrule; the time constant in this case is 2.86 hours. Knowing the time

FIG 10 : COMPARISON OF MEASURED AND FITTED CURVES

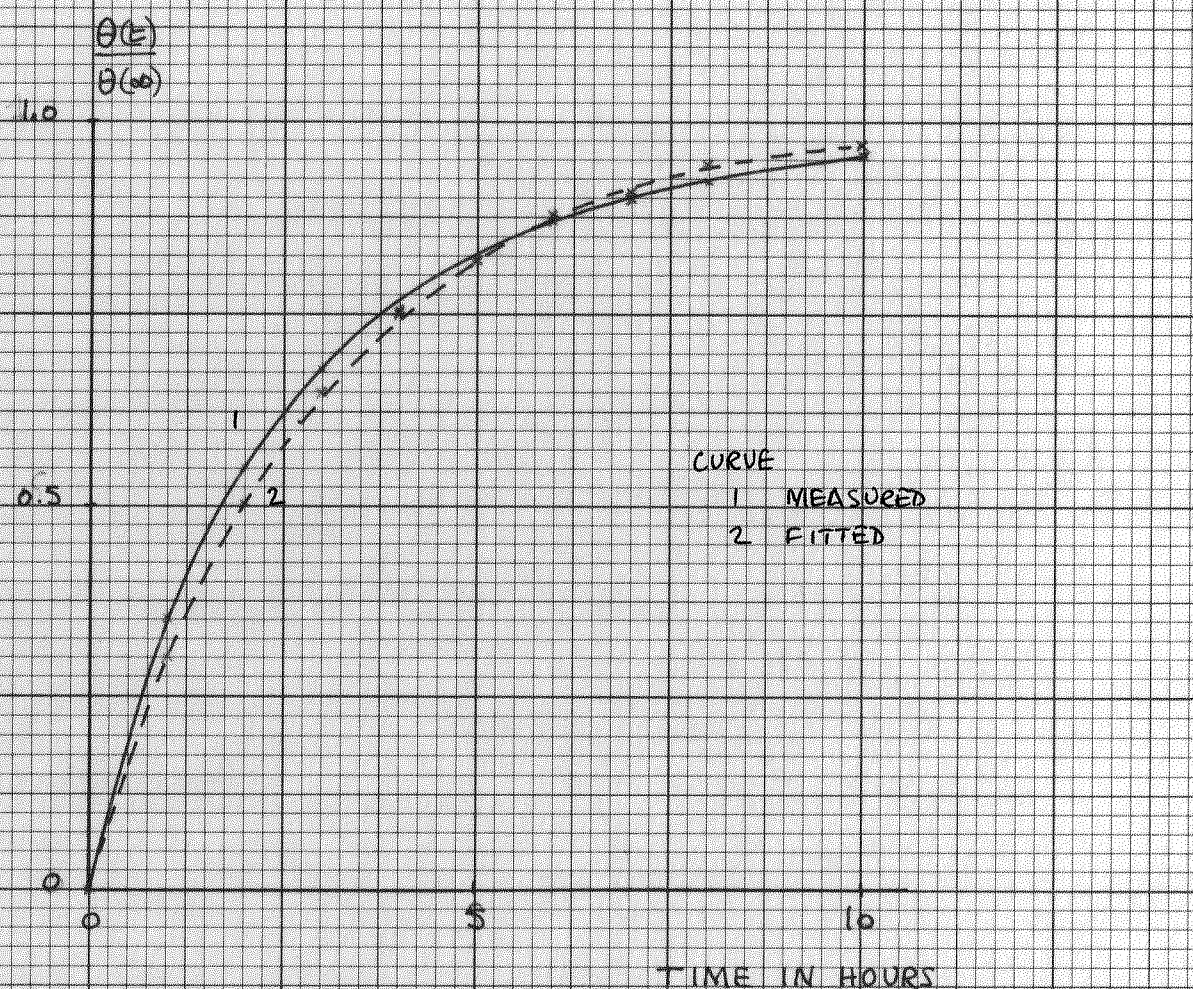

constant, which defines the short-time, transient behaviour of a node and the thermal resistance between the node and the cable sheath, the equivalent capacitance to be lumped at the node may be calculated. The data measured from the analog is shown in Table 1; with this data set, the capacitance and resistance profiles of the insulation may be drawn so that, although the mesh used in the digital simulation does not correspond with the mesh used in the analog, insulation resistances and equivalent capacitances can be determined for use in the program.

As a preliminary to the digital investigation of oil oscillation and to help in the appreciation of the problem, the cooling effect of a uni-directional oil-flow is studied using the method due to Weedy[28]. A sheath cooled cable system is investigated and conditions near the end of the cooled length, where the cable conductor temperature rise is 65°C, are studied. Since oil and conductor temperatures are interdependent, an iterative process is used. Oil temperature rises are, initially, set equal to those of the conductor without oil flow, and, starting in the cable section remote from the joint, the gain in oil temperature passing through the joint is calculated. The heat transfer mechanism is described by the following equations.

Enthalpy change, q_1, in the oil passing through, and carried out of, the section is

$$q_1 = \omega \, Cp \, (\theta_1 - \theta_2)$$

where θ_1 and θ_2 are the entrance and exit oil temperatures.

TABLE 1

Thermal resistances and capacitances measured from the analog

Node	Length (cm)	Resistance* (°C/W)	Capacitance* (J/°C)
A (Ferrule)	15.9	82.8	123.5
B	20.32	98.7	88.3
C	20.32	98.7	82.8
D	20.32	89.5	88.1
E	20.32	68.9	107.2
F	20.32	58.9	121.8
G	20.32	47.7	139.6
H	20.32	47.7	120.7
J	20.0	47.6	120.3
K	20.0	47.6	120.3
L	40.0	47.6	111.2
M	40.0	47.6	111.2
N	60.0	47.6	99.8
P	80.0	47.6	99.8
Q	100.0	47.6	99.8

* N.B. Resistance and capacitance values are for 1 cm length.

Heat, q_2, lost to the oil through convective heat transfer is

$$q_2 = (\theta_{cond} - \tfrac{1}{2}(\theta_1 + \theta_2)) \frac{1}{R_h}$$

θ_1 is initially assumed to be 65°C and the value of θ_2 varied until q_1 and q_2 are equal. The final value of θ_2 is then taken as the value of θ_1 for the next section and so on through the cable and joint. The set of oil temperatures thus obtained is imposed on the analog and the modified conductor temperatures obtained. The process is then repeated with the successive sets of modified conductor temperatures until further iteration produces no appreciable change in the oil and conductor temperatures. The conductor temperature profile obtained in this way is that existing when the oil has been circulating for a long time.

The conductor and oil temperature profiles obtained with an oil flow rate of 5 cm^3/s are shown in Fig. 11 where they are compared with the conductor temperature profile without circulation. The ferrule temperature rise is seen to fall to a value of 86°C in the 'stable condition' compared with a no flow value of 102°C; the 'stable condition' is defined as that condition with oil circulation for which the ferrule temperature is no longer falling. The difference between the ferrule temperatures with and without circulation for any given flow rate is called the ferrule temperature alleviation for that flow rate. Thus, the ferrule temperature alleviation for a unidirectional flow of 5 cm^3/s is (102 - 86)°C, i.e. 16°C. Ferrule temperature alleviation

FIG 11: CONDUCTOR AND OIL TEMPERATURE PROFILES - UNIDIRECTIONAL FLOW

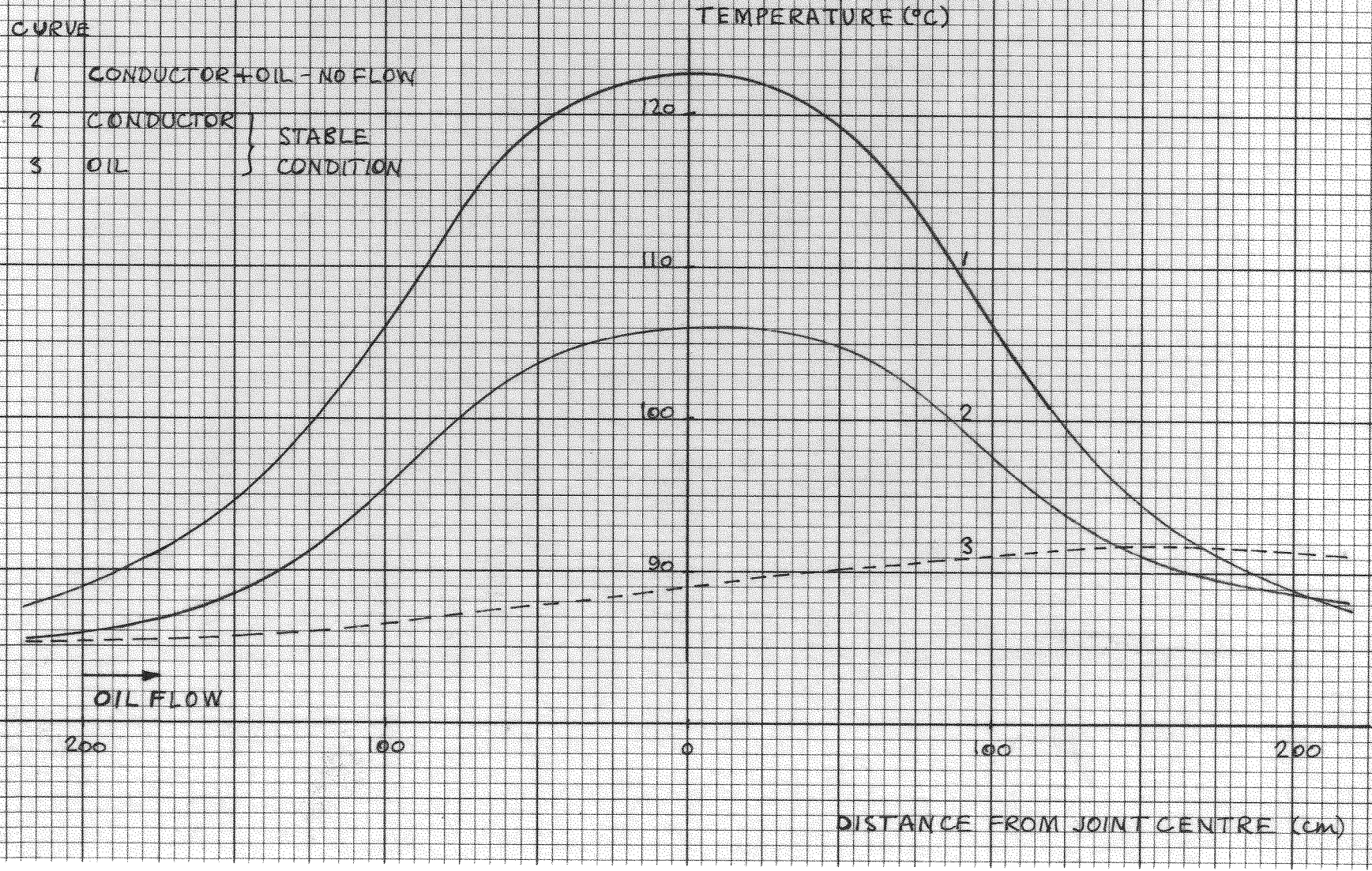

is plotted as a function of flow rate in Fig. 12. It is interesting to note that the rate of increase of temperature alleviation falls off with increasing flow rate. It should be noted that no temperature correction has been applied to the results obtained with the analog and that the values of losses used are evaluated for an 65°C temperature rise.

The remaining data to be obtained for inclusion in the program are the allowable flow rates and cycle times. These are limited by the pressure available to maintain flow and the volume of oil which can be absorbed in the downstream pressure tank; this last limitation imposes a limit on the product of flow rate and the half-cycle time. It is in fact possible to use flow rates of up to 60 cm^3/s (48 gal/h) for both the duct sizes (i.e. 12 mm and 16·5 mm diameters) normally used in EHV cable construction, although for the smaller duct size flow rates in excess of 40 cm^3/s are not recommended because of the higher Reynolds numbers experienced (Appendix 7). It will be shown later that there are other reasons for the limitations applied to flow rate and cycle time.

The oil velocity profile used is assumed to be a square wave. This represents the optimum case of zero time required to effect flow reversal; however, too short a flow reversal time is to be avoided because of the very high transient pressure changes produced. Flow reversal will require a finite time and to simulate this, a velocity profile with a 30 seconds delay is used

FIG 12: FERRULE TEMPERATURE REDUCTION v OIL FLOW RATE

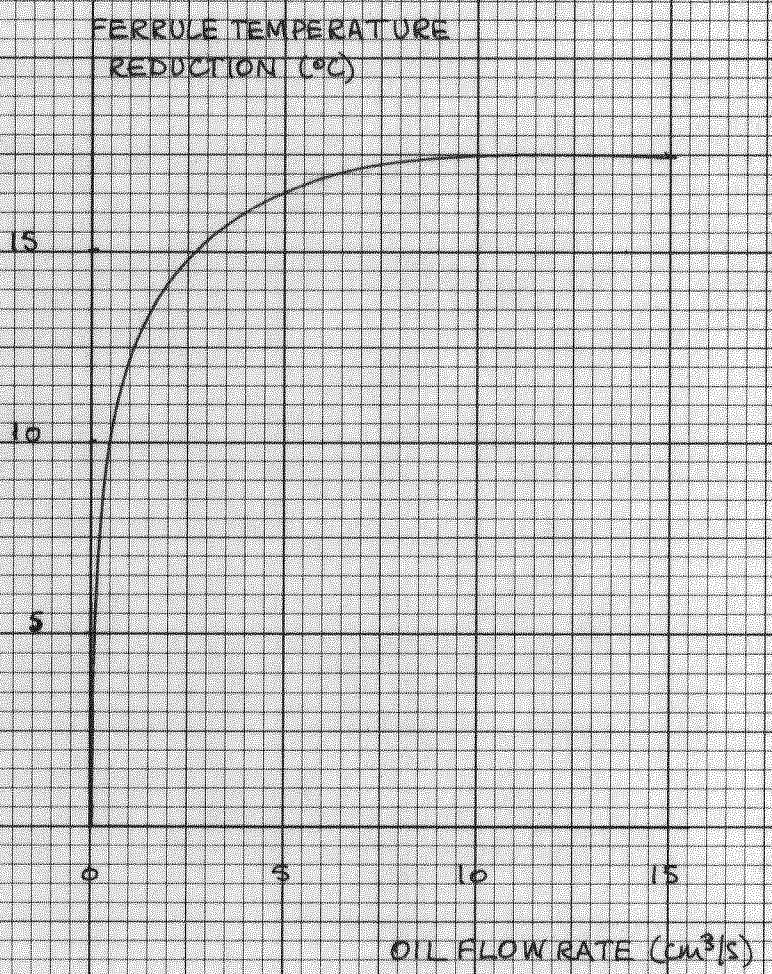

(Fig. 13) so that the flow velocity is assumed to be zero for 30 seconds at flow reversal; this represents the worst case.

In developing the model for digital solution, a compromise has to be made between fine subdivision of the system which would give high accuracy in solution but be expensive in computation time, and a coarse division, which is economic in time but less accurate. The joint-cable is therefore divided to give a fine mesh at, and near to, points of interest, in this case the joint ferrule, becoming more coarse in the cable remote from the joint. In accordance with this requirement, the first model used was obtained from the analog due to Perkins. This model divides a half-joint and associated cable into 15 subdivisions and utilizes the half-ferrule as one subdivision. Because the behaviour of both halves of the joint is not the same with oil flow, the whole joint had to be included in the model so that there were 30 subdivisions, comprising the joint and 3.6 m of cable on each side of the joint. However, the temperature of the oil entering the system did not remain fixed but increased with time; to remedy this, the length of cable considered was increased. The result was that a second model was developed in which the oil entering and leaving the extremities of the cable had the same temperature, which did not increase with time. The model contains 80 nodes and comprises a joint with 500 m of cable each side; this, however, is not representative of cable systems.

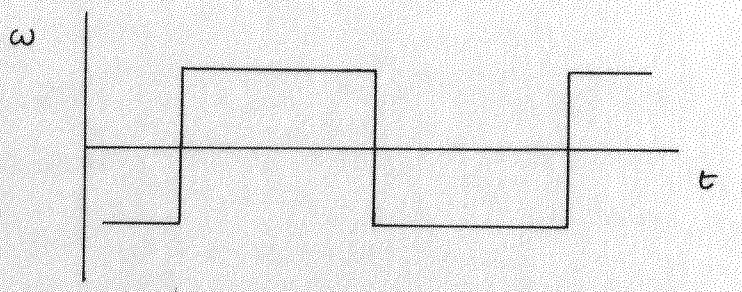

Standard Square Wave

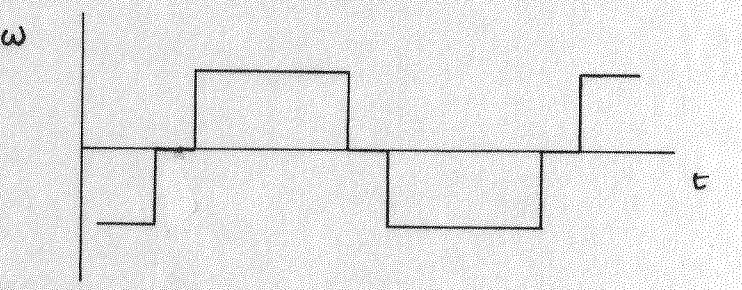

Delayed Square Wave

FIG 13: FLOW PROFILES

In an endeavour to make the model more closely resemble a real situation, the system of Fig. 14 is used. It represents a system comprising 700 m of cable containing two 400 kV normal through joints, the centres of which are equidistant from the centre of the system; the system is divided into 80 sections. The joint ferrule is considered as two sections which are the smallest subdivisions, being 15 cm long. The length of sections increases until out in the cable the subdivision is coarsest and the section length is 4m. The nodal region lengths and their associated resistance and capacitance are shown in Table 2.

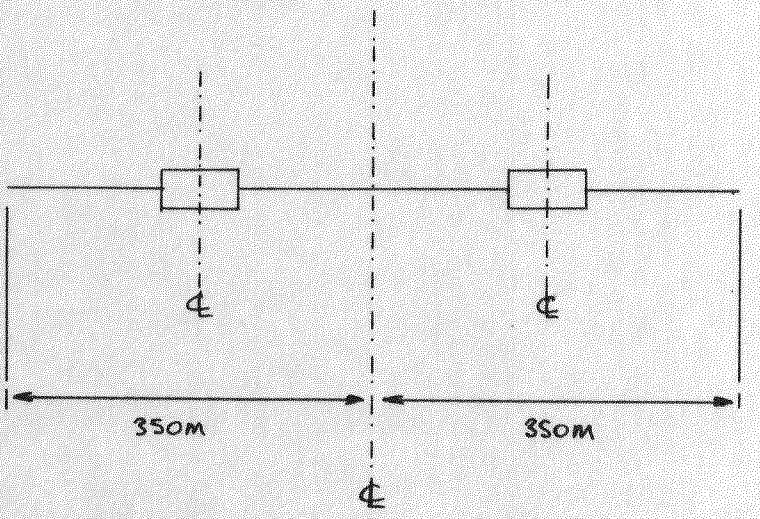

FIG 14: JOINT-CABLE SYSTEM

TABLE 2

Thermal resistances and capacitances used in the digital simulation

Node	Length (cm)	Resistance* (°C/W)	Capacitance* (J/°C)
1	4320.0	47.6	99.8
2	4320.0	47.6	99.8
3	2160.0	47.6	99.8
4	2160.0	47.6	99.8
5	2160.0	47.6	99.8
6	1455.0	47.6	99.8
7	250.0	47.6	99.8
8	120.0	47.6	99.8
9	120.0	47.6	99.8
10	90.0	47.6	99.8
11	60.0	47.6	105.0
12	60.0	47.6	110.0
13	30.0	47.6	115.0
14	30.0	47.6	120.3
15	30.0	47.7	122.5
16	30.0	52.5	133.0
17	30.0	68.8	110.0
18	30.0	89.5	88.3
19	30.0	96.5	88.3
20 (Ferrule)	15.0	82.8	124.5

* N.B. Resistance and capacitance values are for 1 cm length.

CHAPTER 4

RESULTS FOR 3 in^2, 400 kV THROUGH JOINT

This chapter is concerned with the response to oil oscillation of conductor temperatures in the 3 in^2, 400 kV joint described in Appendix 3. The oil oscillation is assumed to start at time zero, and the system is assumed to have been previously running with 2200 MVA load for such a time that the temperature distribution is steady. Although temperatures quoted previously in Chapter 3 were temperature rises measured against water temperature, temperatures quoted in this, and subsequent, chapters will be actual temperatures above $0^{o}C$; this is a more convenient practice and the implications of temperatures more readily understood. The water temperature is, again, assumed to be $20^{o}C$. The periodic time for oil oscillations is 20 minutes unless stated otherwise.

The steady state conductor temperature distribution measured from the analog is compared, in Fig. 15, with the distribution obtained using the digital computer simulation described in Table 2 above. The agreement between the two sets of results is good, and at no point over the whole length of the cable and joint does the difference between the two profiles exceed $2^{o}C$. Using both digital and analog methods, the conductor and oil temperature profiles for a 5 cm^3/s unidirectional flow, in the 'stable-condition' (i.e. that condition at which the ferrule temperature

FIG 15: CONDUCTOR TEMPERATURE PROFILES

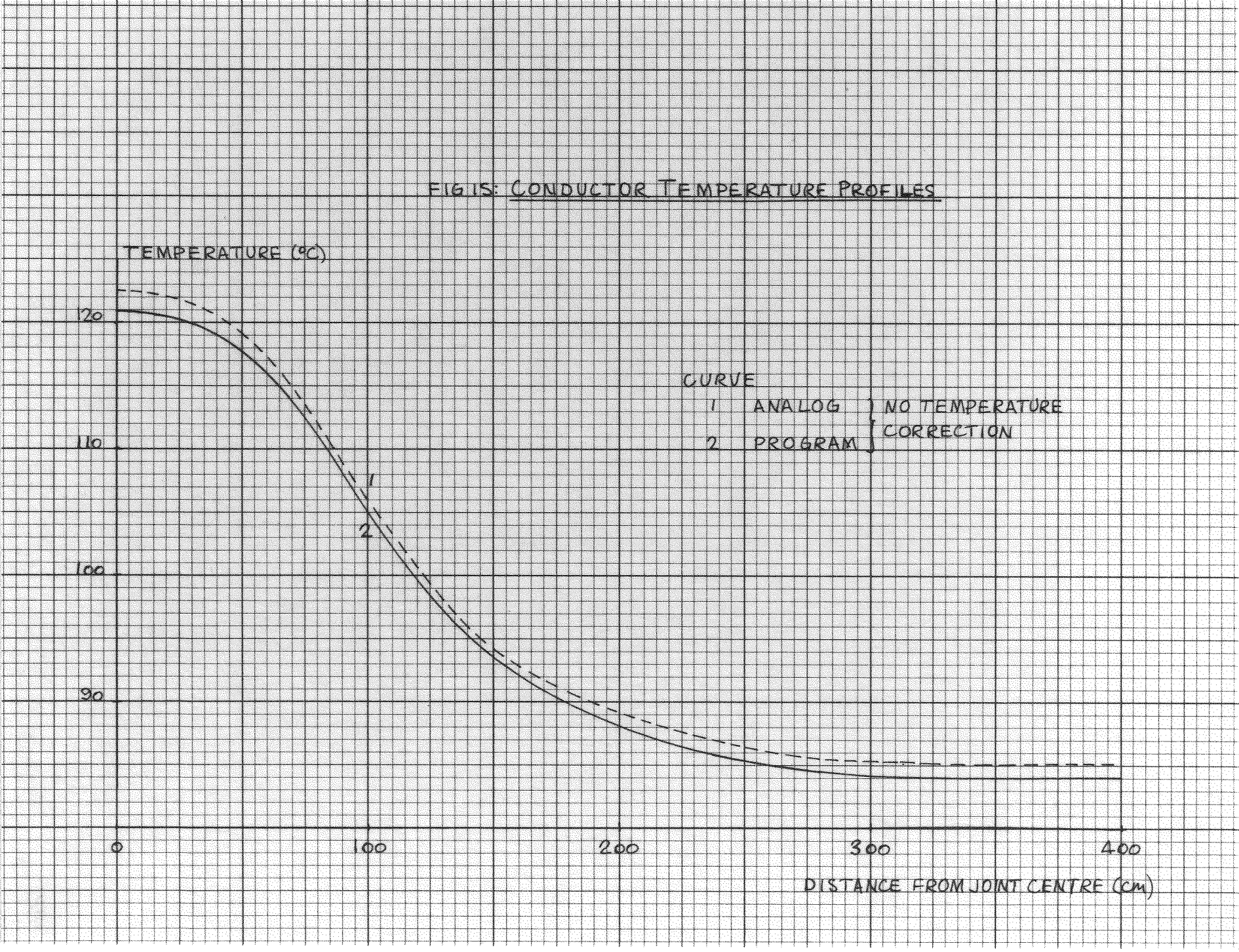

reaches a steady value), are shown in Fig. 16, and once again the agreement between the two sets of results is good, the maximum difference between them being 2°C. The variation of ferrule temperature alleviation with flow-rate is shown in Fig. 17 and the results agree fairly well.

These results show that the digital simulation compares favourably with the analog, and the method is, therefore, acceptable. It should be noted, however, that the results from the analog are less accurate than those obtained digitally because the analog represents only the half-joint and its proper working is dependent on the validity of the image theory. With oil flow, the two halves are behaving differently, and the image theory breaks down. The errors produced in this way should be small and within the limits of accuracy of the analog.

The results obtained for unidirectional flow were obtained with the copper losses calculated at 85°C and uncorrected for the temperature dependence of the conductor resistance. This temperature dependence is allowed for by the factor $(1 + \alpha(\Delta T))$, where α is the temperature coefficient of resistance for the conductor material and (ΔT) is the difference between the actual conductor remperature and the 85°C reference. The result of including the temperature correction is that the ferrule temperature increases to 115.7°C from 100.8°C. Corrected and uncorrected temperature profiles are compared in Fig. 18; the difference between the curves is greatest at the joint-centre and

FIG 16: CONDUCTOR AND OIL TEMPERATURE PROFILES - UNIDIRECTIONAL FLOW

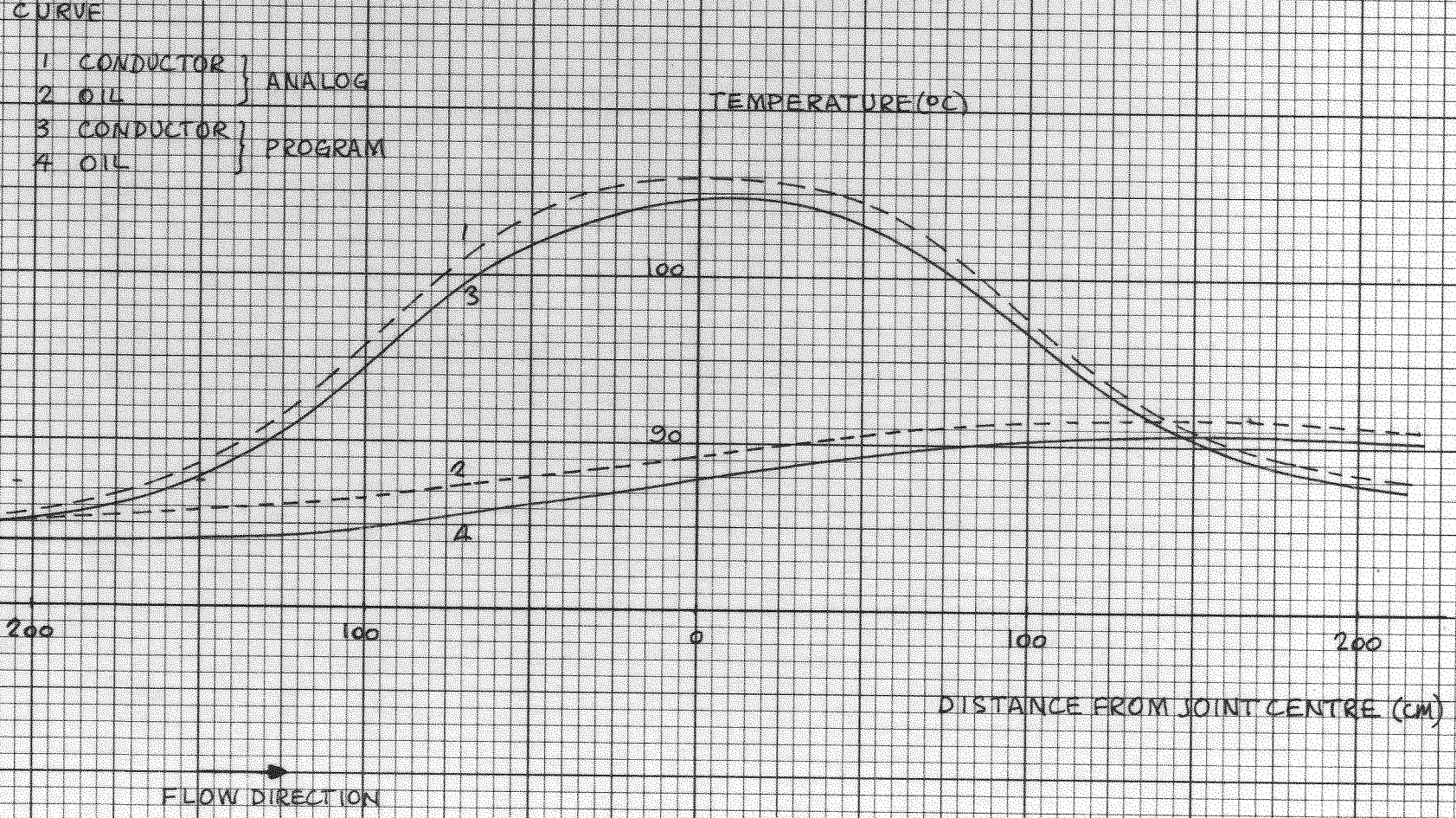

FIG 17: FERRULE TEMPERATURE REDUCTION v OIL FLOW RATE

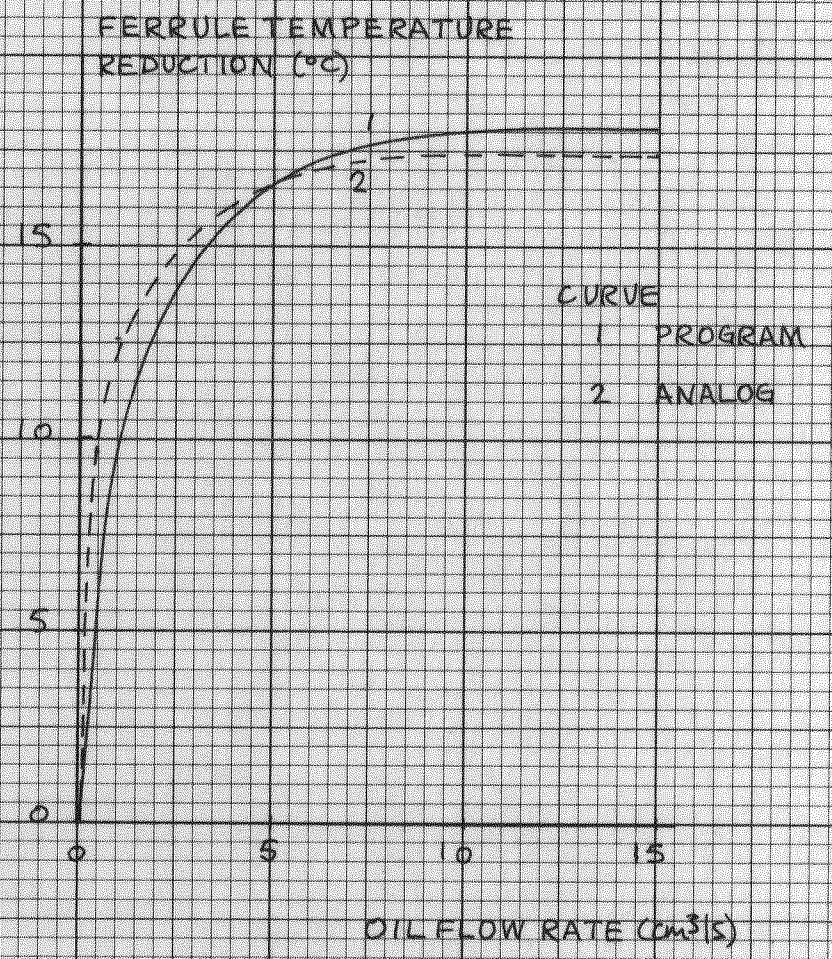

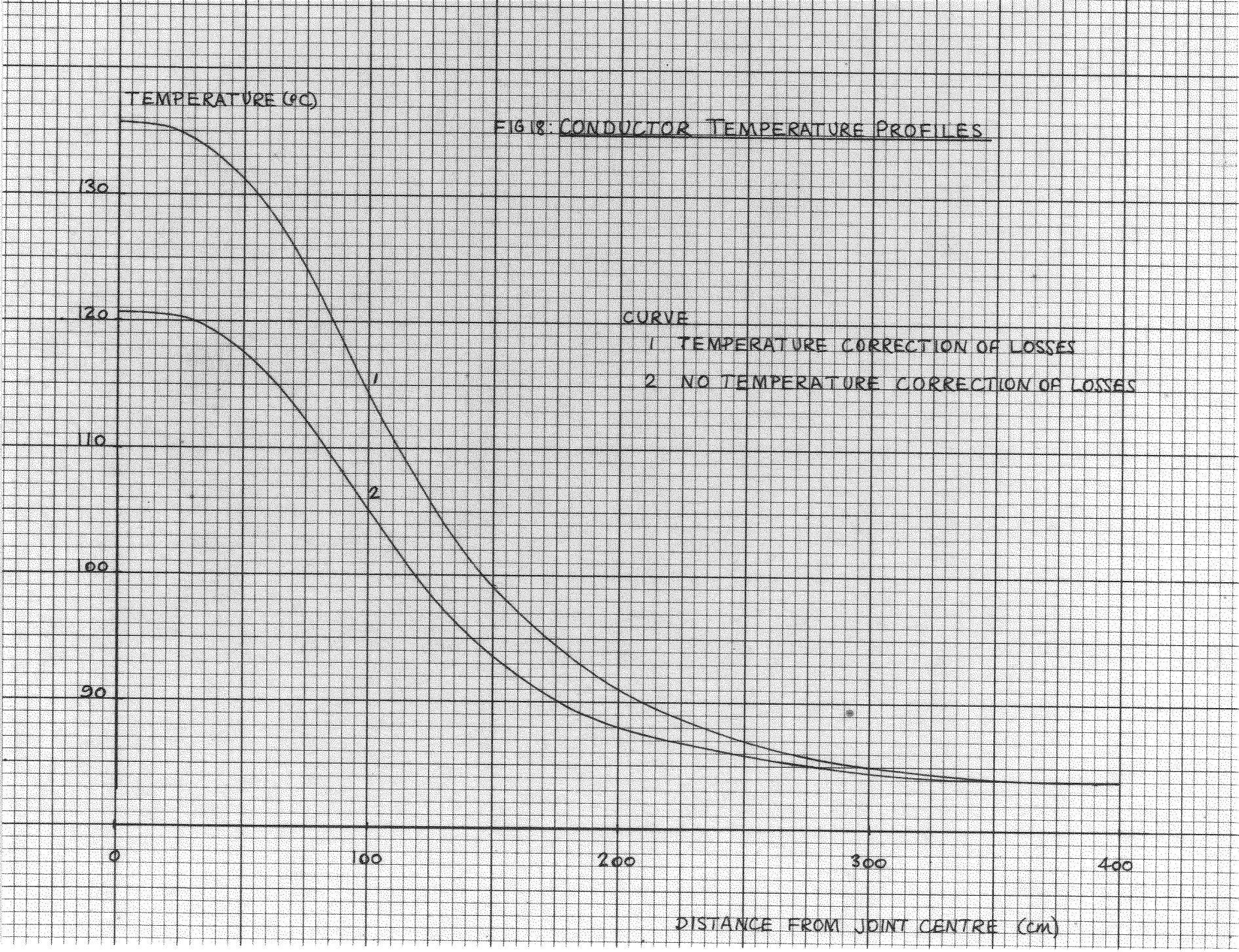

FIG 18: CONDUCTOR TEMPERATURE PROFILES

CURVE

1 TEMPERATURE CORRECTION OF LOSSES

2 NO TEMPERATURE CORRECTION OF LOSSES

reduces in the remote cable as the conductor temperature approaches 85°C. Fig. 19 shows the effect of temperature correction on the 'stable-condition' conductor temperature profile obtained with a 20 minute cycle, 5 cm^3/s oil flow; the ferrule temperature alleviation is seen to be 24.6°C rather than 14.7°C. It is obvious that the effect of temperature correction is significant and cannot be ignored. All results quoted, subsequently, are corrected for the temperature dependence of the conductor resistance.

'Stable-condition' temperature profiles in the conductor and the duct-oil obtained with an oil flow-rate of 5 cm^3/s are compared, in Fig. 20, with the pre-oscillation temperature profile. The oil temperature is seen to rise to a peak on the downstream side of the joint-centre. Although the rate of fall of temperature of oil leaving the joint is less than its rate of rise entering, the temperature of the oil leaving the upstream joint returns to its starting value before entering the downstream joint. The fact that the oil temperature profile peaks on the downstream side of the joint centre implies that, when the flow direction reverses, the peak must cross the joint centre. This is illustrated in Fig. 21 which shows the variation of conductor temperature with time at three positions in the joint-cable system. Fig. 21 has been obtained using a 5 cm^3/s oil flow-rate with a 40 min. oscillation cycle. The 'ripple' associated with the movement of the oil temperature profile peak can be seen; the periodic time of this

FIG 19: CONDUCTOR TEMPERATURE PROFILES - WITH AND WITHOUT TEMPERATURE CORRECTION

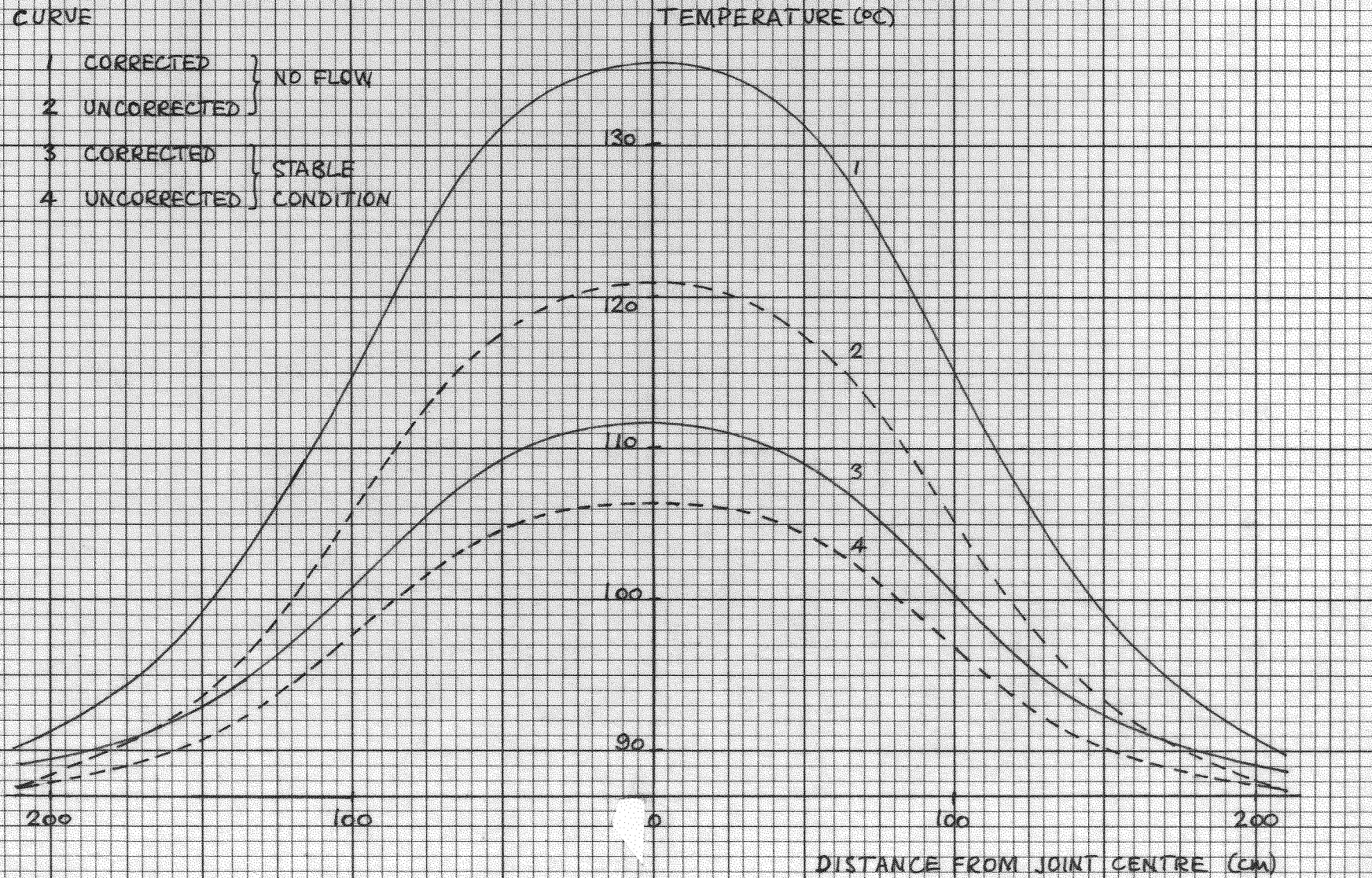

FIG 2a : CONDUCTOR AND OIL TEMPERATURE PROFILES

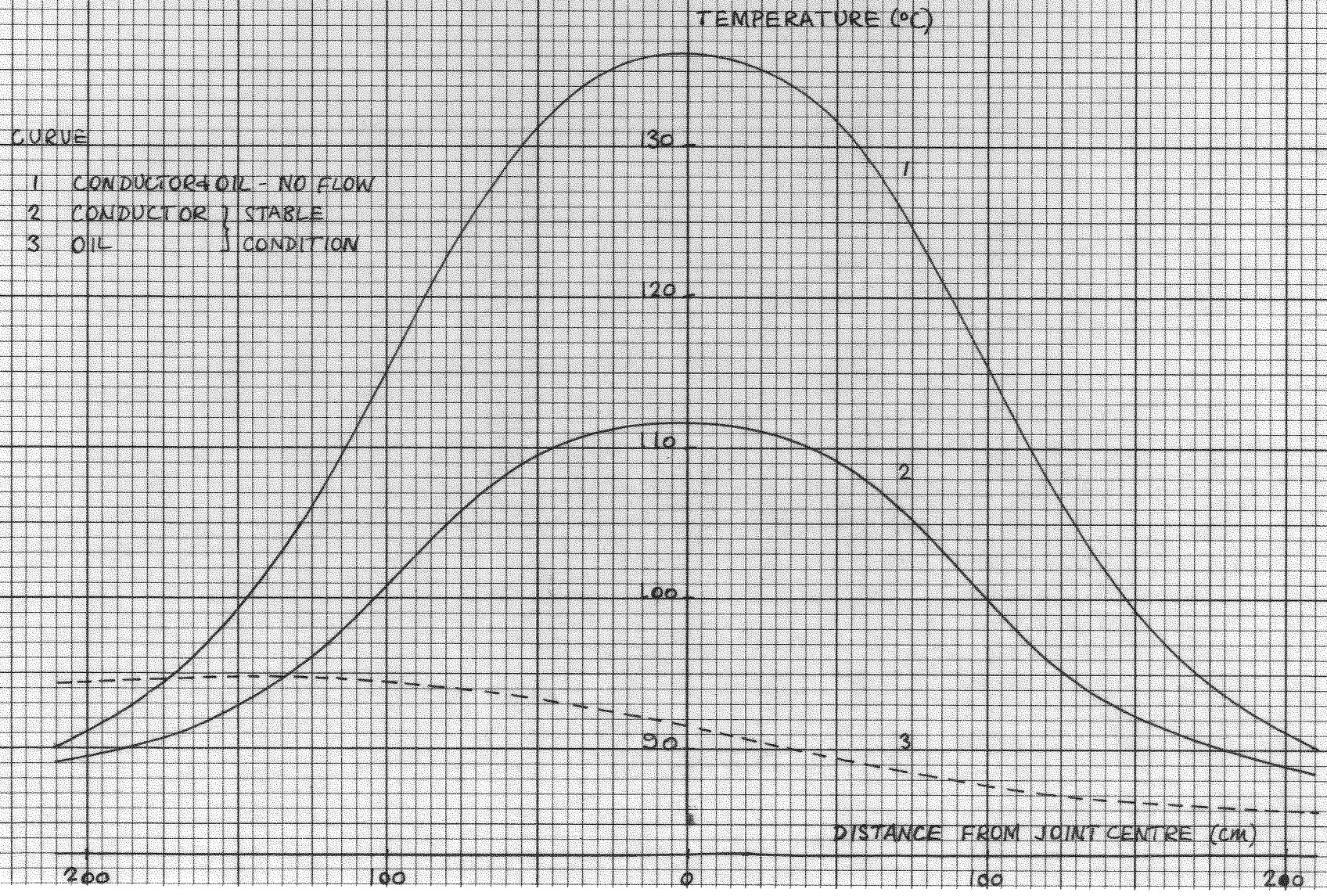

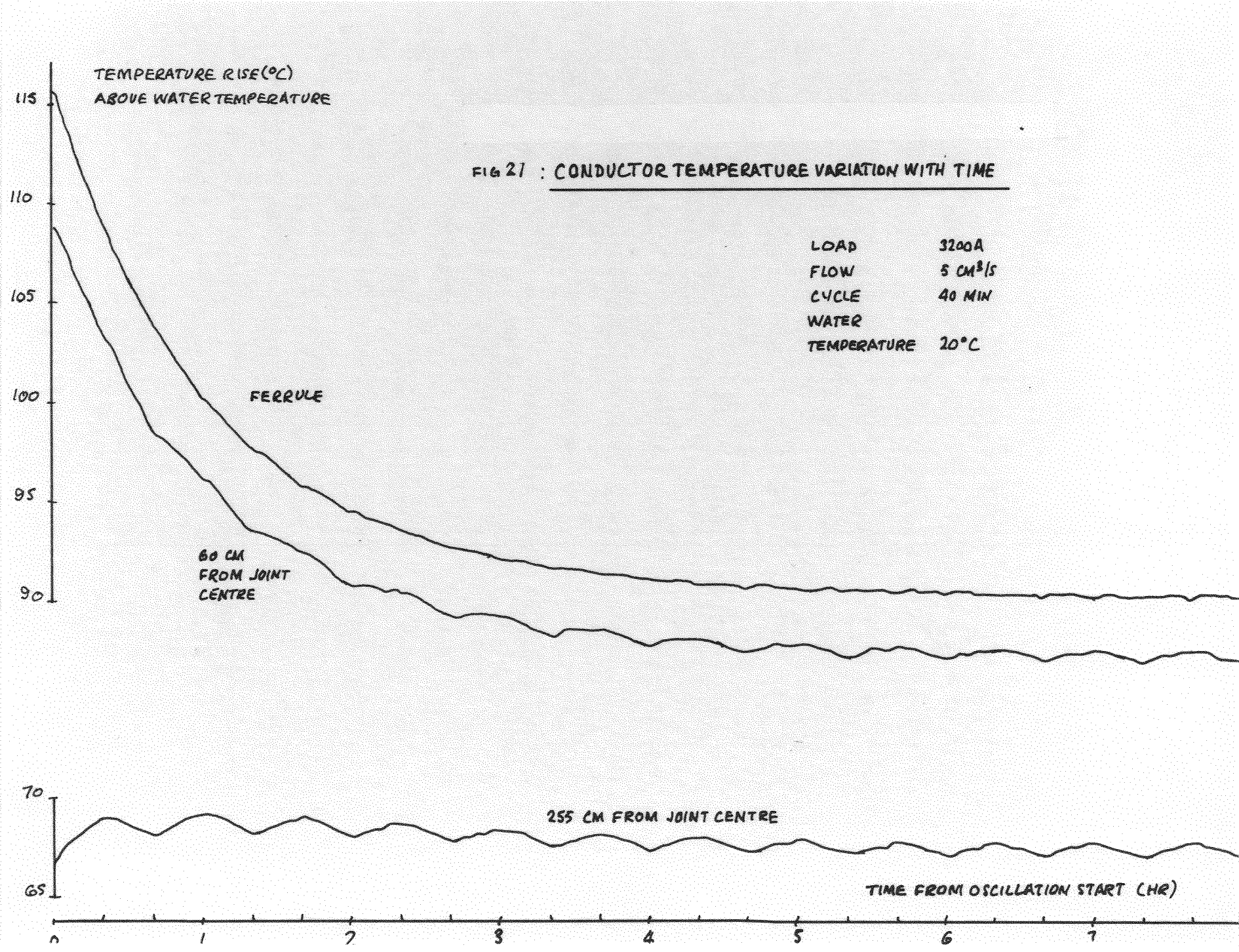

FIG 21 : CONDUCTOR TEMPERATURE VARIATION WITH TIME

ripple, measured from the curve for the remote cable conductor is 40 min., the same as the oil oscillation cycle time.

The stable-condition temperature profiles in the conductor, for several values of oil flow-rate with a 20 min. oscillation cycle, are shown in Fig. 22, compared with the pre-oscillation profile. It is seen that, as flow-rate increases, the rate of improvement in conductor temperature falls off. Although there is a $5^{o}C$ spread in the conductor temperatures at 200 cm, the temperatures, in all cases, converge on the pre-oscillation value in the remote cable. The 'smoothed' curves of Fig. 23 show the reduction of ferrule temperature with time for oscillation conditions described for Fig. 22, and the reduction in the rate of improvement of conductor temperature can be observed.

After 1½ hours of oscillation, the ferrule temperature alleviation in all cases is at least 70% of its final value, and after three hours, even for the slowest flow (2.5 cm^3/s), is within 90% of the stable-condition value. After six hours, the temperatures have steadied down, excepting the ripple indicated in Fig. 21. As the oil flow-rate increases, the initial gradient of the temperature-time curves increases, implying a reduction in the time constant. This increase in gradient can be explained by considering Equation (11) of Chapter 2; dividing through by Δt and re-arranging, we obtain

$$\frac{\Delta\theta_{o_{m+1}}}{\Delta t} = \frac{H_{o_n}}{C_{o_n}} \Delta\theta_r + \frac{\omega Cp}{C_{o_n}} \Delta\theta_o$$

FIG 22: CONDUCTOR TEMPERATURE PROFILES

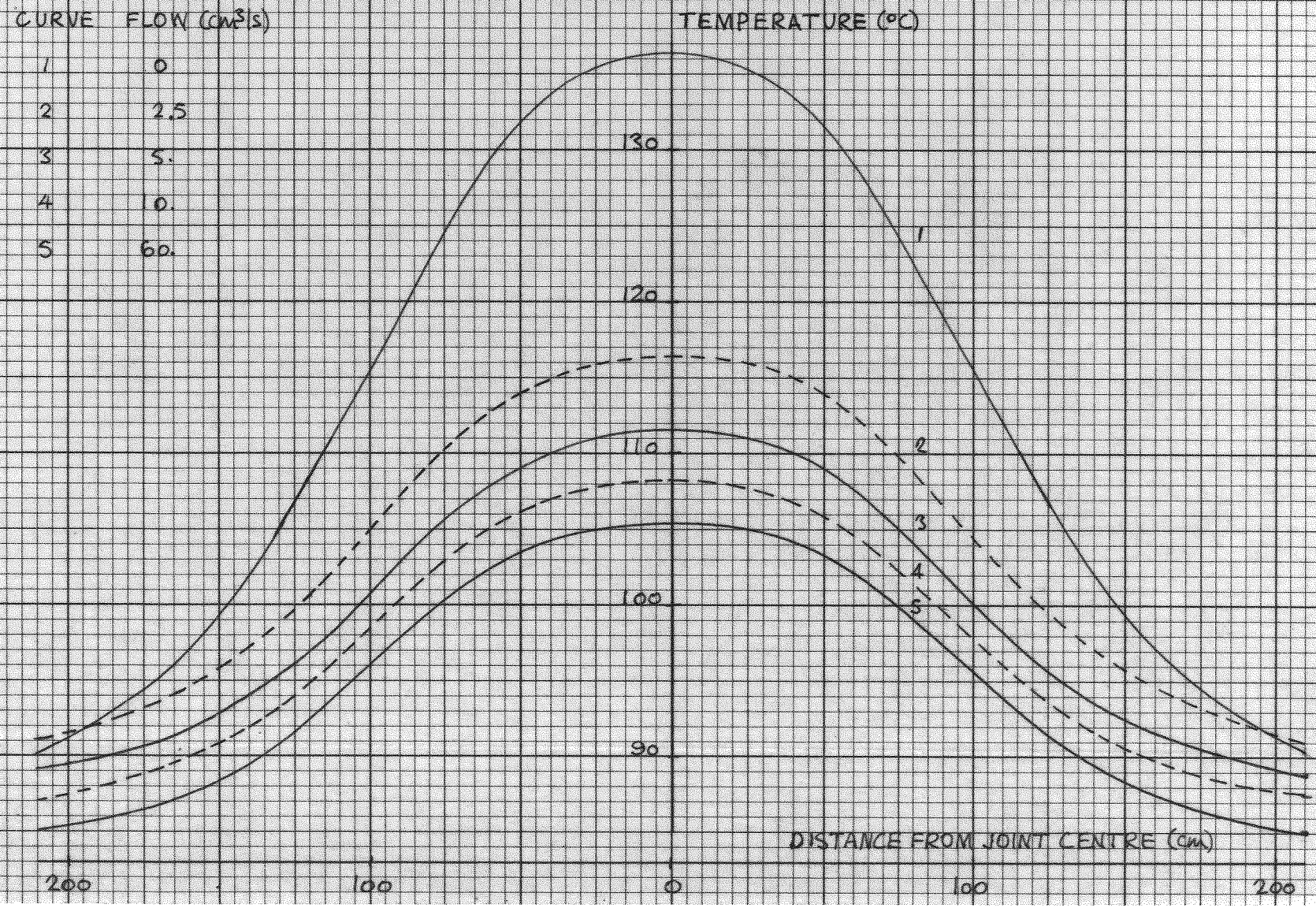

FIG 23: FERRULE TEMPERATURE VARIATION WITH TIME

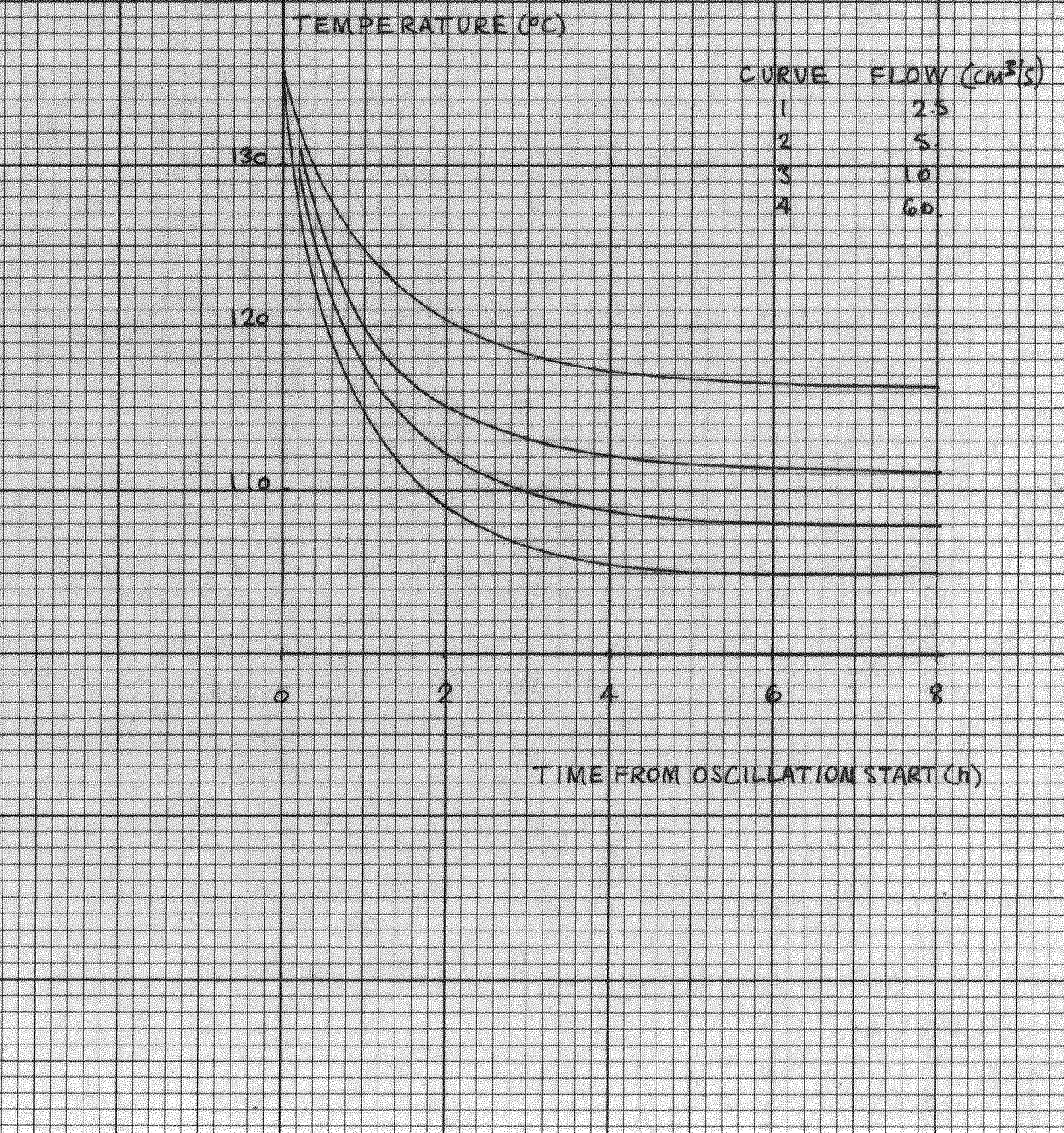

FIG 24: FERRULE TEMPERATURE REDUCTION v OIL FLOW RATE

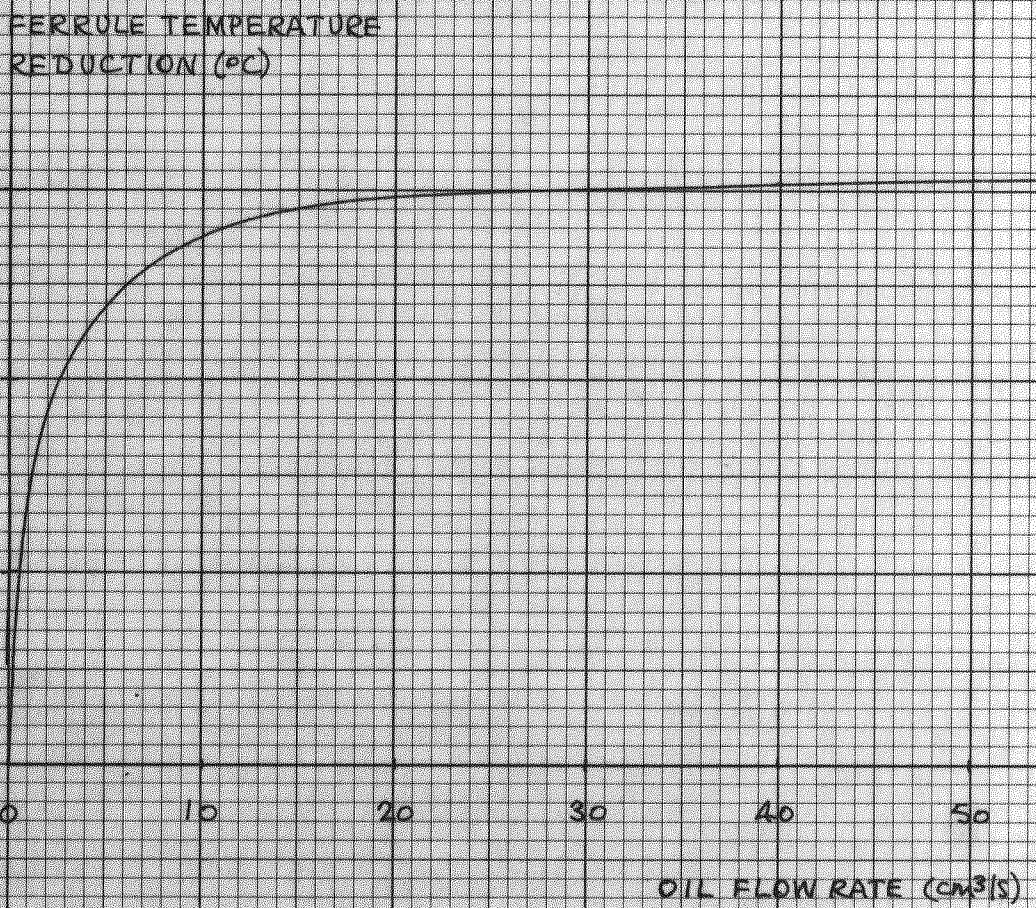

where $\Delta\theta_{o_{m+1}} = \theta'_{o_{m+1}} - \theta_{o_{m+1}}$

$\Delta\theta_r = \theta_n - \frac{1}{2}(\theta_{o_m} + \theta_{o_{m+1}})$

$\Delta\theta_o = \theta_{o_{m+1}} - \theta_{o_m}$

From this equation, we see that, in the coefficients of the temperature terms, all of the factors are constant except for the flow-rate, hence, the dependence of $\frac{d\theta}{dt}$ on ω.

The reduction in the rate of conductor temperature improvement is illustrated by the curve in Fig. 24 where ferrule temperature alleviation, θ_R, is plotted as a function of flow-rate. This curve may be fitted with an expression of the form:

$$\text{temperature alleviation, } \theta_R = \frac{\omega}{\alpha + \beta\omega}$$

where α and β are constants and ω is the flow-rate. This is the Frohlich Equation. It should be noted that $\frac{1}{\alpha}$ is equal to the temperature alleviation at infinite flow rate and $\frac{1}{\beta}$ is equal to the gradient of the curve at zero flow. (See Appendix 8)

The equation

$$\theta_R = \frac{\omega}{(.0432 + .0319\,\omega)}$$

provides a good fit to within less than 1% over the range 5-60 cm^3/s.

The relationship between ferrule temperature alleviation and cycle time for constant flow rate (= 5 cm^3/s) is illustrated in Fig. 25. The curve is seen to be of the same general shape as that of Fig. 24, and an equation of the same form may be used to fit it. The equation

$$\theta_R = \frac{T}{(.0756 + .0371T)}$$

yields results agreeing with the measured values to within 1% over the range 10-60 min.

The equations quoted above may be combined to yield the equation

$$\theta_R = \frac{35.4\ \omega T}{(\omega + 1.36)(T + 2.04)}$$

This equation gives values for ferrule temperature alleviation which are in good agreement with those obtained from the program.

These results have been obtained assuming the square wave velocity profile shown in Fig. 13, and these are therefore the best results which can be expected with oscillatory flow. Values for ferrule temperature alleviation obtained with the flow profile involving a 30s delay at reversal are, even for the maximum flow rate, $2^{\circ}C$ less than the results shown for the normal square wave profile. Because of this, the profile used to obtain all subsequent results is the square wave profile involving no delay at flow reversal. Although the curves of Figs. 24 and 25 show that

FIG 25: FERRULE TEMPERATURE REDUCTION v PERIODIC TIME

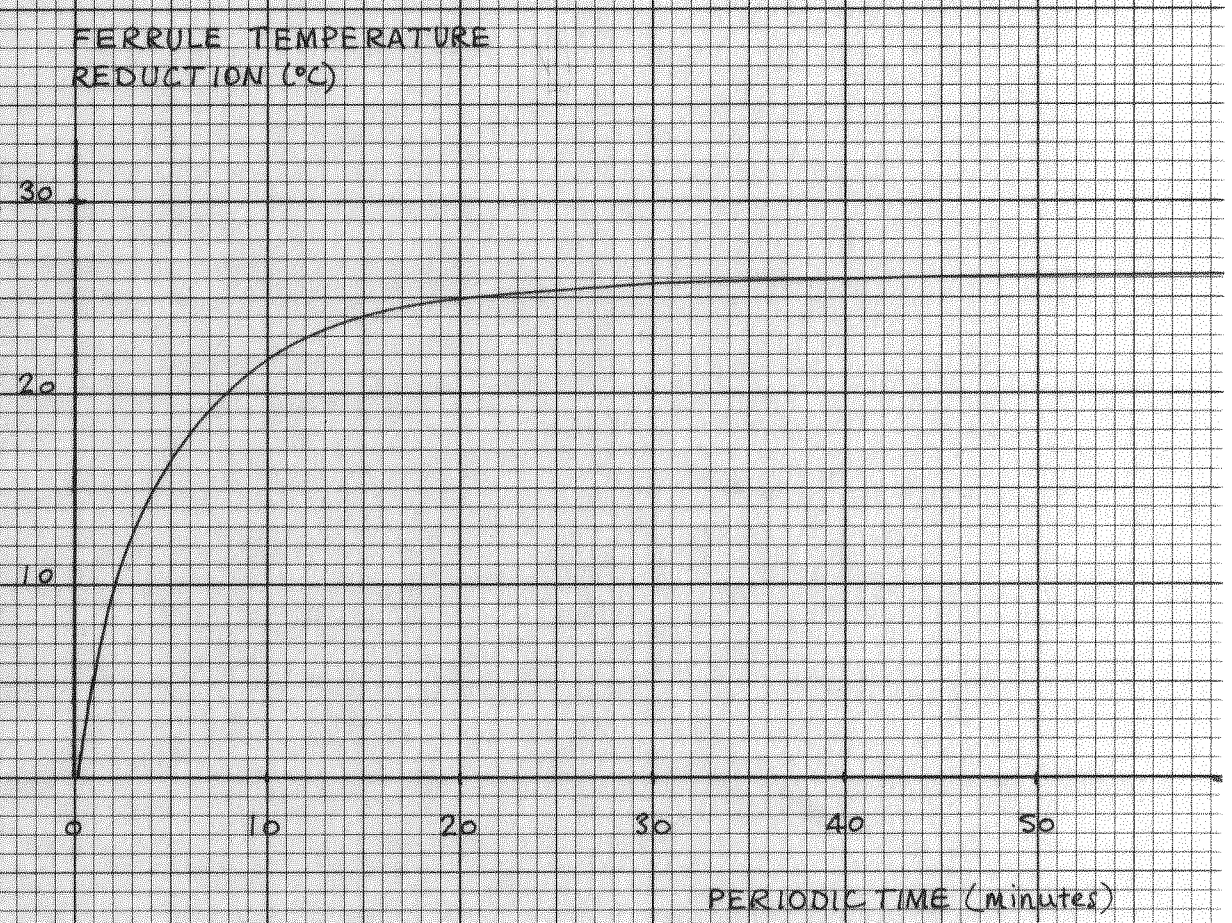

ferrule temperature alleviation increases with increasing flow-rate and/or cycle time, it is apparent that beyond a certain limit any increase in alleviation becomes progressively more expensive. Optimum flow-rate and cycle time for this 3 in^2, 400 kV cable and through joint are 20 cm^3/s (16 gal/h) and 20/30 minutes respectively.

Effect of Nusselt number variation

The value for Nusselt number assumed in the investigation so far is that obtained for laminar flow in a smooth tube. The duct of an EHV cable contains a metal helix, and it has been assumed that the boundary layer thickness is such that the effect can be ignored. However, it has been suggested[29] that the Nusselt number of the flow is lower than predicted because the oil contained between the interstices of the oil duct helix is stagnant and the major part of the heat transfer, thus, occurs across the surface of the helix itself. On the other hand, some investigators[30] have suggested that the effect of the helix would be rather to throw the oil flow and thus effectively increase the heat transfer at the oil surface.

Fig. 26 shows the effect on ferrule temperature of varying the Nusselt number of a 5 cm^3/s flow between limits of 2.42, corresponding to a heat transfer conductor per cm length of the 1.65 cm duct of .01 $W/^oC$, and 12.1 (.05 $W/^oC$ per cm length). The oil temperature profiles are omitted, and it should be noted that,

FIG 2.6: CONDUCTOR TEMPERATURE PROFILES - EFFECT OF NUSSELT NUMBER VARIATION

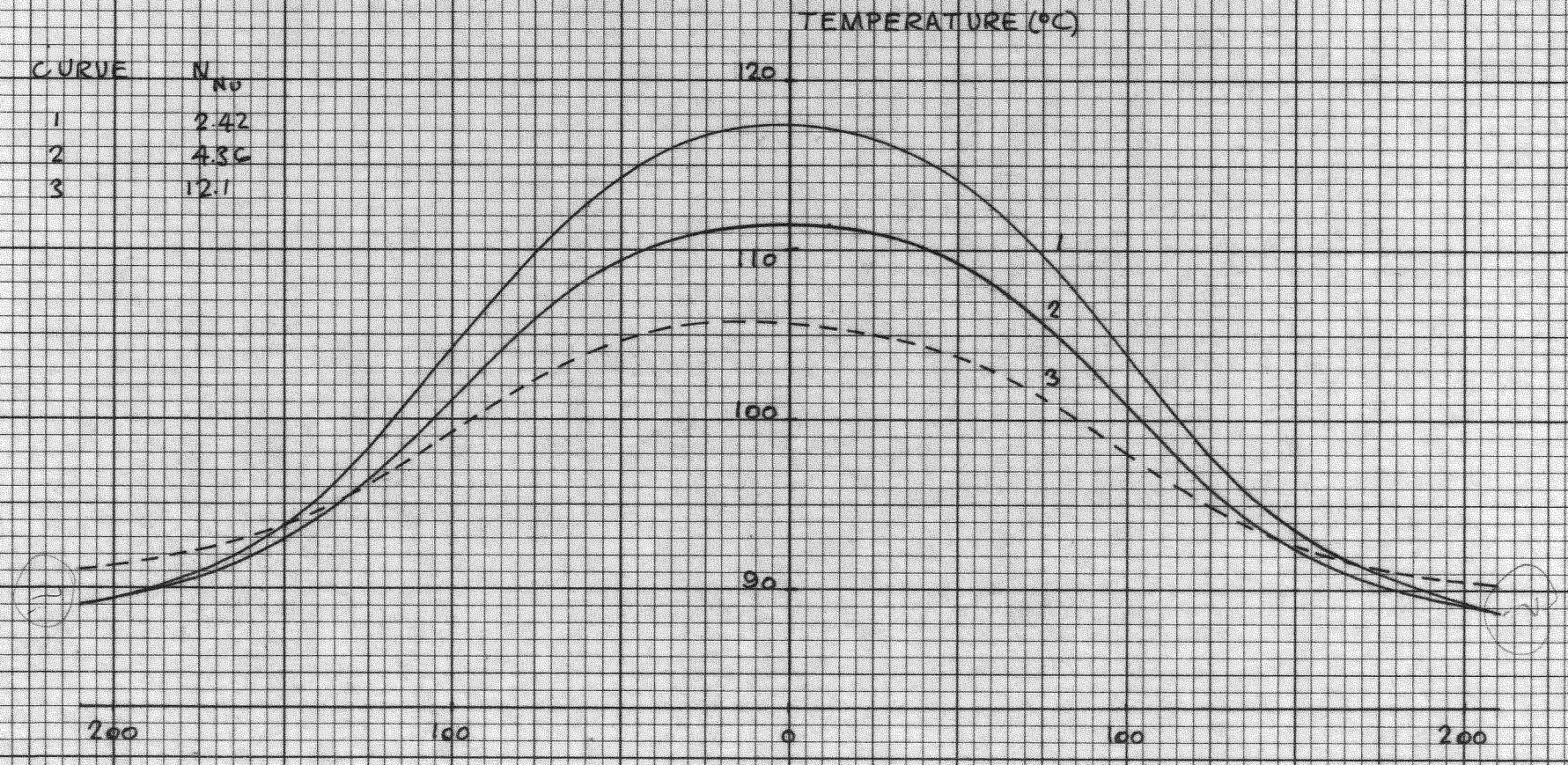

although oil temperatures did vary considerably with Nusselt number, the temperatures in the remote cable remain unchanged. For a five times increase in heat transfer coefficient, the extra reduction in ferrule temperature is of the order of $10^{o}C$. This may be explained by considering the distribution of the heat transferred from the conductor to the oil between the capacitances due to flow (ω Cp) and to the volume of the nodal region (Cp x volume). To a first approximation, we may say that the heat absorbed by the 'flow capacitance' is carried out of the region while the heat absorbed by the 'oil volume capacitance' produces the transient rise in the oil temperature. A greater part of the heat will be absorbed by the oil volume capacitance than by the flow capacitance so that, should the heat transfer be increased, the oil temperature will tend to rise. This rise in oil temperature will reduce the temperature difference across the oil heat transfer conductance and also the heat transferred across it which means that the conductor temperature reduction will be less than would otherwise be expected. Thus, although the value of the heat transfer coefficient, and hence the Nusselt number, is important, the determining factor in heat removal and ferrule temperature reduction is the oil flow-rate.

Although the effect of oil flow is to reduce the ferrule temperature by amounts which make the effort involved worthwhile, it is apparent that further reduction would be advantageous. One method which has been suggested is artificial increase of the oil

heat transfer coefficient at the ferrule. This can be achieved by use of a 'turbulence promoter' which may possibly consist of a metal helix or gauze inserted into the duct.

The curves of Figs. 27-30 illustrate the effects of such promoters covering:

1. the whole joint region, extending for a distance 1.5 m each side of the joint centre (joint turbulence);
2. the ferrule region, extending over the centre 30 cm of the joint (ferrule turbulence).

The comparative effects of a 5 cm^3/s flow with an induced joint turbulence with a Reynolds number of 2000 are illustrated in Fig. 27. It can be seen that the temperature profile over most of the joint length is lower with induced turbulence and the ferrule temperature alleviation is increased from 24.7°C to 30.7°C, a gain of 6°C. Fig. 28 shows the profiles obtained with a 60 cm^3/s flow, with and without an induced joint Reynolds number of 10^4. The effect of the induced turbulence is very dramatic; the temperature profile being almost flat and the ferrule temperature alleviation almost doubled.

The Reynolds number of artificially induced turbulence cannot be predicted with any accuracy so that it is necessary to use a flow-rate which will remove the heat transferred from the conductor. The importance of this consideration is illustrated by the curves plotted in Fig. 29. The profiles obtained for a 5 cm^3/s

FIG 27: CONDUCTOR TEMPERATURE PROFILES - EFFECT OF INDUCED TURBULENCE

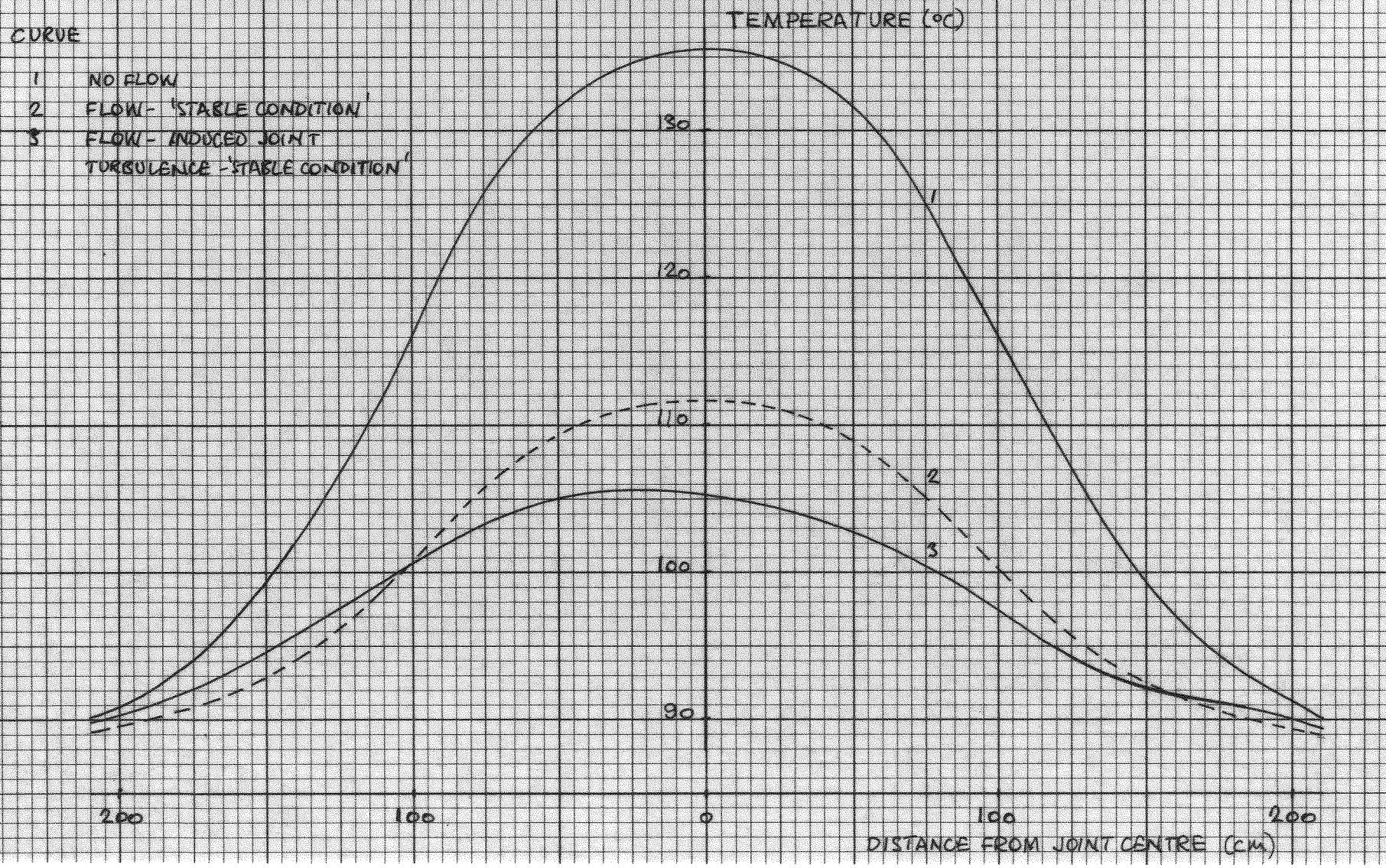

FIG 28: CONDUCTOR TEMPERATURE PROFILES - EFFECT OF INDUCED TURBULENCE

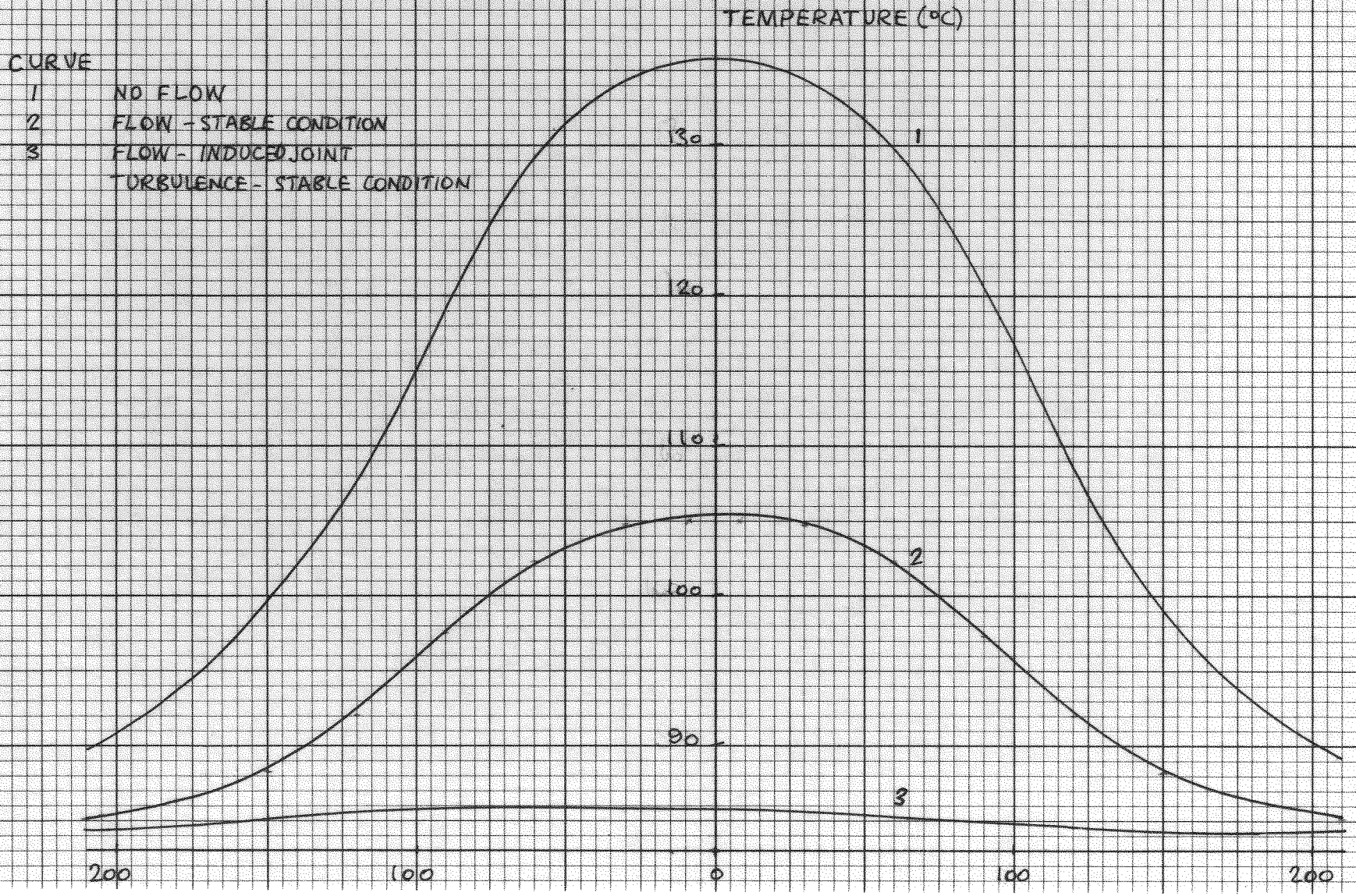

FIG 29 : CONDUCTOR TEMPERATURE PROFILES - EFFECT OF INDUCED TURBULENCE

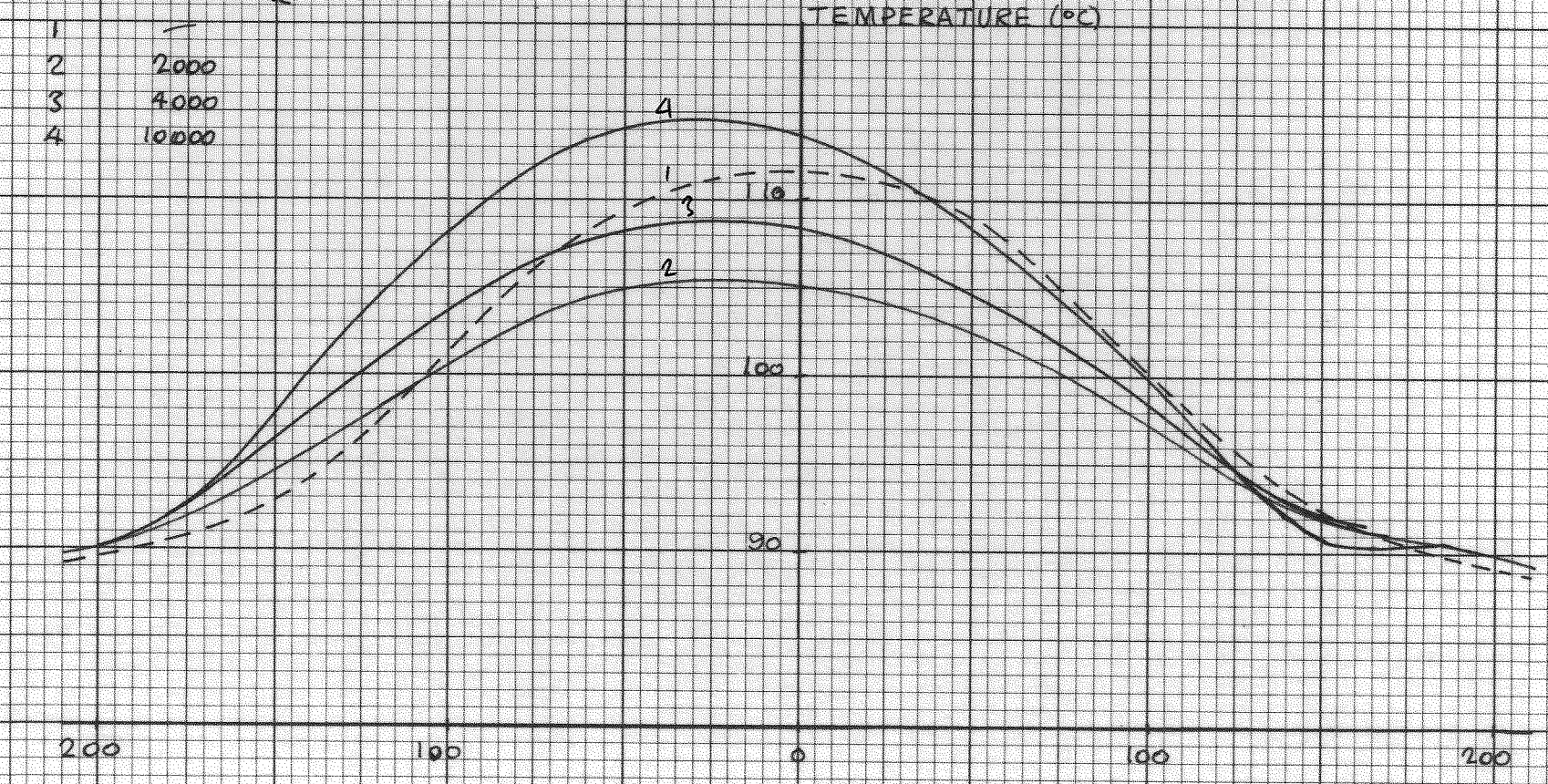

flow with induced joint Reynolds numbers of 2000, 4000 and 10000 are compared with the profile obtained with no induced turbulence. Ferrule temperature alleviation decreases with increasing Reynolds number and the alleviation for the flow with the highest Reynolds number is less than that obtained with no turbulence. This reinforces the deduction made above, from the results shown in Fig. 26, that the determining factor in heat removal is the oil flow-rate.

The improvement in ferrule temperature alleviation obtained by inducing a turbulence in the ferrule is illustrated in Fig. 30. The conductor temperature profiles for 5 cm /s and 60 cm /s flow rates with and without induced ferrule turbulence, are compared with the pre-oscillation profile. The effect at the ferrule is very marked, and a comparison of ferrule temperature alleviation becomes less meaningful. The efficiency of the method can best be illustrated by a comparison of temperatures at the points in the conductor associated with the peaks in the temperature profile. These peaks occur for both flows at positions 60 cm upstream and downstream of the joint centre; for the 5 cm^3/s flow, turbulence in the ferrule produces a further reduction in temperature of about 4^oC and, for the 60 cm^3/s flow, a reduction of about 7^oC.

It is apparent that, for the faster flows, induced turbulence over the whole joint is a more efficient method of obtaining further improvement in ferrule alone. However, the improvements obtained with ferrule turbulence are worthwhile, and the promoter

FIG 30: CONDUCTOR TEMPERATURE PROFILES: EFFECT OF INDUCED TURBULENCE

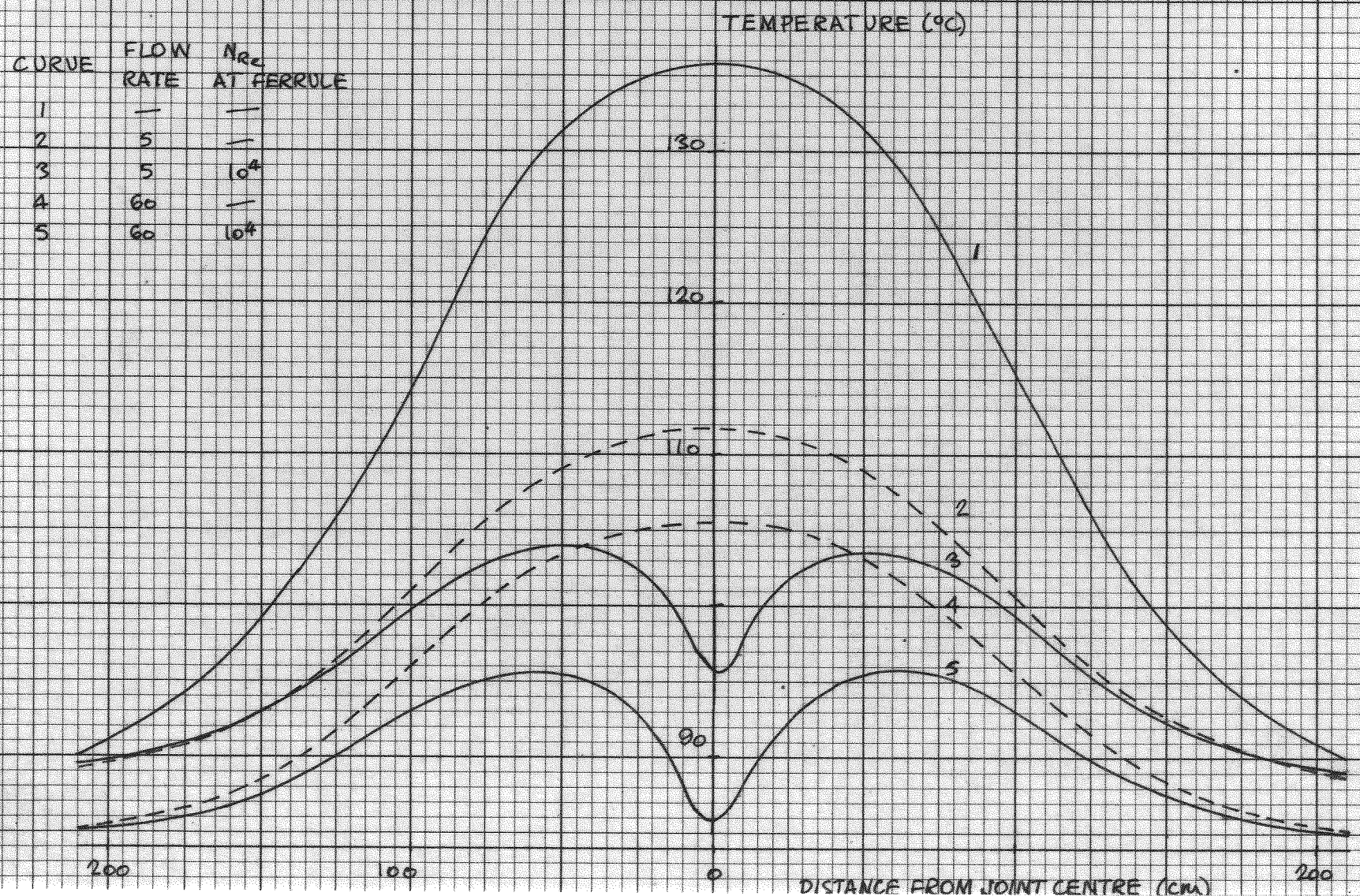

to produce ferrule turbulence will be less expensive and more easily installed. There is also a pressure loss associated with the use of a promoter and this will be less the shorter the length involved; this is an important consideration because of the limited pressures available, in present day designs, for maintaining oil movement. On balance then, it would appear that induced turbulence in the ferrule is the better method.

Some investigators, as discussed in Chapter 3, dispute the idea of a constant value for Nusselt number, when considering problems with temperature distributions such as exist in buried cables; rather one should consider the Nusselt number as a function of distance from the 'thermal entrance'. A thermal entrance is always associated with a change in temperature gradient. If we consider the temperature distribution for the 400 kV cable and joint shown in Fig. 18, it is apparent that one such change in temperature gradient occurs at the joint ferrule. The position of the other is somewhat arbitrary and is assumed, for the purposes of this investigation, to be 180 cm from the joint centre, which corresponds with a node in the model. The relationship used to evaluate the Nusselt number is that quoted in Chapter 3 and derived by Sieder and Tate.

$$N_{Nu} = 1.86 \left(\frac{\mu_b}{\mu_\omega} \right)^{.14} \left(N_{Re} \, N_{Pr} \, \frac{D}{L} \right)^{1/3}$$

The Nusselt numbers are calculated in the program and the factor $\left(\frac{\mu_b}{\mu_\omega} \right)^{.14}$ is assumed to be unity; this is an allowable

approximation since, even if the ratio should vary between 0.5 and 2.0, the maximum error recorded in the value of the heat transfer coefficient is less than 10%. For a 5 cm^3/s flow, the heat transfer conductance profile through the cable and joint is illustrated in Fig. 31. There are always two peaks in the profile, the upstream one associated with the thermal entrance at the approach to the joint and the other at the ferrule. At nodes outside the region 180 cm each side of the joint centre, the heat transfer conductance per cm length is taken to be 0.018 $W/^oC$, corresponding with a Nusselt number of 4.36.

Curve 3 in Fig. 32 shows the effect of the $(\frac{D}{L})$ term on the stable-condition conductor temperature profile. The profile is reduced over the region of higher Nusselt numbers, and the ferrule temperature alleviation is increased by 5^oC. The effect of the sharp change in heat transfer coefficient at the ferrule can be seen. The profile obtained with a constant Nusselt number (= 4.36) and induced turbulence at the ferrule is shown as curve 4 for comparison. Apart from the region 60 cm either side of the joint centre, the two profiles compare quite well, so that profiles obtained using constant Nusselt number and ferrule turbulence can be used to give a good approximation to the profile with $N_{Nu} = f(\frac{D}{L})$.

The curves in Figs. 33 and 34 compare conductor temperature profiles for two flows (5 cm^3/s and 20 cm^3/s) with $N_{Nu} = f(\frac{D}{L})$ with and without induced turbulence ($N_{Re} = 10^4$) at the ferrule.

FIG 31 : HEAT TRANSFER CONDUCTANCE PROFILE FOR 1.65 cm DUCT AND 5 cm^3/s FLOW

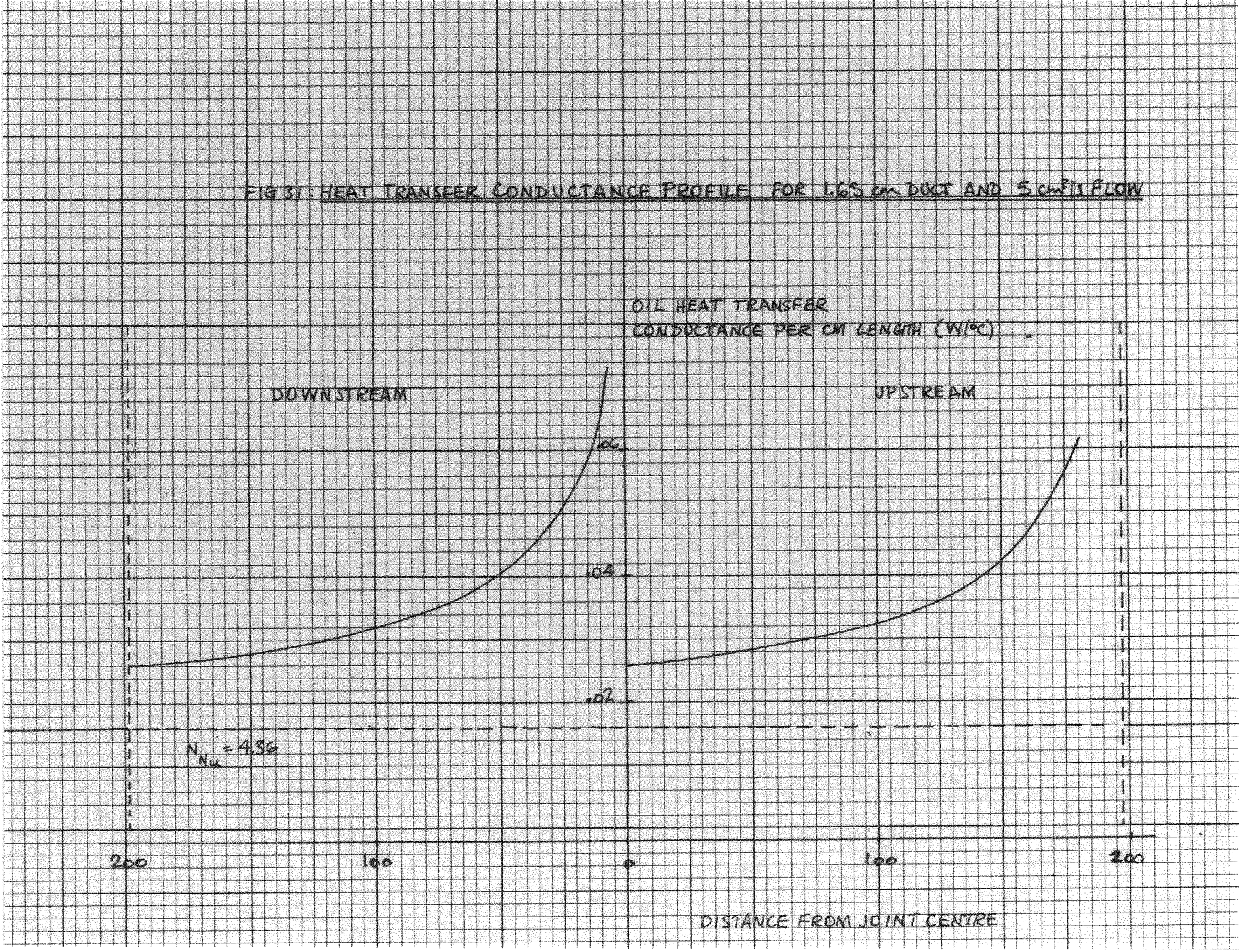

FIG 32: CONDUCTOR TEMPERATURE PROFILES - EFFECT OF NUSSELT NUMBER VARIATION

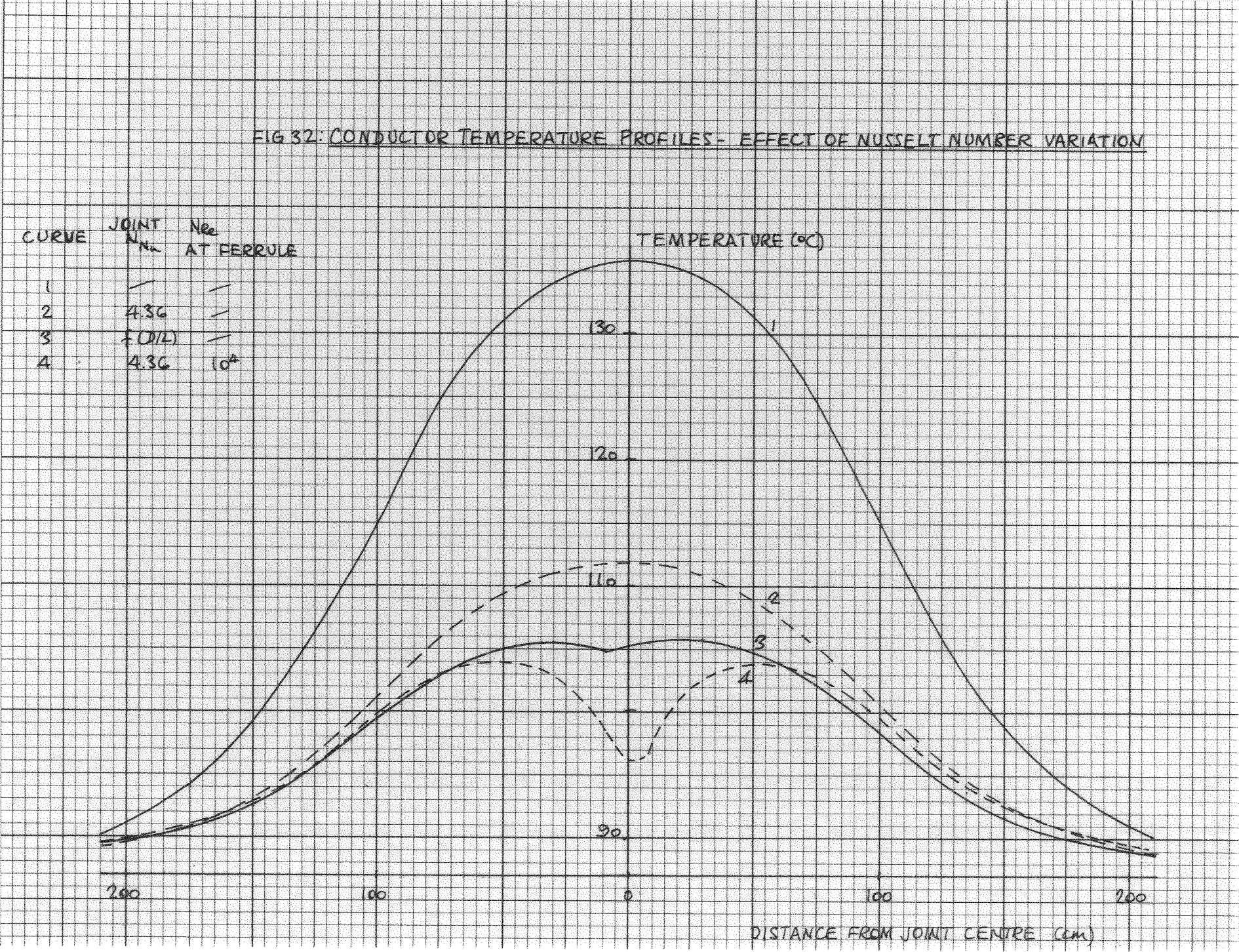

FIG 33: CONDUCTOR TEMPERATURE PROFILES - EFFECT OF NUSSELT NUMBER VARIATION

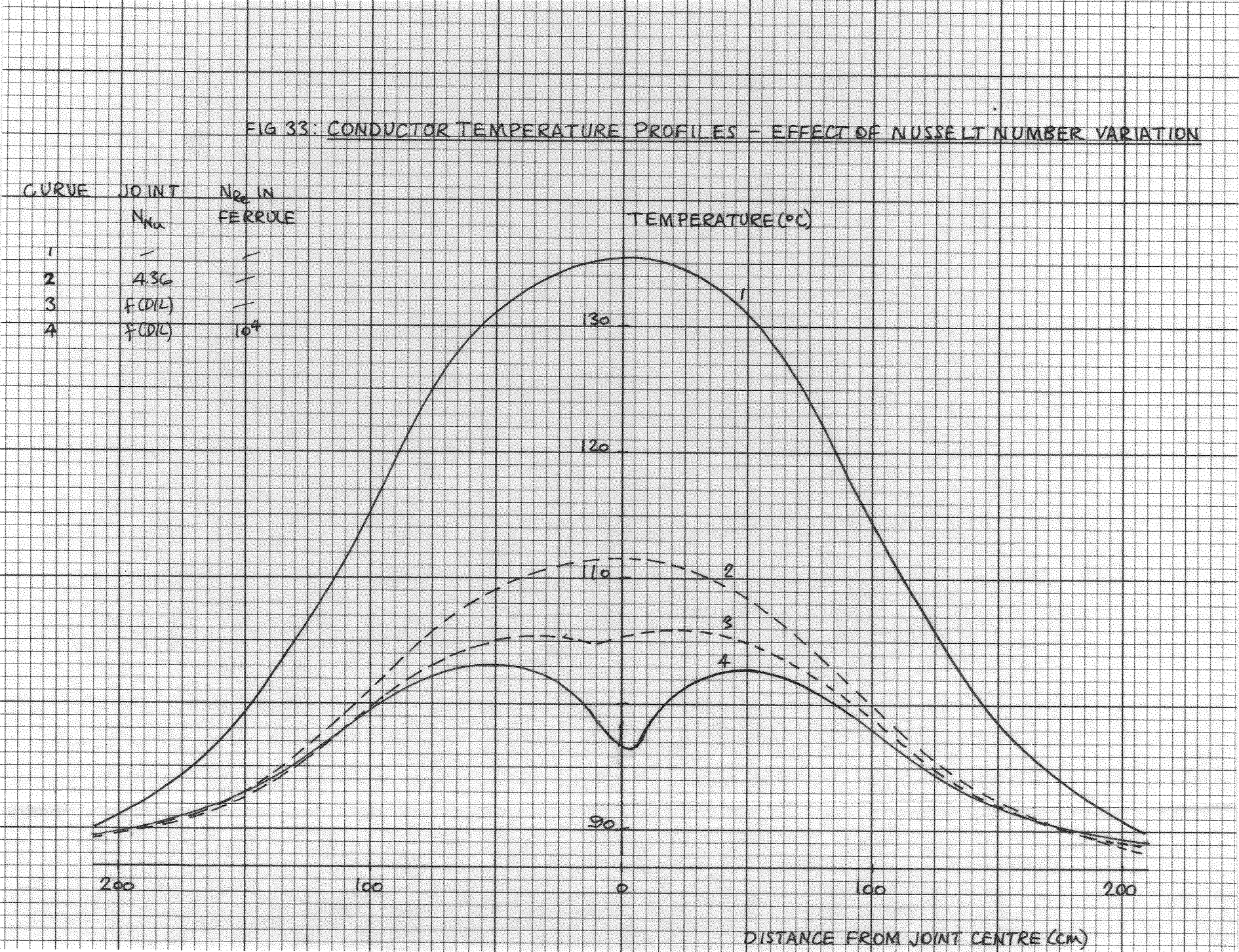

FIG 34: CONDUCTOR TEMPERATURE PROFILE - EFFECT OF NUSSELT NUMBER VARIATION

CURVE	JOINT N_{Nu}	N_{Re} IN FERRULE
1	—	—
2	4.36	—
3	f(D/L)	—
4	f(D/L)	10^4

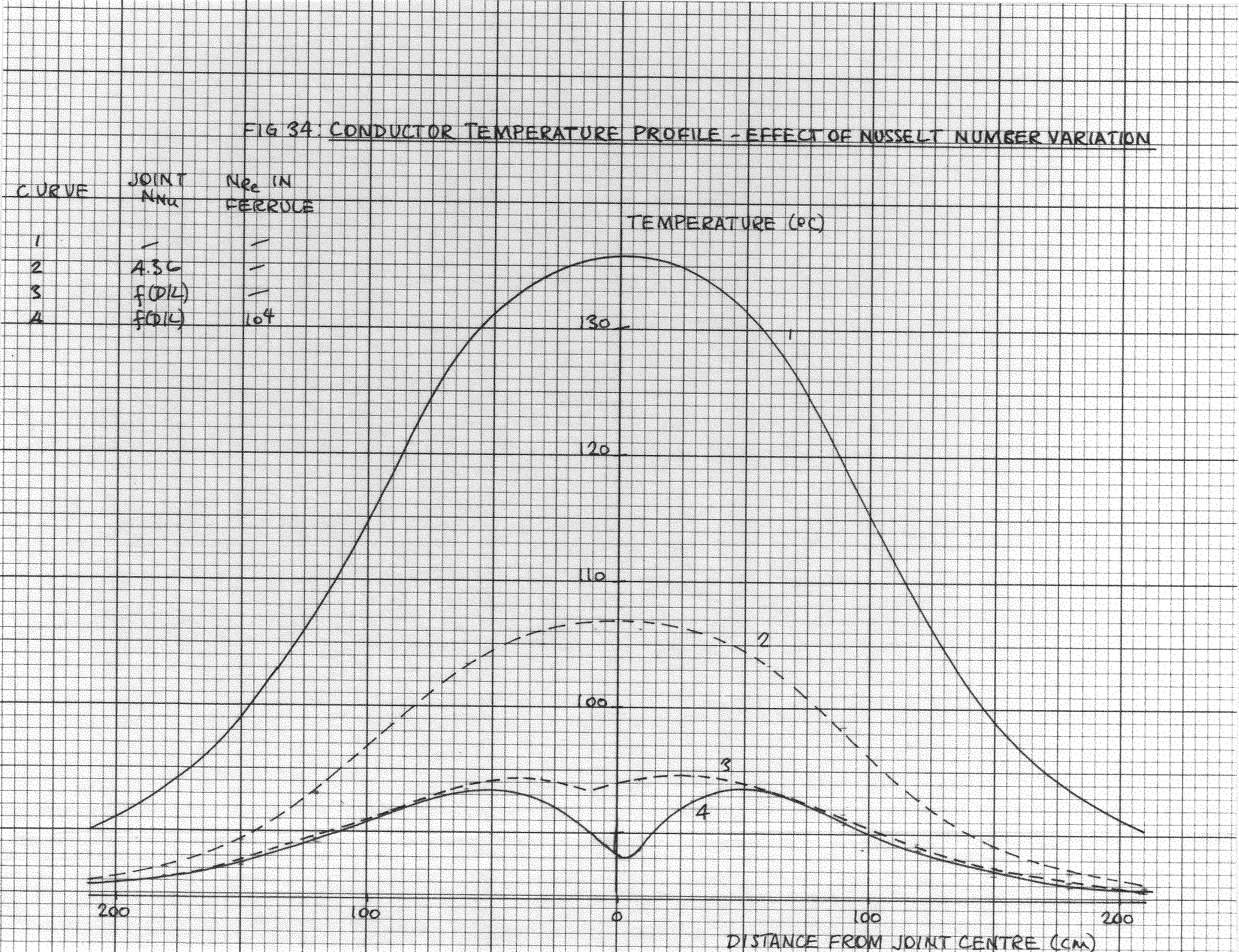

Although the ferrule temperature is depressed, the reduction overall is only slight, so that, if Nusselt number is indeed dependent on a thermal entrance effect, there is little advantage to be gained from inducing turbulence in the ferrule.

It can be considered that the result obtained with $N_{Nu} = f\left(\frac{D}{L}\right)$ are the optimum and indicate what could possibly be achieved using oil oscillation. However, the results obtained assuming constant Nusselt number (= 4.36) are worthwhile, if pessimistic, and probably provide a more satisfactory basis for a design.

CHAPTER 5

DEVELOPMENT OF THE GENERALIZED PROGRAM

Chapter 4 describes the performance of a 400 kV, 3 in^2 joint, forced cooled at the sheath; the benefits of oil oscillation in the conductor duct are obvious. This chapter describes the development of a generalized program from the program used to obtain the results shown in Chapter 4. The essential difference between the latter program and the generalized one is that, in the first, the parameters used, including losses and thermal resistances and capacitances, are measured from the analog due to Perkins and, in the generalized program, all values used are calculated internally from the system parameters which are read in as data.

The heat input is assumed concentrated at the conductor nodes and consists of copper and dielectric losses. Since the sheath is in direct contact with the cooling water, any sheath loss may be ignored in the model used. Copper losses are calculated using the equation

$$W_{Cu} = I^2 R_\ell$$

where R_ℓ is the effective electrical resistance of the conductor in the nodal region.

Dielectric losses are obtained from the equation

$$W_d = 2\pi f C_\ell V^2 \tan \delta$$

where V is the system voltage to earth, C_ℓ the electrical capacitance of the cable in the nodal region and f the system frequency. The thermal resistances in the conductor and insulation are obtained using Equations (12) and (13) of Chapter 3.

$$R_{cond} = \frac{g_c x}{A} \tag{12}$$

$$R_{ins} = \frac{g_i}{2\pi\ell} \ln \frac{r_i}{r_c} \tag{13}$$

where g_c and g_i are the conductor and insulation thermal resistivities, A the conductor cross-section, x the distance between adjacent nodes, ℓ the nodal region length and r_c and r_i the conductor and insulation outer radii. The heat transfer resistance between the conductor and the duct oil is obtained from the equation

$$R_h = \frac{1}{h\, A_o}$$

where h is the heat transfer coefficient defined by the Nusselt number of the flow and A_o is the 'wetted area' of the duct within the nodal region.

The parameters so far discussed are calculated without difficulty; the main problem is the determination of the equavalent thermal capacitance to be lumped at the conductor. The values of thermal capacitance used in Chapter 4 have no actual physical significance but serve merely to define the short-time transient behaviour of the conductor. The difficulty, in fact is

to allow for the effect on the conductor of the distributed thermal capacitance of the cable insulation. Van Wormer[31] has suggested that the insulation thermal capacitance may be assumed to be lumped partly at the conductor and partly at the sheath in such proportions that the total quantity of heat stored in the dielectric is not altered. It can be shown that the fraction, p, of the insulation thermal capacitance concentrated at the conductor is defined by the equation

$$p = \frac{1}{2 \ln \frac{r_i}{r_c}} - \frac{1}{\left(\frac{r_i}{r_c}\right)^2 - 1} \qquad (18)$$

where r_i and r_c are the insulation and conductor outer radii. It should be noted that this method for distributing thermal capacitance makes no allowance for the distributed dielectric loss. The dielectric loss is divided equally between conductor and sheath, and, since the system is sheath-cooled, the effect of the loss injected, and the thermal capacitance lumped, at the sheath may be neglected.

Applying Equation (18) at each node in the network model of the 3 in^2, 400 kV joint and cable studied in Chapter 4 and substituting the values of the conductor and insulation radii at each node, values for the factor 'p' ranging from 0.3 in the joint to 0.4 in the remote cable are obtained. Using these values of 'p' to calculate the fraction of the insulation thermal capacitance to be lumped at the conductor and adding in the thermal

capacitance of the conductor, the values for equivalent thermal capacitance which result range from a maximum of 190 J/°C per cm length in the joint to 110 J/°C per cm length in the remote cable. Comparing these values of thermal capacitance with those quoted in Table 2, it is seen that the calculated ferrule thermal capacitance is 50% higher than that obtained from the analog while the value calculated for the cable approximates to the mean of the measured values. Fig. 35 compares temperature rise transients at the joint ferrule and the remote cable conductor obtained by Perkins[20] with those obtained using:

1. the model derived from measurements on the analog and studied in Chapter 4;
2. the model used in the generalized program with the thermal capacitance per cm length at each node set equal to the value for the remote cable (110 J/°C per cm length).

The agreement between the three sets of results is good, so that the equivalent thermal capacitance utilized in the program is the sum of the conductor thermal capacitance plus a fraction, defined by Equation (18), of the cable insulation thermal capacitance.

The conductor temperature profiles obtained with the 'analog program' (i.e. the program used to study the model derived from the Perkins' analog) and with the generalized program are shown in Fig. 36. The agreement between the two profiles is good, and the difference between the two curves does not exceed 2°C over the

FIG 35 : TRANSIENT TEMPERATURE RISE

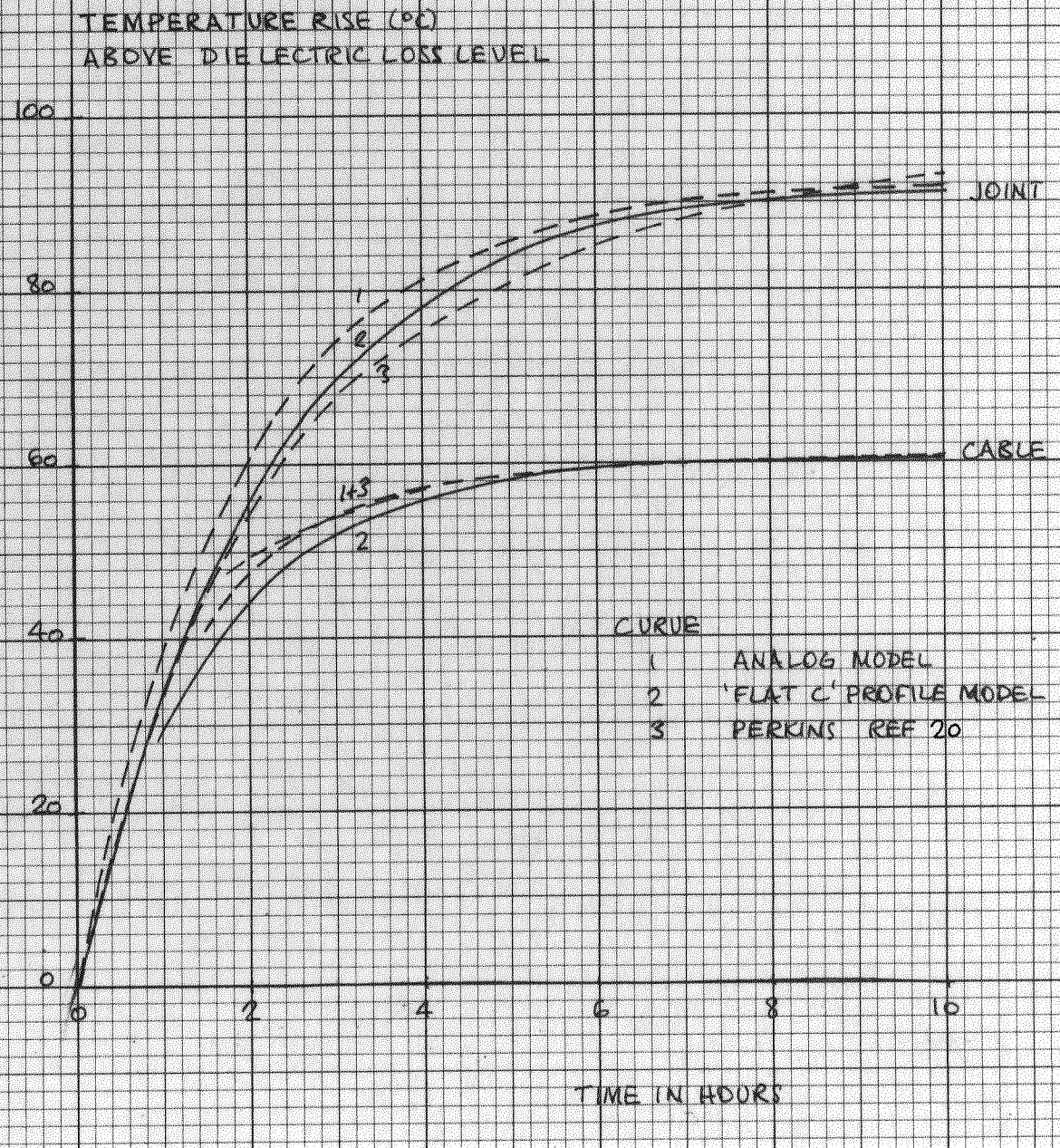

FIG 36: CONDUCTOR TEMPERATURE PROFILES

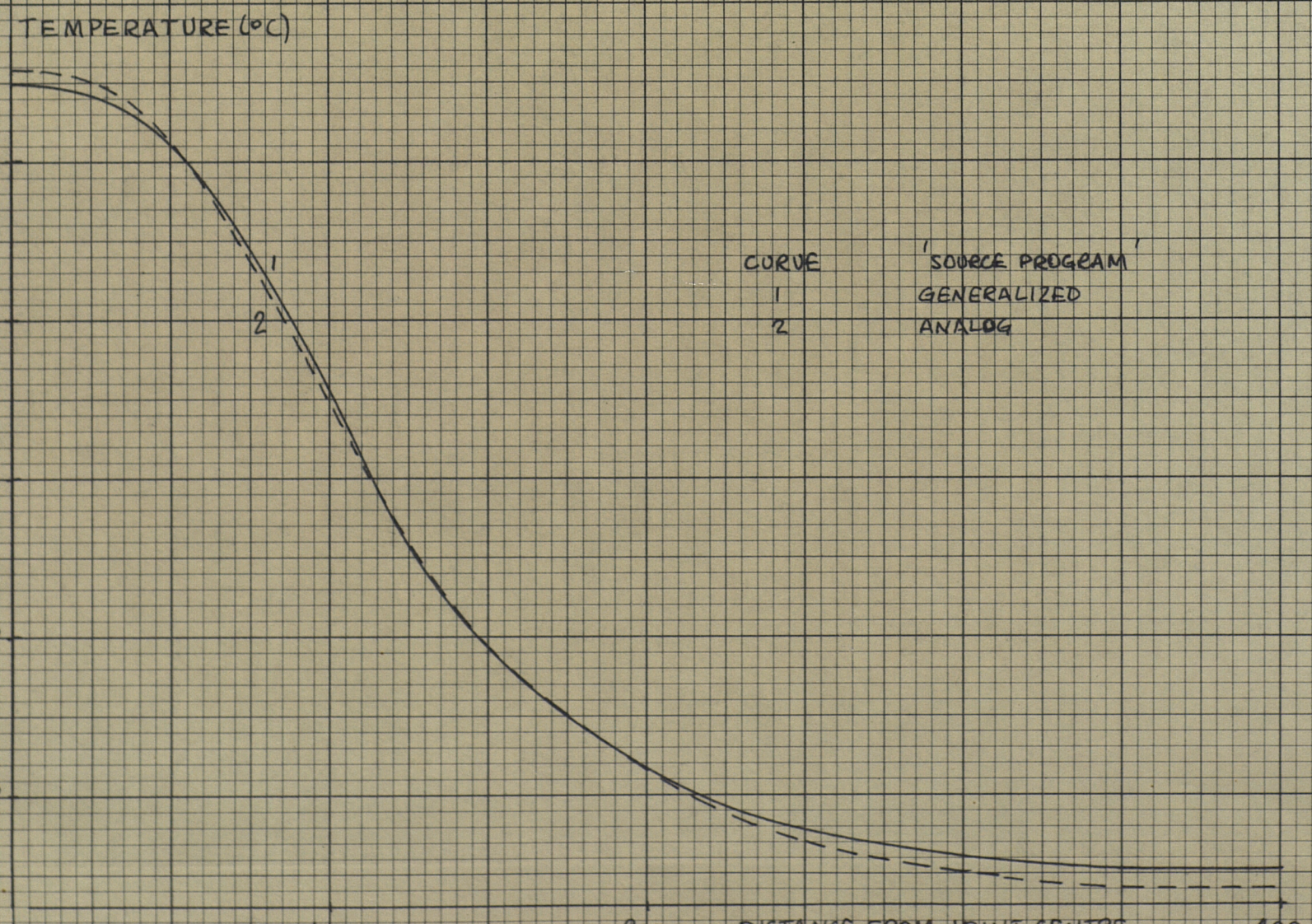

length of the model. Table 3 compares the ferrule temperature alleviation, for several flow rates with 20 minute oscillation period, obtained with the two programs. In Fig. 37, plots of reduction of ferrule temperature with time for a 5 cm^3/s, 20 minute period oscillation obtained with the two programs are compared. The rate of fall of temperature obtained using the generalized program is similar to that obtained using the 'analog program'. The results obtained with the generalized program compare favorably, in all respects, with the results obtained using the Perkins' model so that the method used to simulate capacitance in the generalized program is acceptable.

Effect of natural convection in the joint oil between paper and shell

The model used in the generalized program to obtain the results shown in Figs. 36 and 37 and Table 3 assumes that there is natural convection in the joint oil, the correction for which is proportional to a Rayleigh number based on the oil thickness and the existence of an $8^{o}C$ temperature difference across the oil at 2200 MVA loading. However, as discussed in Chapter 3, normal design practice is to treat the joint as though the dielectric were composed entirely of paper, and Fig. 38 compares profiles obtained for the joint and 3 in^2 cable described in Tables 4 and 5, assuming:

1. convection in the joint oil with an $8^{o}C$ temperature difference across the oil;

FIG 37: FERRULE TEMPERATURE VARIATION WITH TIME

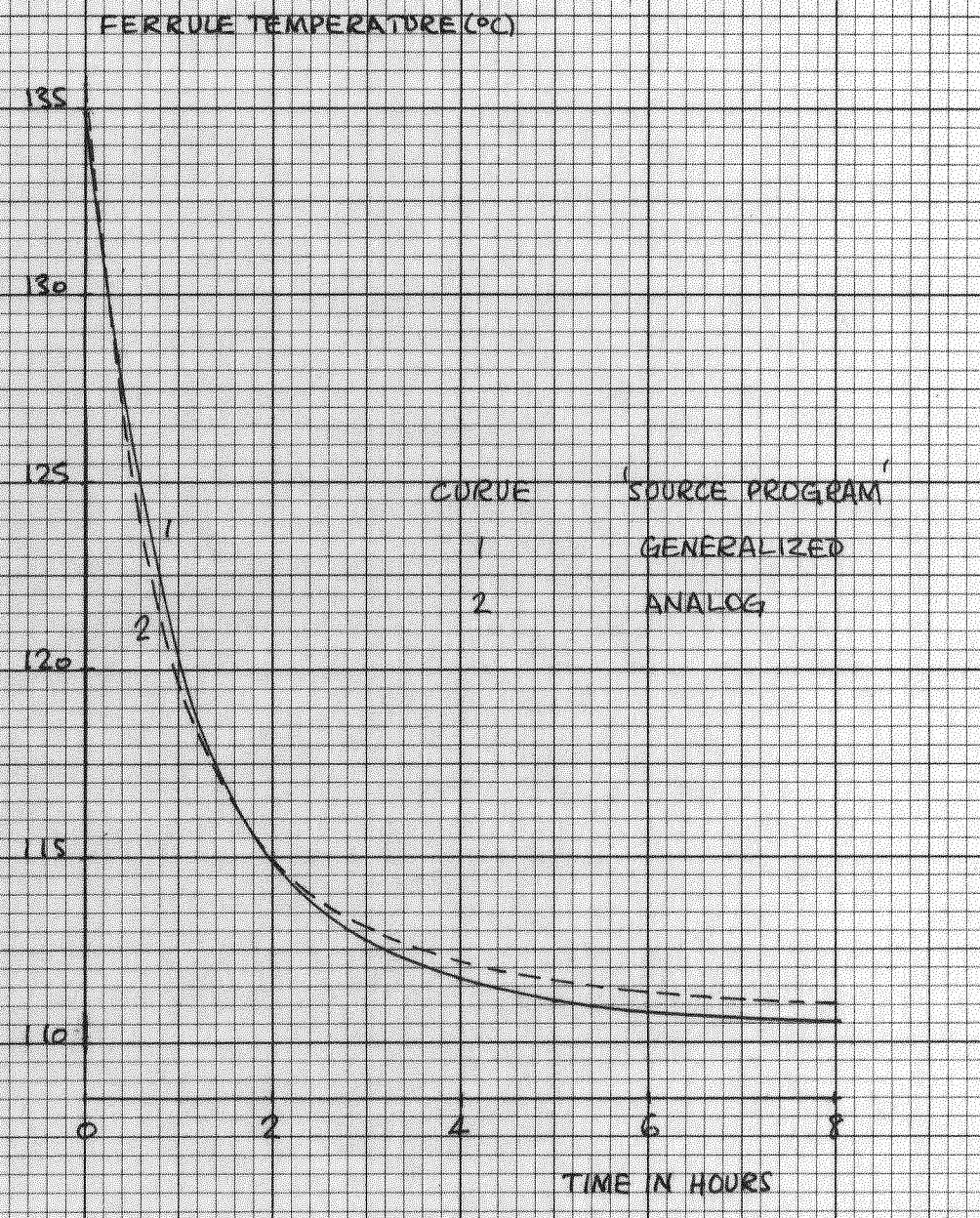

TABLE 3

Ferrule Temperature Alleviation

Flow Rate (cm^3/s)	Temperature Alleviation (^oC)	
	Analog Program	Generalized Program
2.5	19.6	19.3
5.0	24.7	24.3
10.0	27.7	27.3
20.0	29.5	29.1

TABLE 4

Dimensions of 400 kV Straight Joints

Outside diameter of joint dielectric	(cm)	20.24
Outside diameter of joint spinning	(cm)	20.80
Outside diameter of joint box	(cm)	30.4 - 40.5
Maximum height of joint box and filler	(cm)	57.00

TABLE 5

Dimensions of 400 kV Oil-filled Cables

Cable conductor cross-section, in^2		2.0	3.0
Oil duct diameter	(cm)	1.2	1.2
Conductor outside diameter	(cm)	4.72	5.79
Dielectric outside diameter	(cm)	9.98	10.62
Sheath outside diameter	(cm)	10.69	11.35
Servings outside diameter	(cm)	11.58	12.24
Conductor a.c. resistance at 85°C	μΩ/cm/core	0.184	0.128

2. a joint dielectric consisting entirely of paper.

The difference in ferrule temperature is 15°C and can be explained by the fact that the insulation thermal resistance at the ferrule is 92°C/W per cm length assuming joint oil convection and 100°C/W per cm length assuming a dielectric composed entirely of paper. Thus it can be seen that for the shell cooled joint this assumption introduces an error which cannot be neglected.

The convention of considering the joint dielectric as being composed entirely of paper has been developed for, and used with, normally loaded, direct-buried cables. The copper losses, for the 400 kV, 3 in^2 cable considered, with a normal winter load of 1100 MVA, are 0.32 W per cm length per phase (dielectric losses are 0.15 W per cm length per phase) and the thermal resistance between the joint conductor and the ground surface is approximately 200°C/W per cm length. It can thus be seen that, in the direct-buried condition, convection effects in the joint oil can be safely ignored. The temperature of the joint ferrule will be 90-95°C above ambient, and ignoring convection will produce an increase of 5% in the thermal resistance, causing the calculated temperature to exceed the actual by a few degrees, thus giving a pessimistic answer. However, the difficulties involved in neglecting convection effects in the joint oil for the sheath-cooled system with 2200 MVA load, where copper losses are 1.27 W per cm length per phase (dielectric losses remaining roughly the same) and the thermal resistance between conductor and shell is 100°C/W per cm

length, are apparent and well illustrated by the curves in Fig. 38. Bearing these arguments in mind, the model used is designed assuming that the joint dielectric is entirely paper so that the program developed and the results obtained may be useful in practical design.

Typical results for generalized program

Values for temperature alleviation have been obtained for a series of flow rates, with a 20 minute oscillation period, using the joint described in Table 4 and the cables described in Table 5. The essential differences in design between the cables and joint used here and those used by Perkins are:

1. the 1.2 cm conductor oil-duct (compared with 1.65 cm);
2. the smaller joint insulation diameter (20.4 cm compared with 22.8 cm) due to the smaller oil annulus.

Temperature alleviation for the various oil flow rates are shown in Fig. 39 for two cable sizes. The 3 in^2 cable is assumed loaded at 2200 MVA (corresponding with a conductor current of 3200 A) and the 2 in^2 at 1600 MVA (corresponding with a conductor current of 2350 A). For the 3 in^2 cable the ferrule temperature before oscillation is 152.1°C and the remote cable conductor temperature is 85°C; the corresponding temperatures for the 2 in^2 cable are 147.4°C and 84°C, the water temperature in both cases is assumed to be 20°C.

FIG 38: CONDUCTOR TEMPERATURE PROFILES

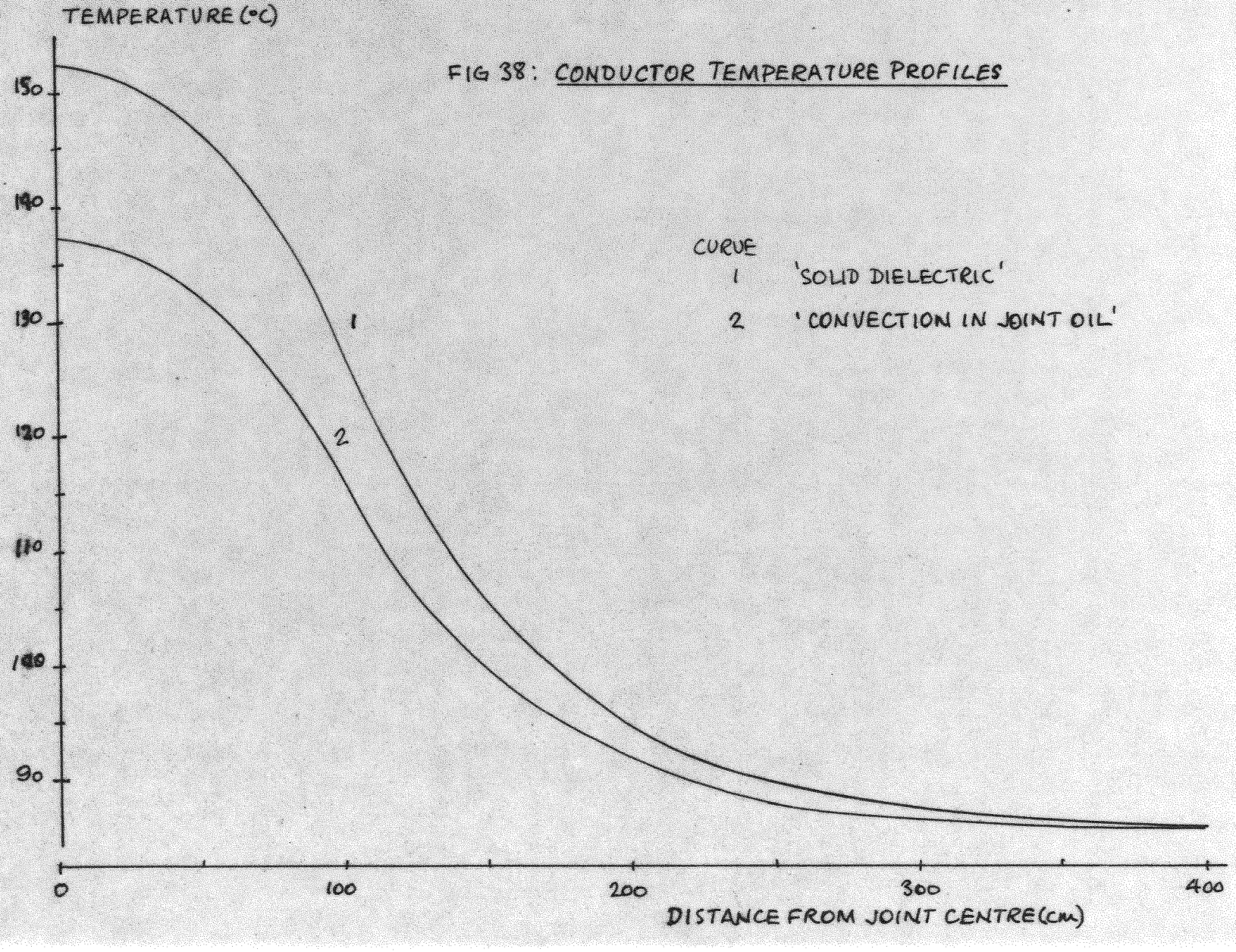

FIG 39: FERRULE TEMPERATURE REDUCTION v OIL FLOW RATE

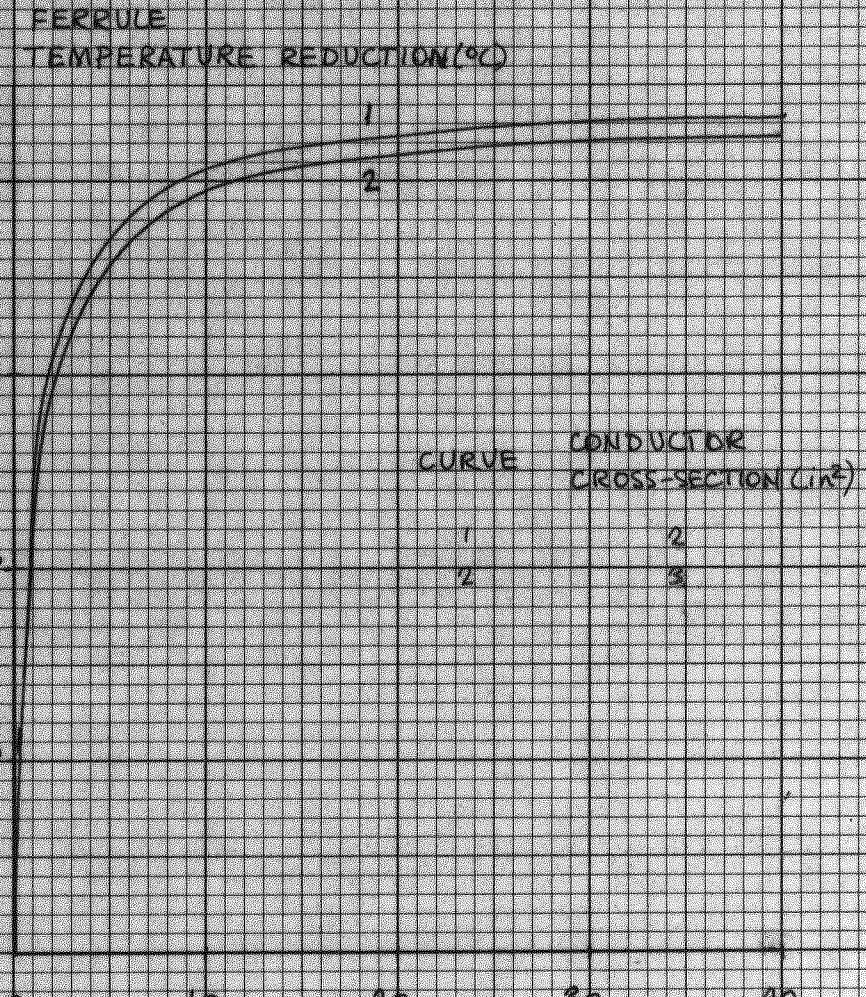

Results have been obtained for the low thermal resistance joint designed by the Pirelli-General Cable Co. Ltd.[33] In this joint, part of the paper of the joint dielectric is replaced with epoxy resin which has the advantage that it has a thermal resistivity 20% that of paper although its dielectric strength is similar to that of paper. In the design of the resin joint, the diameter of the paper section of the dielectric is equal to the cable insulation diameter and the overall diameter of the joint dielectric is bigger than the diameter of a conventional joint. The thermal resistance between conductor and shell for the resin joint is 60°C/W per cm length compared with 100°C/W per cm length for the conventional joint. The steady-state conductor temperature profile for the resin joint is shown in Fig. 40 where it is compared with the stable-condition temperature profile obtained with a 5 cm^3/s flow with 20 minute oscillation period. The beneficial effect of introducing the epoxy resin is apparent, the ferrule temperature being 102°C, and the ferrule temperature alleviation with the 5 cm^3/s flow 8°C. For the high-load, shell-cooled cable system considered, it is seen that the resin joint runs at an acceptable temperature even without cooling by oil circulation.

These results illustrate the wide range of application of the generalized program. Appendix 5 contains a listing of the generalized program and describes the assembly of the data for the program.

FIG 40 : CONDUCTOR TEMPERATURE PROFILES

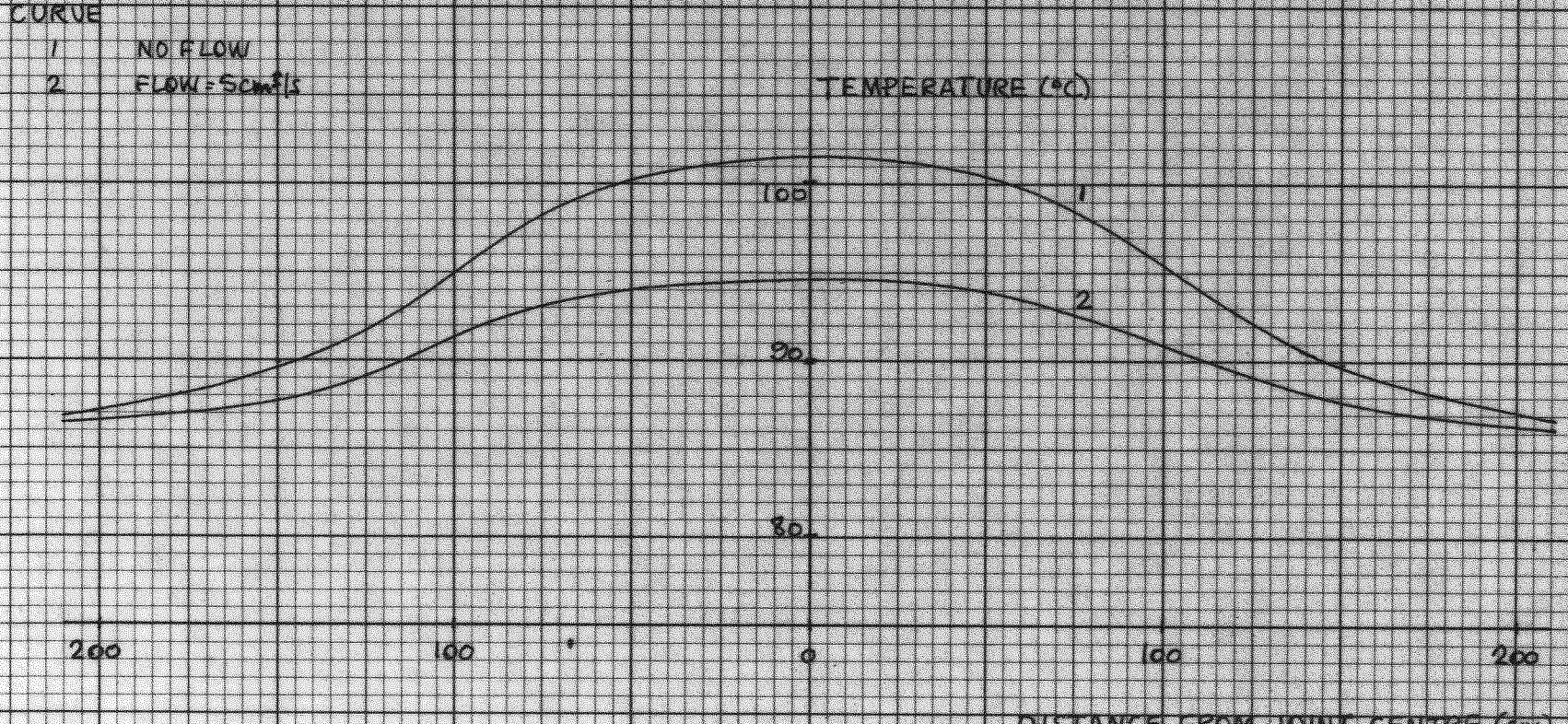

CHAPTER 6

THERMAL INSTABILITY IN A 400 kV JOINT AND CABLE

To investigate thermal instability in a cable dielectric, the radial temperature distribution in the dielectric must be known. Thus, it is clear that the program described in Chapter 5 cannot be used because of the lumped representation of the dielectric thermal resistance and capacitance. To overcome this, a mesh program, described in Appendix 9, has been developed; in this program the dielectric is considered in four sections. The joint model used is illustrated in Fig. 41 and a comparison of this with Fig. 47 will show that the representation has, for ease of calculation, been idealized. The joint investigated is described in Table 4 and the cable in Table 5.

The model used is divided into 20 nodal sections along the length of the cable and contains a half joint and several metres of cable. The smallest subdivision is 16 cm corresponding to the half-ferrule, and the subdivisions become progressively longer into the cable, the largest being 10 m at the section remotest from the ferrule. To investigate the integrally cooled cable, a mesh containing 6 nodes radially is used; the six nodes are situated - one in the conductor, four in the dielectric and the sixth in the sheath; this last is held constant at 20°C.

The main problem which arises in the treatment of instability is obtaining a functional relationship between dielectric loss

angle and temperature. Many investigators use a piece-wise-linear approximation, which is acceptable for the temperature range encountered in the study of temperature distribution in the steady state or transient temperature rises after load changes. Because of the steeply rising nature of the curve at the temperatures at which instability could occur, it was felt that this method would not prove useful. The relationship used is a function of the form shown below, which was obtained from a cable manufacturer:

$$\tan \delta = f(T, T^2, T^3, T^4, T^5)$$

where T is the dielectric temperature and lies in the range $60^{\circ}C < T < 170^{\circ}C$.

In the program, the value of tan δ for temperatures below $60^{\circ}C$ is set equal to the value at $60^{\circ}C$, and for temperatures above $170^{\circ}C$ the expression is assumed to hold true, since instability sets in at temperatures only a little above $170^{\circ}C$. Because the value of tan δ at $85^{\circ}C$ (= 0.0018) obtained from the expression is lower than the values assumed so far in the investigation, the function, when used in the program, is normalized against its value at $85^{\circ}C$. Tan δ is then obtained by multiplying the normalized value of the function by the power factor assumed for the dielectric; that is 0.003 in the cable and 0.008 in the joint. This treatment depends on the validity of assuming that the impurities which are producing the dielectric loss are in such small concentrations that they will behave in the same manner, independent of their concentration.

The fault level for which the 400 kV transmission system is designed is 50 kA and this is the value of fault current used in these calculations. The definition of failure is more problematical; although no difficulty in this direction is encountered with the physical system, in the digital model some arbitrary limit must be set. Failure, due to instability, is said to occur when the temperature of any point in the joint or cable exceeds 1000°C. This is an entirely artificial barrier and will be recognised as such by the temperature levels measured in the system during the faults applied.

Two distinct points of failure can be recognised; these are marked in Fig. 41 as failure point I, located in the dielectric adjacent to the conductor at the node in the cable closest to the joint, and failure point II, located in the dielectric at the joint ferrule. Fig. 42 shows the variation of temperature with time, at failure point I, for several fault times, while Fig. 43 shows the variation of temperature with time at failure point II for the same fault times. The rate of change of temperature is much greater at point I than at point II; this is due to the higher dielectric losses at point I coupled with its much lower thermal resistance to ambient. Table 7 shows the losses in mW/cm^3 for the cable and joint in the steady state; rows 1-14 represent the cable, 15-20 the joint; row 1 represents the conductor and rows 2-5 the dielectric. Failure point I is at node (2,14) and failure point II at node (2,20).

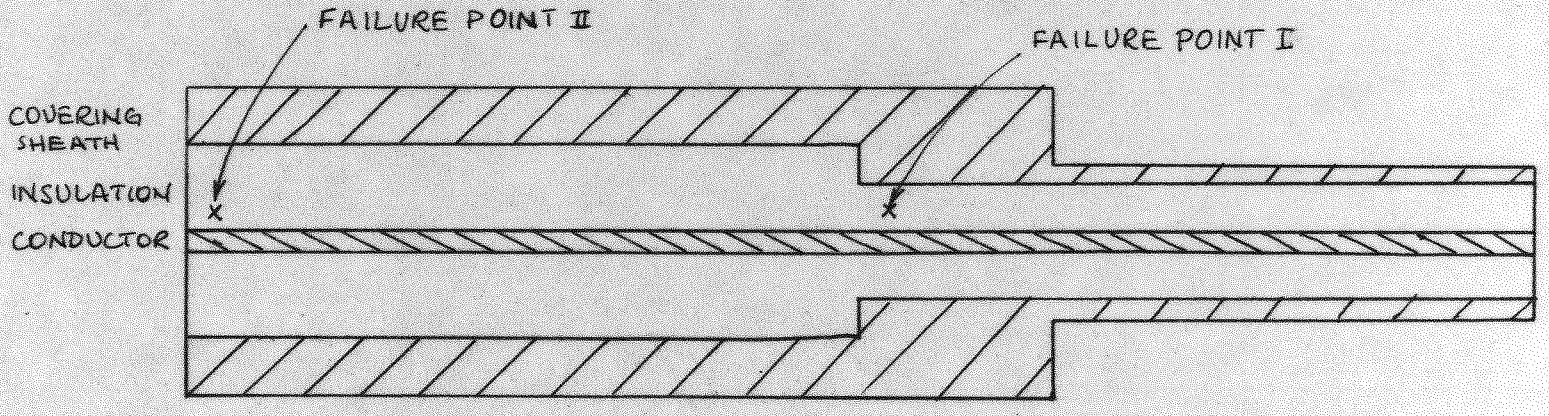

FIG 41: IDEALIZED JOINT

FIG 42: TRANSIENT TEMPERATURE RISE - FAILURE POSITION I

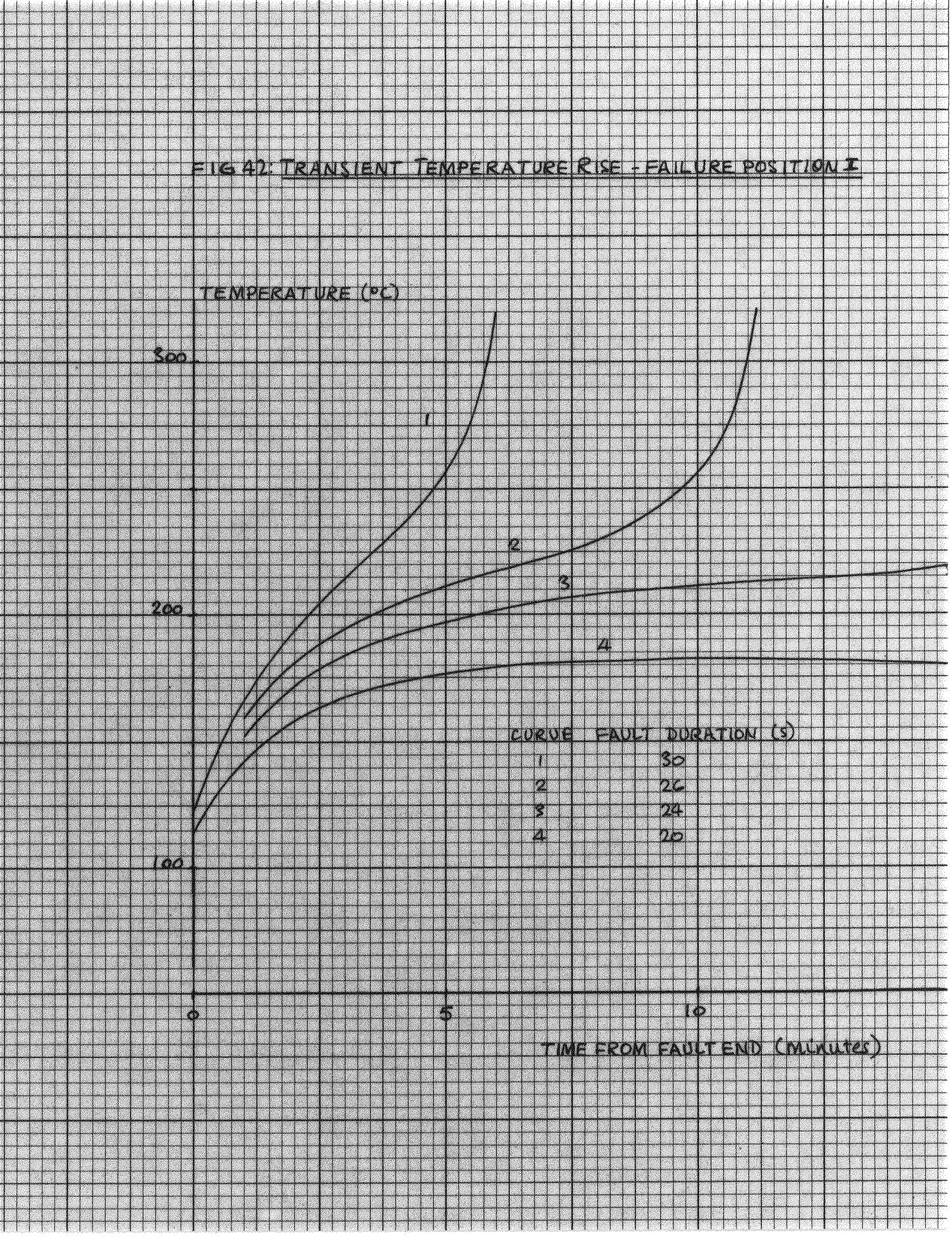

FIG 43 : TRANSIENT TEMPERATURE RISE - FAILURE POSITION II

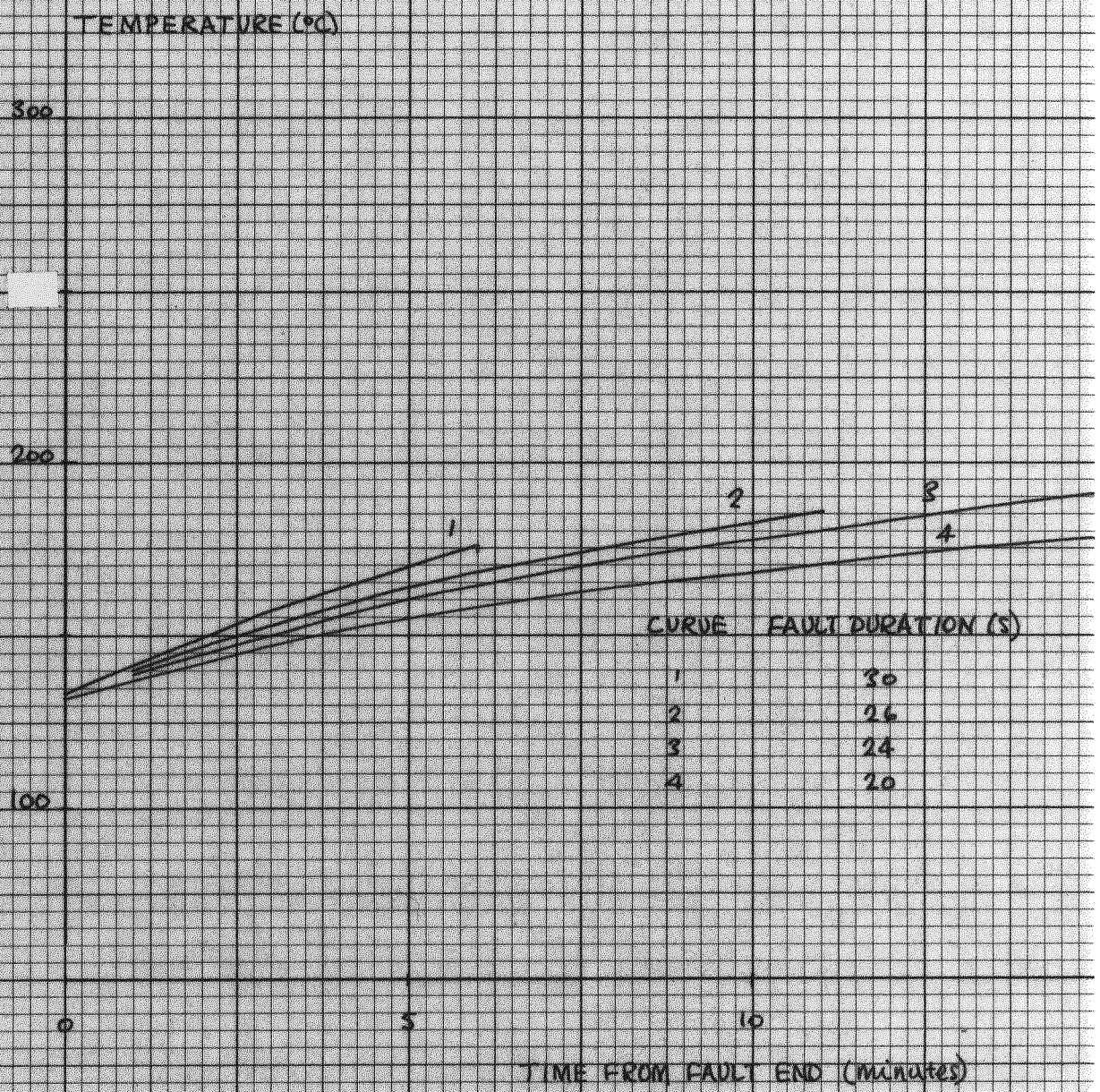

TABLE 7

Rate of heat generation (mW/cm^3)

	1	2	3	4	5
1	65.5	.459	.316	.231	.176
2	65.5	.459	.316	.231	.176
3	65.5	.459	.316	.231	.176
4	65.5	.459	.316	.231	.176
5	65.5	.459	.316	.231	.176
6	65.6	.459	.316	.231	.176
7	65.7	.459	.316	.231	.176
8	66.2	.459	.316	.231	.176
9	67.0	.459	.316	.231	.176
10	68.1	.459	.317	.231	.176
11	69.6	.459	.317	.231	.176
12	71.0	.460	.317	.231	.176
13	72.8	.460	.317	.231	.176
14	75.1	.462	.317	.231	.176
15	78.3	.204	.091	.052	.033
16	80.8	.205	.091	.052	.033
17	82.7	.206	.091	.052	.033
18	84.0	.206	.091	.052	.033
19	84.9	.207	.091	.052	.033
20	85.2	.207	.091	.052	.033

Table 8 lists fault times and failure positions along with the time to failure, which is defined as the time from the end of the fault to the point when the temperature at the failure positions reaches 1000°C. For a fault time between 22 and 24 seconds the failure position changes. Figs. 44 and 45 show the variation of temperature with time for the two failure points, Fig. 44 representing a fault time of 26 seconds and Fig. 45 one of 20 seconds. The failures in this instance illustrate the third kind of instability discussed in Chapter 1, where generated losses exceed the dissipated losses.

The table of losses shows that dielectric losses in the steady state at failure point I are more than twice as large as those at failure point II. This difference is due almost entirely to the much greater electric stress in the cable. The factors which determine failure are the thermal resistances to ambient and the level of the generated losses. In the integrally cooled case, the sheath is assumed to be in direct contact with the water so that only the resistance of the dielectric need be considered. The thermal resistance to ambient of failure point II is twice that of failure point I so that the slope of the dissipation curve for failure point II will be less than the slope of the curve for point I. Although the generated loss curve for failure point I lies higher than that for failure point II, the slope of the dissipation curves is so different that the intersection of the curves for loss generation and dissipation for point II will be at a higher

FIG 44 : TRANSIENT TEMPERATURE RISE - 26 S FAULT

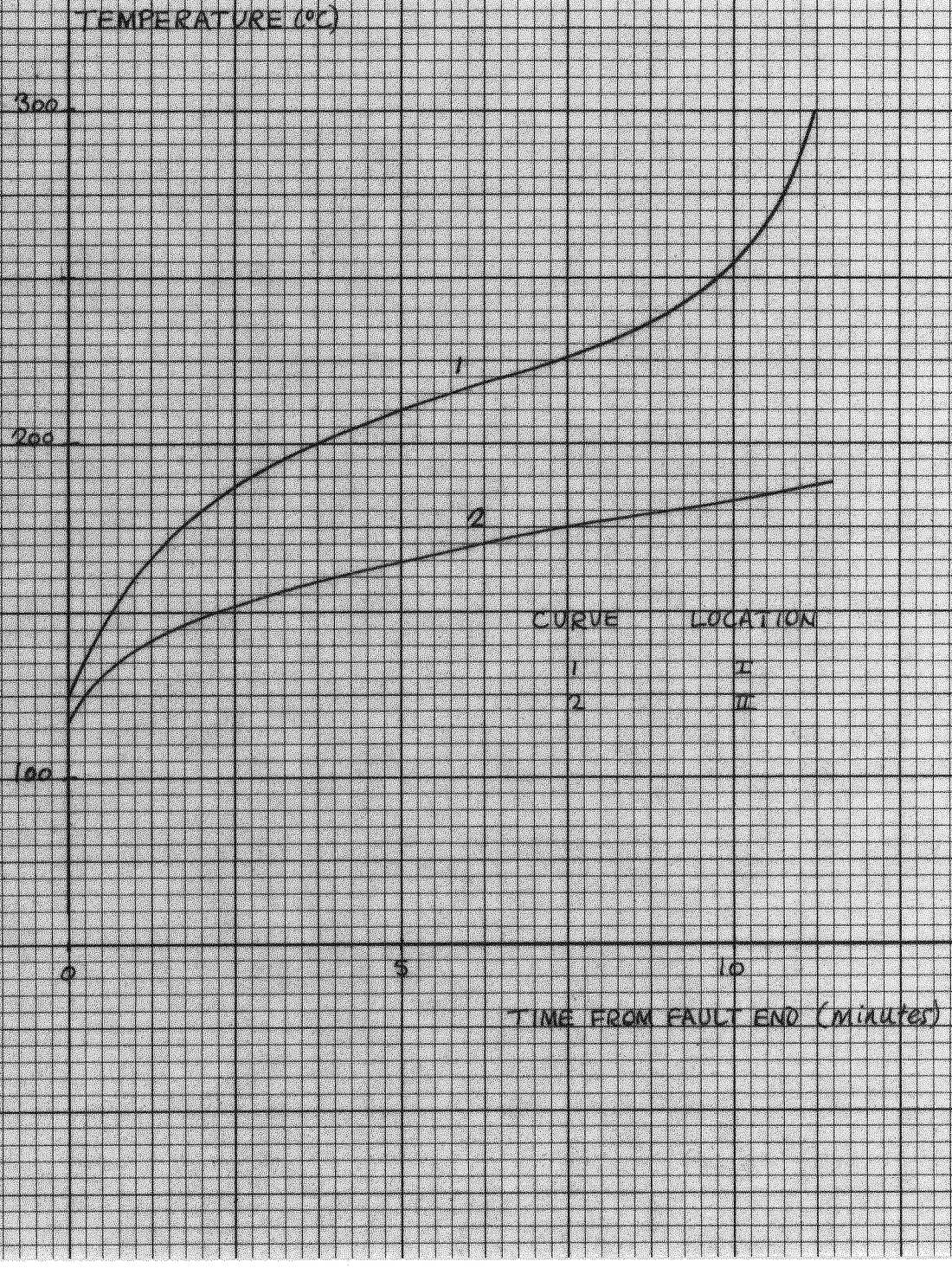

FIG 45 : TRANSIENT TEMPERATURE RISE - 20 S FAULT

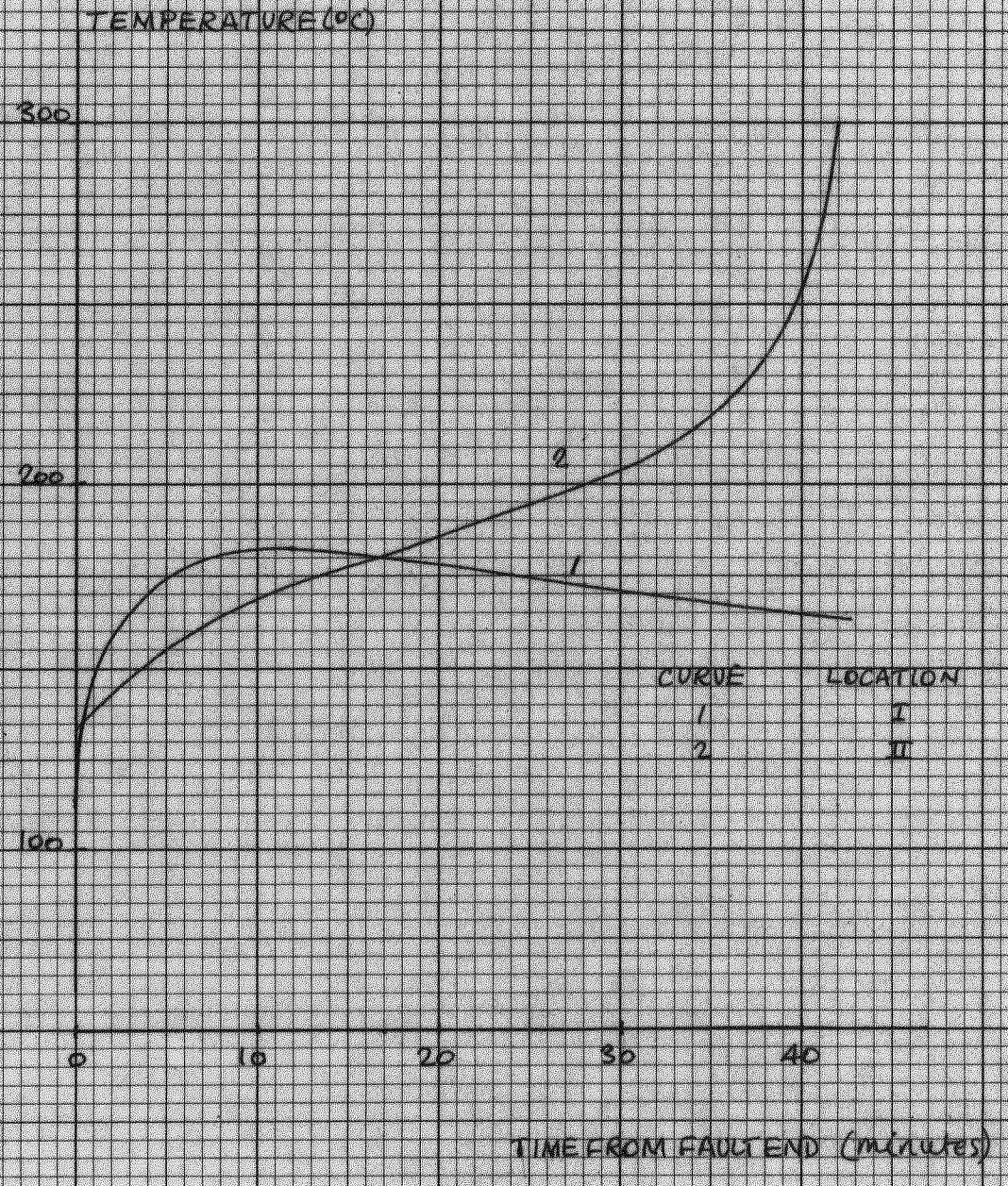

TABLE 8

Fault durations, positions and times to failure

Fault time (s)	Failure point	Time to failure h : m : s
30	I	0 : 06 : 12
26	I	0 : 11 : 24
24	I	0 : 24 : 22
22	II	0 : 34 : 54
20	II	0 : 42 : 48
15	II	1 : 41 : 35
10	II	7 : 34 : 00

temperature than that for point I. So, failure will occur at point I in preference to point II unless the fault level and/or duration is not sufficient to trigger instability at point I. For all the fault times used, the temperature at the ferrule continues to rise till failure, but at point II temperatures reach a maximum and then fall for fault times less than 24 seconds.

The fault times used in obtaining these results are very much longer than would be realised in practice so that the results show the inherent stability of the 3 in^2 cable. The temperatures in the steady-state are higher than would be acceptable in practice, but the results are useful in that they help in the understanding of the process of instability. With oil oscillation, temperatures in the joint ferrule would be 40°C-50°C lower, and the ability of the cable to withstand the fault durations considered here would consequently be considerably improved. No results have been obtained for the cable cooled by oil oscillation because of the long computation times and the large core storage required.

Another way in which instability may be induced is by an increase in the resistance to ambient of the medium surrounding the cable. This has been simulated with the present model by allowing the sheath to float; this is equivalent to an infinite resistance between the sheath and ambient. Such a situation could arise due to a failure of the coolant supply and a partial vacuum forming in the pipe. This is an extreme case, and in practice the results of coolant failure would not be so severe. Fig. 46 compares the

FIG 4C: RADIAL TEMPERATURE PROFILE - REMOTE CABLE

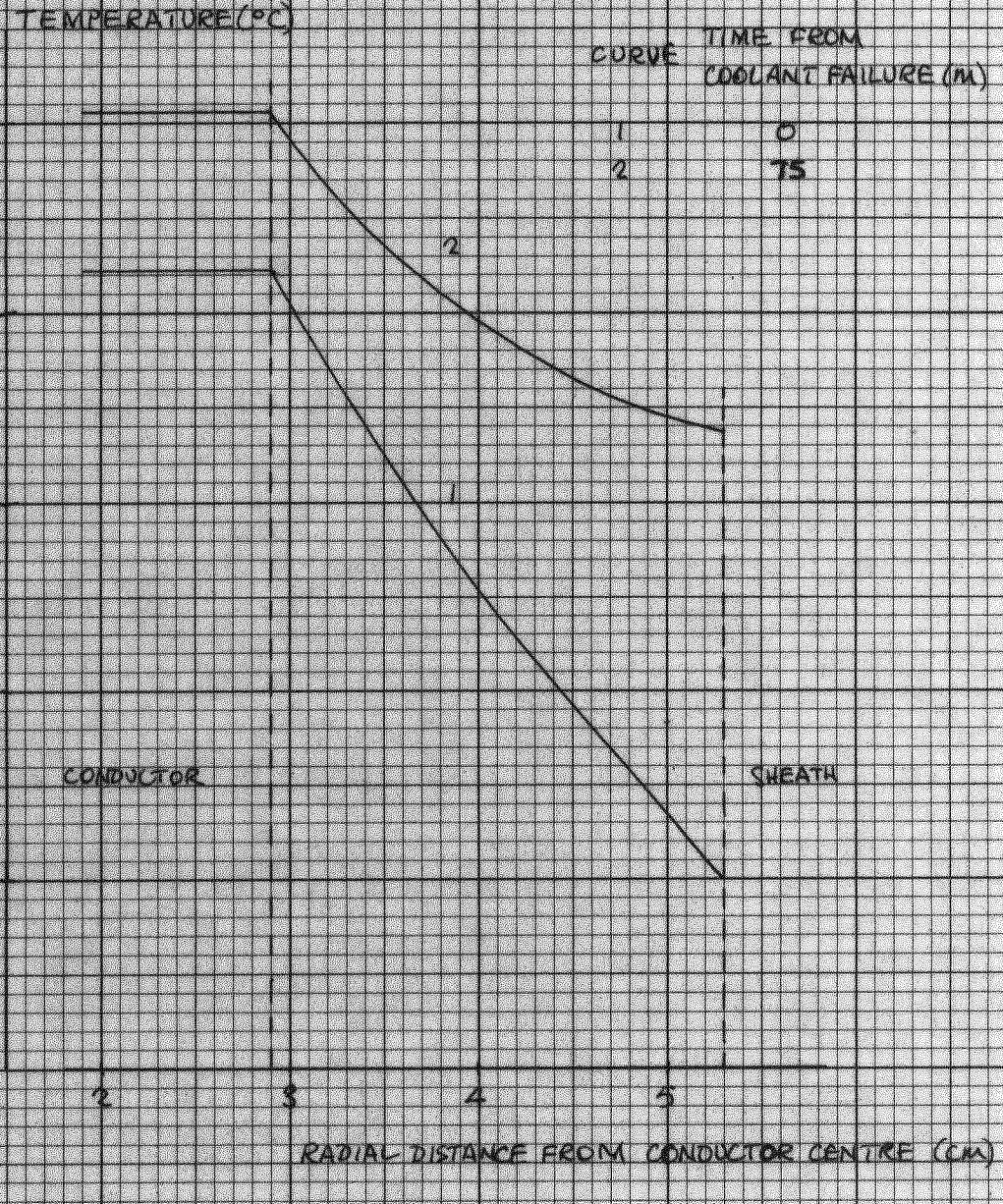

temperature profile through the cable with the sheath held at 20°C to the profile at time 75 minutes after failure of the coolant supply. Although the temperatures have increased, the temperatures in the insulation doing so at a faster rate than the conductor temperature, they are not excessively high. The cable fails over 3 hours after the coolant failure, so that this is a further illustration of the stability of the 3 in^2 cable.

CONCLUSIONS

The work on oil oscillation indicates that a worthwhile reduction in hot-spot temperature can be obtained with oil oscillation. It has been shown that the limit imposed by the joint on the current carrying capacity of a cable system is less severe with cooling by oil oscillation. For the 3 in^2, 400 kV joint and associated cable studied in the initial part of the investigation, the various parameters of the system are related by the following expression:

reduction in hot-spot temperature,

$$\theta_R = \frac{35.4\ \omega T}{(\omega + 1.36)\ (T + 2.04)}$$

where ω is the oil flow rate in cm^3/s and T the periodic time of the oscillation in minutes. In the expression, the variation in conductor resistance is accounted for; this effect is quite significant.

As the oil flow rate and/or oscillation periodic time increase, the relative improvement in hot-spot temperature is reduced. The optimum flow rate and periodic time associated with the particular system described by the equation above are 20 cm^3/s (16 gal/h) and 20/30 minutes respectively. Increases above these values bring very small extra return, although, if increases in T and ω can be easily obtained, small further increases in θ_R will result.

Doubt has been expressed over the value of N_{Nu} used, so results were obtained for Nusselt numbers of 2.42 and 12.1. These results showed that the thermal capacity of the fluid, rather than the Nusselt number of the flow, was the important factor in determining the reduction in hot-spot temperature obtained.

Results obtained for induced turbulence show that inducing turbulence in the joint produces much larger reductions in the hot-spot (joint ferrule) temperature. Results also show that inducing turbulence in the whole joint is no more effective in reducing ferrule temperatures than induced turbulence in the joint ferrule alone. Investigation of the effects of the thermal entrance on the heat transfer characteristic of the joint shows that these are significant. Results obtained assuming thermal entrance effects are equivalent to those obtained assuming an induced turbulence with a high Reynolds number. It is felt that in practice the reductions obtained would lie between those obtained assuming a constant Nusselt number and those obtained assuming thermal entrance effects.

The generalised program developed for the analysis of oil oscillation in general cable systems has been used to obtain results for several different types of cable. The program is simple to use and economical both in storage and computation time.

Thermal instability in an EHV cable and joint, integrally cooled, has been studied and the particular cable is shown to be

stable. It is impossible to induce thermal instability by faults of the current level and time duration obtainable in practice.

The study of instability has been confined to an intensely cooled cable, and it is suggested that the work be extended to cover the directly buried cable.

APPENDIX 1

Thermal Constants

Material	Resistivity (^{o}C cm/W)	Specific Heat (J/^{o}C gm)	Density (gm/cm^{3})
Oil	700.0	2.0	0.89
Paper	500.0	1.60	1.05
Copper	0.26	0.39	8.93
Lead	2.9	0.13	11.37
Bitumen	615.0	1.25	1.25
P.V.C.	540.0	1.5	0.92
Butyl	305.0		
Glass Fibre	480.0		
Soil	120.0	1.02	1.75

APPENDIX 2

Calculation of optimum transmittable power for a buried cable

The calculations in this Appendix are based on the report presented by the Chairman of the CIGRE-Committee No. 2 to the CIGRE in 1964[4].

Consider a three phase buried cable system consisting of 3 cables buried at a depth 'h' below the ground surface and laid horizontally with spacing 's' between centres. The system voltage is V (phase to earth) and the rated current I. The conductor diameter is d, the insulation diameter D and the inner and outer serving diameters D_s and D_s'.

The temperature rise of the conductor is therefore

$$\theta = (I^2R_{ac} + \tfrac{1}{2}W_d)\,R_1 + (I^2R_{ac} + W_d)\,R_2 + (I^2R_{ac} + W_d)\,R_3$$

where W_d is the dielectric loss.

R_1 is the insulation thermal resistance.

R_2 is the cable serving thermal resistance.

R_3 is the soil thermal resistance.

$$W_d = 2\pi f\, CV^2 \tan\delta$$

where $C \left(= \dfrac{2\pi\,\varepsilon_o\,\varepsilon_r}{\ln D/d}\right)$ is the cable capacitance

and $\tan\delta$ is the insulation power factor.

$$R_1 = \frac{g_1}{2\pi} \ln \frac{D}{d}$$

$$R_2 = \frac{g_2}{2\pi} \ln \frac{D_s'}{D_s}$$

$$R_3 = \frac{g_3}{2\pi} \left[\ln \frac{h}{D_s'} + \ln \left(\frac{4h^2 + s^2}{s^2} \right) \right]$$

where g_1, g_2 and g_3 are the insulation, serving and soil thermal resistivities.

For the cases considered, the depth and spacing are the same and the variation in the inner and outer serving diameters such that the ratio alters only slightly so that we may, sensibly, write

$$R_2 = \frac{a\, g_2}{2\pi}$$

$$R_3 = \frac{b\, g_3}{2\pi}$$

Substituting for W_d in the equation for θ and re-arranging the terms, we obtain an expression for the current capacity of the cable, assuming a maximum temperature rise of θ.

$$I = \left[\frac{\theta - 4\pi^2 f\, \varepsilon_o\, \varepsilon_r\, V^2 \tan \delta\, (R_1 + 2\,(R_2 + R_3))}{2 \ln \frac{D}{d}\, R_{ac}\, (R_1 + R_2 + R_3)} \right]^{\frac{1}{2}}$$

Substituting for R_1, R_2 and R_3 in the above equation we obtain

$$I = \left[\frac{1}{\ln \frac{D}{d} R_{ac}} \quad \frac{2\theta - 4\pi^2 f \varepsilon_o \varepsilon_r V^2 \tan \delta \left[g_1 + 2(ag_2 + bg_3)/\ln \frac{D}{d} \right] \frac{1}{2\pi}}{2(g_1 + (ag_2 + bg_3)/\ln \frac{D}{d}) \frac{1}{2\pi}} \right]^{1/2}$$

Now, if the maximum stress at the conductor surface is E_m,

$$E_m = \frac{2V}{d \ln \frac{D}{d}}$$

and substituting for $\ln \frac{D}{d}$ and multiplying both sides by 3V, we obtain the optimum transmittable power

$$P = \left[\frac{9\pi E_m d V^2}{R_{ac}} \quad \frac{(2\theta - 2\pi f \varepsilon_o \varepsilon_r V \tan \delta \left[Vg_1 + 2E_m d(ag_2 + bg_3) \right])}{Vg_1 + E_m d(ag_2 + bg_3)} \right]^{1/2}$$

APPENDIX 3

Construction of 400 kV Joint and Analog

The joint studied is a 3 in^2, 400 kV normal through joint, rated at 1100 MVA winter loading. The joint is shown in Fig. 47, and the principle cable dimensions are listed in Table 9. The conductor a.c. resistance at 85°C is 0.124 μΩ per cm length. The power factor of the joint is assumed to be 0.008, and that of the cable 0.003.

Because the thermal field in the joint is symmetrical about the centre line of the joint ferrule, only one half of the joint need be studied. The joint and cable can be considered as a thermal resistance-capacitance network which is obtained by sub-dividing the joint-cable into small volumes which are then represented by their thermal resistances in the reference directions and their thermal capacitances (volume x specific heat). The problem is simplified from three to two dimensions by assuming that the cable sheath and joint shell are isothermal circumferentially (this has been shown to be valid[15] by experiments using a finely divided mesh in which sheath and spinning are fully represented). Longitudinal heat flow in the dielectric is negligible and therefore not considered. Outside the cable and joint, the longitudinal thermal resistance of the soil is neglected, giving an equivalent network which represents the

FIG47 STRAIGHT THROUGH JOINT FOR 400 KV CABLE

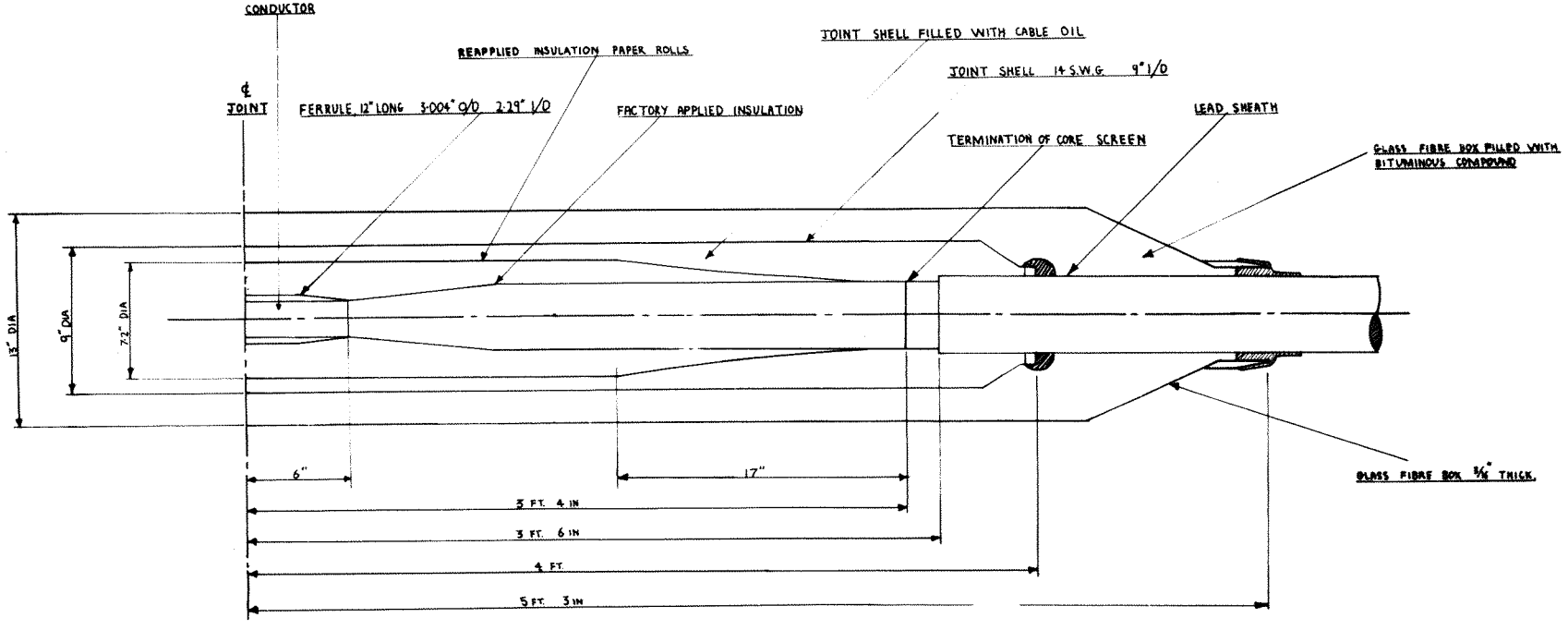

TABLE 9

Dimensions of 400 kV, 3 in^2 oil-filled cable

Oil duct diameter	(cm)	1.65
Conductor outside diameter	(cm)	5.80
Dielectric outside diameter	(cm)	10.55
Sheath outside diameter	(cm)	11.50
Servings outside diameter	(cm)	12.46
Conductor a.c. resistance at 85°C	μΩ/cm/core	0.124

effective resistance in the soil from the joint (cable) surface to the ground surface.

The subdivision in the joint is shown in Fig. 48, the smallest section corresponding to the half-ferrule. A length of cable 360 cm each side of the joint is considered and divided into 7 sections which become progressively longer away from the joint. The electrical analog is shown in Fig. 49, and this is derived from the thermal network using the following scaling factors (the terms on the left represent analog parameters):

$$C_e \ (F) = 2 \times 10^{-11} \ C_T \quad (J/^oC)$$

$$R_e \ (\Omega) = 2.78 \times 10^{-4} \ R_T \quad (^oC/W)$$

$$t_e \ (s) = {}^1/(18 \times 10^5) \ t \quad (s)$$

$$I \ (A) = 3.6 \times 10^{-5} \ Q \quad (W)$$

These factors give convenient electrical values and times which enable transients to be recorded on a CRO. The capacitances are connected between the appropriate nodes and the ground surface.

Copper and dielectric losses are calculated assuming a conductor temperature of 85°C and are injected at the appropriate nodes in the conductor and insulation. Dielectric losses are corrected in the steady state for temperature dependence using an iterative process, but are assumed constant over the transient. Copper losses are corrected in steady state for temperature dependence by an iterative process and are also corrected over the transient by the RC injection circuits used.

FIG 48 400 KV CABLE JOINT SHOWING RADIAL AND LONGITUDINAL SECTIONS

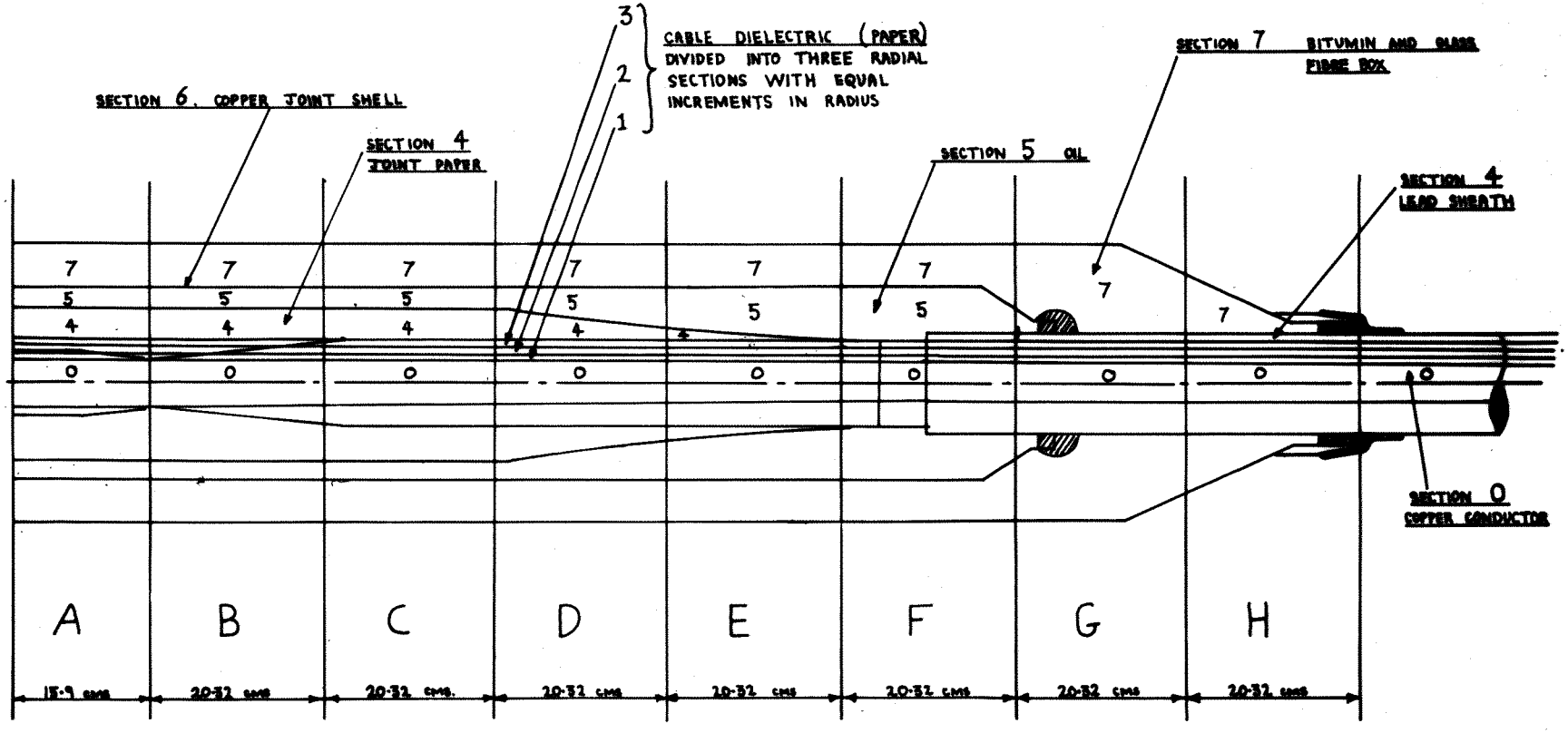

FIG 49 ELECTRICAL ANALOGUE CIRCUIT OF JOINT AND CABLE

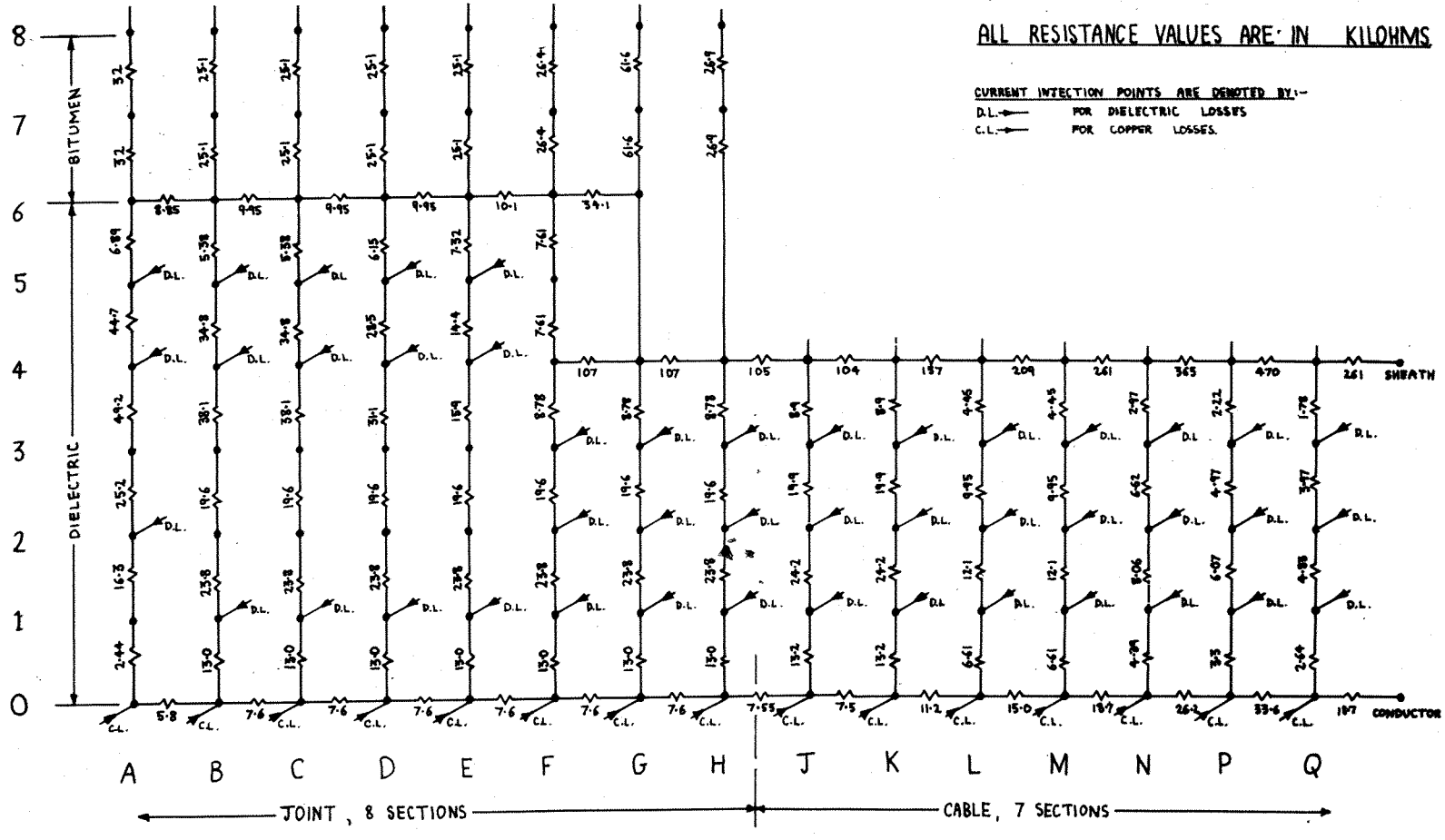

Provision is made in the analog for simulation of water cooling, three methods of cooling are used:

1. separate water pipes, involving the use of 4 butyl rubber pipes of 7.62 cm bore laid in the horizontal formation illustrated in Fig. 4;
2. integral cooling, where the water is assumed to be in direct contact with the cable sheath (joint shell);
3. separate pipe cooling with joint shell cooling.

APPENDIX 4

Development of equations for solution of oil flow in a duct

In the following description it should be noted that the subscript 'n' is used for nodes located in the conductor (duct wall) and 'm' for nodes in the oil; the relationship between 'n' and 'm' is that 'n' is at the centre of the nodal region and 'm' is at the downstream boundary of the region.

Flow in a duct

Consider the system shown in Fig. 8 which represents a nodal element in a duct wall losing heat to oil flowing inside the duct. The following assumptions are made:

1. there is no capacitance in the duct wall;
2. there is no thermal conduction along the fluid; this is valid since the thermal resistivity of the oil is 700°C cm/W compared with .26°C cm/W for the duct wall;
3. there is no heat generation in the oil and heat flow is from the duct wall to the oil.

To formulate the nodal energy balance, three energy terms must be considered:

1. the heat lost to the oil through convective heat transfer

$$H_{o_n} (\theta_n - \theta_{av}), \quad \text{where} \quad \theta_{av} = \frac{\theta_{o_m} + \theta_{o_{m+1}}}{2}$$

2. the enthalpy change in the oil passing through, and carried out of, the region

$$\omega \, Cp \, (\theta_{o_{m+1}} - \theta_{o_m})$$

3. the energy flow rate involved in the transient temperature rise of the oil within the element over the finite time step, Δt,

$$\frac{C_{o_n}}{\Delta t} \, (\theta'_{o_{m+1}} - \theta_{o_{m+1}})$$

This last term should contain the temperatures θ'_{av} and θ_{av} but, since the average fluid temperature contains both inlet and outlet temperatures, the use of the average temperatures would require a solution for two unknown temperatures after the time step. As recommended by Dusinberre[26], the downstream values will be used to represent the average.

The nodal energy balance is, therefore,

$$H_{o_n} \left(\theta_n - \frac{(\theta_{o_m} + \theta_{o_{m+1}})}{2}\right) = \omega \, Cp \, (\theta_{o_{m+1}} - \theta_{o_m}) + \frac{C_{o_n}}{\Delta t} \, (\theta'_{o_{m+1}} - \theta_{o_{m+1}})$$

and re-arranging the equation, we obtain

$$\theta'_{o_{m+1}} = \frac{H_{o_n} \Delta t}{C_{o_n}} \, \theta_n + \frac{(2\omega Cp - H_{o_n})\Delta t}{2C_{o_n}} \, \theta_{o_m} + \left[1 - \frac{(2\omega Cp + H_{o_n})\Delta t}{2C_{o_n}}\right] \theta_{o_{m+1}}$$

For stability in calculation, we require that the coefficients of the temperature terms in the equation for $\theta'_{o_{m+1}}$ be positive. The coefficient of the θ_n term is positive since each term is physically positive. The coefficient of the θ_{o_m} term gives the criterion

$$\Delta t \leq \frac{2C_{o_n}}{2\omega Cp + H_{o_n}}$$

since, for most of the flows considered, $H_{o_n} << 2\omega Cp$, we may rewrite the criterion as

$$\Delta t < \frac{2Cp\ A_d\ \ell_n}{2\omega Cp}$$

where A_d is the duct cross-sectional area and ℓ_n is the length of the nodal region.

It is seen that the time step is directly proportional to the nodal region length so that the time step is dependent on the length of the smallest nodal-region. The time step is also inversely proportional to the oil flow-rate.

Buried cable

Consider the system shown in Fig. 9 which represents a cable section losing heat from the conductor through the insulation to ambient and from the conductor to the oil in the conductor-duct. The cable has a water-cooled sheath and the water temperature is assumed to be uniform along the length of the cable. The following assumptions are made about the cable system:

1. All heat flow, longitudinally, takes place in the conductor; longitudinal heat flow is negligible in the insulation, the thermal resistivity of which is 500°C cm/W compared with .26°C cm/W for the conductor.
2. The distributed capacitance of the insulation is lumped at the conductor.

To write energy balance at node n, six energy terms must be considered:

1. There are heat flows from node n along the conductor to nodes (n-1) and (n+1), from node n through insulation to ambient and from node n into the oil; these are respectively

$$(\theta_n - \theta_{n-1})\, K_{n-1}$$

$$(\theta_n - \theta_{n+1})\, K_n$$

$$\theta_n\, H_{i_n}$$

$$\left(\theta_n - \left(\frac{\theta_{o_m} + \theta_{o_{m+1}}}{2}\right)\right) H_{o_n}$$

2. There is the energy rate involved in the transient temperature change of the conductor within the nodal-region over the finite time-step, Δt,

$$\frac{C_{e_n}}{\Delta t}\,(\theta_n - \theta_n')$$

3. There is the heat injection term due to copper and dielectric losses, q_n.

The energy balance at node n is therefore

$$\theta_n H_{i_n} + (\theta_n - \theta_{n+1})K_n + (\theta_n - \theta_{n-1})K_{n-1} + (\theta_n - (\frac{\theta_{o_m} + \theta_{o_{m+1}}}{2}))H_{o_n} = \frac{C_{e_n}}{\Delta t}(\theta_n - \theta_n') + q_n$$

and re-arranging the equation, we obtain

$$\theta_n' = \frac{K_n \Delta t}{C_{e_n}} \theta_{n+1} + \frac{K_{n-1} \Delta t}{C_{e_n}} \theta_{n-1} + (1 - \frac{\Sigma \Delta t}{C_{e_n}}) \theta_n + \frac{H_{o_n} \Delta t}{2C_{e_n}} (\theta_{o_m} + \theta_{o_{m+1}}) + \frac{q_n \Delta t}{C_{e_n}}$$

where $\Sigma = K_n + K_{n-1} + H_{o_n} + H_{i_n}$.

The coefficient of the θ_n term in these equations gives a time criterion for stability,

$$\Delta t < \frac{C_{e_n}}{H_{o_n} + K_n + K_{n-1} + H_{i_n}}$$

The equations for $\theta'_{o_{m+1}}$ and θ'_n define the longitudinal temperature profiles in both oil and conductor and their variation in time, subject to the space and time criteria being met.

Assuming typical values for oil film thermal conductance (.018 W/°C per cm length) and oil specific heat (1.78 J/°C cm^3) and an oil flow rate of 5 cm^3/s, the limiting nodal region length is found to be 10 m. Using this length in the time criteria established above, we find that for the duct-oil system, the time criterion is about 250 s, and, for the cable, the time criterion is

an order of magnitude higher. Thus the important criteria are the space criterion and the time criterion derived from the equation for $\theta'_{o_{m+1}}$. In practice, however, it is found that there is another important criterion, which is that the temperature coefficients must sum exactly to one. In an iterative process, a coefficient sum of less than one will show as a fictitious heat sink, and, conversely, a coefficient sum of more than one will show itself as a fictitious heat source, both resulting in instability.

APPENDIX 5

Generalized program for oil oscillation

This program solves the equations, derived in Appendix 4, for oil oscillation in the duct of an EHV cable. The model contains two EHV joints and is divided into (ID) nodal regions. The model is considered to be symmetrical about its centre line, so that, since the joints are also symmetrical about their own centre-lines the input data need only describe the nodes 1 to (ID/4) inclusive. The oil velocity has a square wave profile defined by the parameter (2*IT) and the period of investigation is defined by the parameter Iθ such that the period of investigation is (Iθ*IT*DELT) seconds, where DELT is the computation time-step.

The conductor and oil temperature profiles are output at the beginning and end of the investigation period. Temperatures at the joint ferrule and at a point in the remote cable conductor, defined by the parameter JCAB, are output at intervals during the investigation defined by the parameter IC.

ID and JCAB are chosen before the cable description data is assembled; the rest of the parameters depend on the value of the oil flow-rate. Once an oil flow-rate has been determined, the time step, Δt, is evaluated from the inequality

$$\Delta t < \frac{2C_o}{2\omega Cp + H_o}$$

where C_o is the thermal capacitance of the oil in the duct and H_o the heat transfer conductance between the oil and the duct wall for the nodal region considered, ω is the oil flow rate and Cp the oil specific heat. In practice, H_o is very small compared with $(2\omega Cp)$ and the criterion reduces to

$$\Delta t < \frac{2Cp\ A_d\ \ell}{2\omega Cp}$$

where A_d is the duct cross-sectional area and ℓ is the length of the nodal region.

It is seen that the time step is directly proportional to the nodal region length so that the time step is dependent on the smallest nodal region length. The time step is inversely proportional to the oil flow rate.

For the data given here (i.e. duct diameter = 1.2 cm and smallest nodal region length = 15 cm), the maximum time step for a 5 cm^3/s flow is 3.6 s. However, investigation shows that the limiting value of the time step is approximately twice that obtained from the inequality so that the time step corresponding with the 5 cm^3/s flow rate is taken to be 6 s.

Now suppose it is desired to investigate a 5 cm^3/s flow with 20 min cycle and to print out ferrule temperature and conductor temperature at 5m from the joint centre.

We have chosen ID = 80

and so JCAB = 12

The half cycle time is 10 min.

and $$IT = \frac{10 \times 60}{6}$$

$$= 100.$$

The number of oscillations is $$\frac{12 \times 60}{20} = 36$$

and $$I\theta = 72$$

The print out period is 10 minutes

and $$IC = \frac{10 \times 60}{6}$$

$$= 100.$$

Format of Input Data Cards

Numbers on the first card are of type INTEGER (I); all other numbers are of type REAL (F), except for the conductor resistance Cols. 36-43 on Card 3 which is of type E.

Input data should be in c.g.s. units.

1. Control Parameters.

Cols. 1-4 : time for one pass in the oscillation (i.e. half oscillation period) (IT).

Cols. 5-8 : total number of nodes in the model (ID).

Cols. 9-12 : number of passes during period of investigation (IΘ).

Cols. 13-16 : print out frequency (IC).

Cols. 17-20 : identifies node in cable for temperature print out.

2. Cable Details.

Cols. 1-4 : conductor cross-sectional area (AREA).

Cols. 5-10 : conductor radius (RADCON).

Cols. 11-14 : conductor duct diameter (DUCTD).

Cols. 15-20 : system current (AMP).

Cols. 21-27 : system voltage (VOLT).

Cols. 28-30 : system frequency (HERTZ).

3. Material Details.

Cols. 1-5 : paper thermal resistivity (PAPERG).

Cols. 6-10 : paper specific heat (PAPERC).

Cols. 11-14 : cable power factor (PHI).

Cols. 15-17 : paper relative permittivity (EPSILON).

Cols. 18-22 : Nusselt number of oil flow (NNU).

Cols. 23-26 : oil specific heat (CPOIL).

Cols. 27-31 : oil thermal resistivity (OILG).

Cols. 32-35 : conductor specific heat (CUCP).

Cols. 36-43 : effective electrical resistance per cm length of conductor (RSTR).

4. Flow-rate and time step.

Cols. 1-5 : flow rate (W).

Cols. 6-10 : time step (DELT).

5. Nodal region lengths and radii.

This section of data should contain ($\frac{1}{4}$ ID) cards.

Cols. 1-5 : nodal region length (ALEN (J)).

Cols. 6-10 : radius under the sheath (shell) at the centre of the nodal region (RAD (J)).

```
      MASTER HRRCKS
      REAL MULT,KCONV,NNU,NRA
      DIMENSION TCONN(100),TOILN(100)
      COMMON /A/ID,IT,IO,IC/B/I,N,T/C/A(100),B(100),C(100),D(100),E(100
     1),F,G(100),H/D/TCONT(100),TOILT(100)/G/DL,CL/H/IDH
      CALL INPUT
      CALL TCALC
      CALL OUTPUT
      DO 4 N=1,IO
      TCONT(ID+1)=TCONT(IDH+1)
      TOILT(ID+1)=TOILT(IDH+1)
      DO 3I=1,IT
      DO 1 J=2,ID
      TOILN(J)=A(J-1)*TCONT(J-1)+B(J-1)*TOILT(J-1)+C(J-1)*TOILT(J)
      TCONN(J)=D(J)*TCONT(J+1)+G(J)*TCONT(J-1)+E(J)*TCONT(J)+
     1F*TOILT(J)+F*TOILT(J+1)+H*(DL/2.+CL*(1.+.00393*(TCONT(J)-65.)))
1     CONTINUE
      TCONN(1)=TCONN(IDH+1)
      TOILN(1)=TOILN(IDH+1)
      DO 2 J=1,ID
      TOILT(J)=TOILN(J)
      TCONT(J)=TCONN(J)
2     CONTINUE
      TOILT(ID+1)=TOILT(IDH+1)
      TCONT(ID+1)=TCONT(IDH+1)
      IF(((I/IT)+IT).EQ.IT)CALL OUTPUT
3     CONTINUE
      IF(N.EQ.IO)GO TO 4
      CALL REVERS
4     CONTINUE
      WRITE(2,200)
200   FORMAT(////24H PROGRAM HRRCKS COMPLETE ///)
      STOP
      END



      SUBROUTINE INPUT
      REAL NNU
      DIMENSION RAD(100),RADSH(100),HPR(100)
      COMMON/A/ID,IT,IO,IC/B/I,N,T/E/ALEN(100),RPR(100),CK/F/DELT
     1,OILH,OILCAP,CE,CPOIL,W/G/DL,CL/H/IDH,IDQ,JCAB
      PI=3.1416
      READ(1,100)IT,ID,IO,IC,JCAB
100   FORMAT(514)
      IDH=ID/2
      IDQ=ID/4
      READ(1,101)AREA,RADCON,DUCTD,AMP,VOLT,HERTZ
```

```
101   FORMAT(F4.1,F6.3,F4.2,F6.0,F7.0,F3.0)
      READ(1,102)PAPERG,PAPERC,PHI,EPSILON,NNU,CPOIL,OILG,CUCP,RSTR
102   FORMAT(F5.0,F5.2,F4.3,F3.1,F5.2,F4.2,F5.0,F4.2,E8.3)
      READ(1,103)W,DELT
103   FORMAT(2F5.1)
      PERIOD=2*IT*(DELT/60.)
      WRITE(2,105)
105   FORMAT(22H1PROGRAM HRRCKS STARTS ///)
      WRITE(2,106)VOLT,AMP,HERTZ,AREA,DUCTD,W,PERIOD,NNU,RADCON
106   FORMAT(///11H INPUT DATA,//,8H VOLTS= ,F8.0,1OH  :  AMPS= ,F7.0,
     114H : FREQUENCY= ,F4.0,5H HZ :,//,26H CONDUCTOR CROSS-SECTION= ,
     1F4.1,24H SQ CM : DUCT-DIAMETER= ,F4.2,5H CM ://7H FLOW= ,F5.1,
     129H CUCM/S : OSCILLATION PERIOD=,F3.0,11H MIN : NNU=,F5.2,2H ://
     119H CONDUCTOR-RADIUS=  ,F5.2,5H CM :///)
      READ(1,104)(ALEN(J),RAD(J),J=1,IDQ)
104   FORMAT(F5.0, F5.2)
      DO 1 J=1,IDQ
      ALEN(IDH +1-J)=ALEN(J)
      RPR(J)=(PAPERG*ALOG(RAD(J)/RADCON))/(2.*PI)
      HPR(J)=1./RPR(J)
      RPR(IDH +1-J)=RPR(J)
      HPR(IDH +1-J)=HPR(J)
1     CONTINUE
      RADINS=RAD(1)
      OILH=(NNU/(OILG*DUCTD))*PI*DUCTD
      OILCAP=CPOIL*.25*PI*DUCTD*DUCTD
      CABCAP=2.*PI*8.854E-12*EPSILON/(ALOG(RADINS/RADCON)*100.)
      CL=RSTR*AMP**2
      DL=2.*PI*HERTZ*((VOLT*VOLT)/3.)*CABCAP*PHI
      CK=AREA/.26
      VANW=1./(2*ALOG(RADINS/RADCON))-1./((RADINS/RADCON)**2-1)
      CE=AREA*CUCP+PI*(RADINS**2-RADCON**2)*PAPERC*VANW
      DO 2 J=1,IDH
      RPR(IDH +J)=RPR(J)
      HPR(IDH +J)=HPR(J)
      ALEN(IDH +J)=ALEN(J)
2     CONTINUE
      CALL CONSTS
      N=0
      I=0
      T=0
      RETURN
      END
```

```
      SUBROUTINE CONSTS
      REAL MULT, NNU
      DIMENSION CONST(100)
      COMMON/A/ID,IT,IO,IC/C/A(100),B(100),C(100),D(100),E(100),F,G(100
     1),H/E/ALEN(100),RPR(100),CK/F/DELT,OILH,OILCAP,CE,CPOIL
     1,W/G/DL,CL/H/IDH
      H=DELT/CE
      DO 2 J=1,ID
      A(J)=OILH*DELT/OILCAP
      B(J)=(2.*W*CPOIL-OILH*ALEN(J))*DELT/(2.*OILCAP*ALEN(J))
      C(J)=1.-A(J)-B(J)
      IF(J.EQ.ID)GO TO 1
      D(J)=CK*DELT*2./((ALEN(J)+ALEN(J+1))*ALEN(J)*CE)
1     CONST(J)=DELT/(RPR(J)*CE)
2     CONTINUE
      F=OILH*DELT/(2.*CE)
      D(ID)=CK*DELT/(ALEN(ID)*ALEN(ID)*CE)
      DO 3 J=2,ID
      G(J)=CK*DELT*2./((ALEN(J)+ALEN(J-1))*ALEN(J)*CE)
      E(J)=1.-D(J)-G(J)  -F-F-CONST(J)
3     CONTINUE
      G(1)=G(IDH+1)
      E(1)=1.-D(1)-G(1)-F-F-CONST(1)
      RETURN
      END



      SUBROUTINE TCALC
      REAL K,MINIM,M
      DIMENSION M(100),K(100),S(100),P(100),R(100),U(100)
      COMMON/A/ID,IT,IO,IC/D/TCONT(100),TOILT(100)/E/ALEN(100),RPR(100)
     1,CK/G/DL,CL/H/IDH,IDQ
      DO 11 J=1,IDH
11    TCONT(J)=RPR(J)*HEAT
      MINIM=0.001
      THAT=999.
      DO 1 J=1,IDH -1
      M(J)=ALEN(J)/RPR(J)
1     K(J)=CK/((ALEN(J)+ALEN(J+1))/2.)
      K(IDH )=CK/ALEN(IDH )
      M(IDH )=ALEN(IDH )/RPR(IDH )
      DO 2 J=2,IDH
      S(J)=K(J)+K(J-1)+M(J)
      P(J)=K(J)/S(J)
      R(J)=K(J-1)/S(J)
2     U(J)=     ALEN(J)/S(J)
      S(1)=K(1)+K(1)+M(1)
      P(1)=K(1)/S(1)
```

```
      R(1)=K(1)/S(1)
      U(1)=     ALEN(1)/S(1)
3     THAT=THIS
      DO 4 J=2,IDH -1
4     TCONT(J)=TCONT(J+1)*P(J)+TCONT(J-1)*R(J)+U(J)*(DL/2.+CL*(1.+.00393
     1*(TCONT(J)-65.)))
      TCONT(1)=TCONT(2)
      TCONT(IDH )=TCONT(IDH -1)
      DO 5 J=1,IDQ
      STORE=TCONT(J)
      TCONT(J)=TCONT(IDH -J+1)
5     TCONT(IDH -J+1)=STORE
      THIS=TCONT(IDQ )
      IF(ABS(THIS-THAT).GE.MINIM)GO TO 3
      DO 6 J=1,IDH
6     TCONT(IDH +J)=TCONT(J)
      DO 7 J=2,ID
7     TOILT(J)=(TCONT(J-1)+TCONT(J))/2.
      TOILT(1)=TOILT(IDH +1)
      RETURN
      END



      SUBROUTINE OUTPUT
      COMMON/A/ID,IT,IO,IC/B/I,N,T/D/TCONT(100),TOILT(100)/F/DELT/H/IDH
     1,IDQ,JCAB
      IF(N.EQ.0)GO TO 3
      IF(((N/2)*2).EQ.N)GO TO 1
      TMID=(TCONT(IDQ)+TCONT(IDQ+1))/2.
      TCABLE=TCONT(JCAB)
      GO TO 2
1     TMID=(TCONT(3*IDQ)+TCONT(3*IDQ+1))/2.
      TCABLE=TCONT(ID-JCAB+1)
2     WRITE(2,206)N,I,TMID,TCABLE
206   FORMAT(15X,2HN=,I4,3H:I=,I4,1H:,4X,F5.1,6X,F5.1/)
      IF(N.EQ.IO.AND.I.EQ.IT)GO TO 3
      GO TO 4
3     T=((N-1)*IT+I )*DELT/60.)
      IF(N.EQ.0)T=0.
      WRITE(2,200)N,I,T
200   FORMAT(///6H   N =,I4,6H:  I =,I4,//,11H   TIME IS ,F6.2,
     18H MINUTES //)
      WRITE(2,201)
201   FORMAT(// 15H CONDUCTOR TEMP /)
      WRITE(2,202)
202   FORMAT(10H UPSTREAM /)
      WRITE(2,203)(TCONT(J),J=1,IDH)
203   FORMAT(10F10.1)
```

```
      WRITE(2,204)
204   FORMAT(/12H DOWNSTREAM /)
      WRITE(2,203)(TCONT(IDH +J),J=1,IDH)
      WRITE(2,205)
205   FORMAT(///IOH OIL TEMP /)
      WRITE(2,202)
      WRITE(2,203)(TOILT(J),J=1,IDH)
      WRITE(2,204)
      WRITE(2,203)(TOILT(IDH +J),J=1,IDH )
4     RETURN
      END


      SUBROUTINE REVERS
      DIMENSION CS(100),OS(100)
      COMMON/A/ID,IT,IO,IC/D/TCONT(100),TOILT(100)/H/IDH
      DO 1 J=1,IDH
      CS(J)=TCONT(J)
      TCONT(J)=TCONT(ID-J+1)
      TCONT(ID-J+1)=CS(J)
      OS(J)=TOILT(J)
      TOILT(J)=TOILT(ID-J+2)
      TOILT(ID-J+2)=OS(J)
1     CONTINUE
      RETURN
      END


      FINISH
```

APPENDIX 6

The asymptotic value of the Nusselt number of a laminar flow in a duct with linear wall temperature variation

The energy equation describing a general fluid flow may be written

$$\frac{g}{Cp} \quad (\underline{v} \cdot \text{grad } T) \quad = \quad \nabla^2 T$$

where $\underline{v}$ ($= \underline{i}\, v_x + \underline{j}\, v_y + \underline{k}\, v_z$) is the vector velocity, T is the fluid temperature and g and Cp are the thermal resistivity and specific heat of the fluid, respectively.

Considering laminar flow with average velocity $\bar{u}$ in a circular duct, radius R, then the velocity distribution across the duct section is

$$u \quad = \quad \bar{u} \left(1 - \frac{r^2}{R^2}\right)$$

and the energy equation reduces to

$$\frac{\partial^2 T}{\partial r^2} + \frac{1}{r} \frac{\partial T}{\partial r} = \frac{2\bar{u}g}{Cp} \left(1 - \frac{r^2}{R^2}\right) \frac{\partial T}{\partial x}$$

Since we assume that the duct wall temperature is varying linearly, the wall temperature rise may be written as

$$T \quad = \quad Bx + \theta(r)$$

where θ is the fluid temperature rise, at distance x, above the

wall temperature rise, at distance x, and B is a constant.

The energy equation may then be rewritten to give a second-order, ordinary differential equation

$$\frac{d^2\theta}{dr^2} + \frac{1}{r}\frac{d\theta}{dr} = \frac{2\bar{u}gB}{Cp}\left(1 - \frac{r^2}{R^2}\right)$$

which may be re-arranged to give

$$\frac{1}{r}\frac{d}{dr}\left(r\frac{d\theta}{dr}\right) = \frac{2\bar{u}gB}{Cp}\left(1 - \frac{r^2}{R^2}\right)$$

This equation is readily soluble. A straightforward integration and substitution of the boundary conditions ($\theta = 0$ at $r = R$ and $\frac{d\theta}{dr} = 0$ at $r = 0$) gives the equation for the fluid temperature rise.

$$\theta = -\frac{2\bar{u}BR^2g}{16\,Cp}\left(3 - \frac{4r^2}{R^2} + \frac{r^4}{R^4}\right)$$

The temperature gradient at the wall ($r = R$), and normal to it, is

$$\left(\frac{d\theta}{dr}\right)_{r = R} = \frac{\bar{u}BgR}{2Cp}$$

The temperature gradient, and thus the heat flux, at the wall is seen to be independent of the axial distance x. This constant heat flux situation, is to a first approximation, the one which exists in the joint-cable system.

The mean bulk temperature, θ_b, of the flow is defined by

$$\theta_b = \frac{\int \theta \rho \, Cp \, u \, dA}{\int \rho \, Cp \, u \, dA}$$

which because of the assumption of constant properties, reduces to

$$\theta_b = \frac{\int \theta \, u \, dA}{\int u \, dA}$$

and the bulk temperature is

$$\theta_b = \frac{11 \, \bar{u} \, B \, g \, R^2}{48 \, Cp}$$

Thus the Nusselt number based on the diameter, D (= 2R), becomes

$$N_{Nu} = - \frac{2R \left(\frac{d\theta}{dr} \right)_{r = R}}{\theta_b}$$

$$= \frac{48}{11}$$

$$N_{Nu} = 4.36$$

APPENDIX 7

Note on the limits imposed on the oil velocity profile

The main factor involved in limiting oil velocities is the allowable pressure rise due to the flow. There is a fixed maximum pressure allowable in the cable system determined by the maximum permissible mechanical hoop stress in the sheath and the pressure rating of the oil reservoir. In designing cables with reinforced sheaths, a factor of safety of 2 on the basis of the 0.01% proof stress is used[32], so that the maximum continuous operating pressure is 76 psi and 115 psi under transient conditions. The pressure limits are used in the design of aluminium sheathed cables. However, continuous pressure ratings of up to 250 psi are used in gas pressure cable systems, so that it is seen that the limiting pressure in the system is the rated pressure of the oil reservoirs.

The minimum pressure must be such that no voids form in the oil/paper insulation. Allowances must also be made for pressure drops due to the cable circuit route profile. Thus, the total pressure must not exceed the sum of minimum pressure to prevent void formation, pressure drops due to route profile and pressure to maintain oil flow. The present state of design will allow a maximum of 25-50 psi to maintain oil flow.

Pressure drop due to flow

$$\Delta p = \frac{f_D \rho V^2 \ell}{2 g_c D}$$

where f_D is the D'Arcy friction factor and is equal to $64/N_{Re}$ for laminar flow regimes.

Fig. 50 shows pressure drops over 1000m (representing the approximate distance between stop-joints and hence pressure tanks) for the two standard duct sizes.

Although the pressure drop for 60 cm^3/s flow in the 12 mm duct is less than 50 psi, and within the allowable maximum, the Reynolds number of the flow is 2450 so that the flow regime is transitional if not turbulent and the equation for Δp may not apply. For the 16.5 mm duct, the pressures are well within the limits, and the flow is always laminar.

The cycle time is limited both by the capacity of the pressure tanks and by the oil flow rate. The capacity of the pressure tanks will determine the volume of oil which can be absorbed at the downstream end of the system, and hence the cycle time will be determined for any flow rate since the volume of oil displaced during each half of the oscillation cycle is equal to the product of the half-cycle time and the oil flow rate.

FIG 5a: PRESSURE DROP v OIL FLOW RATE

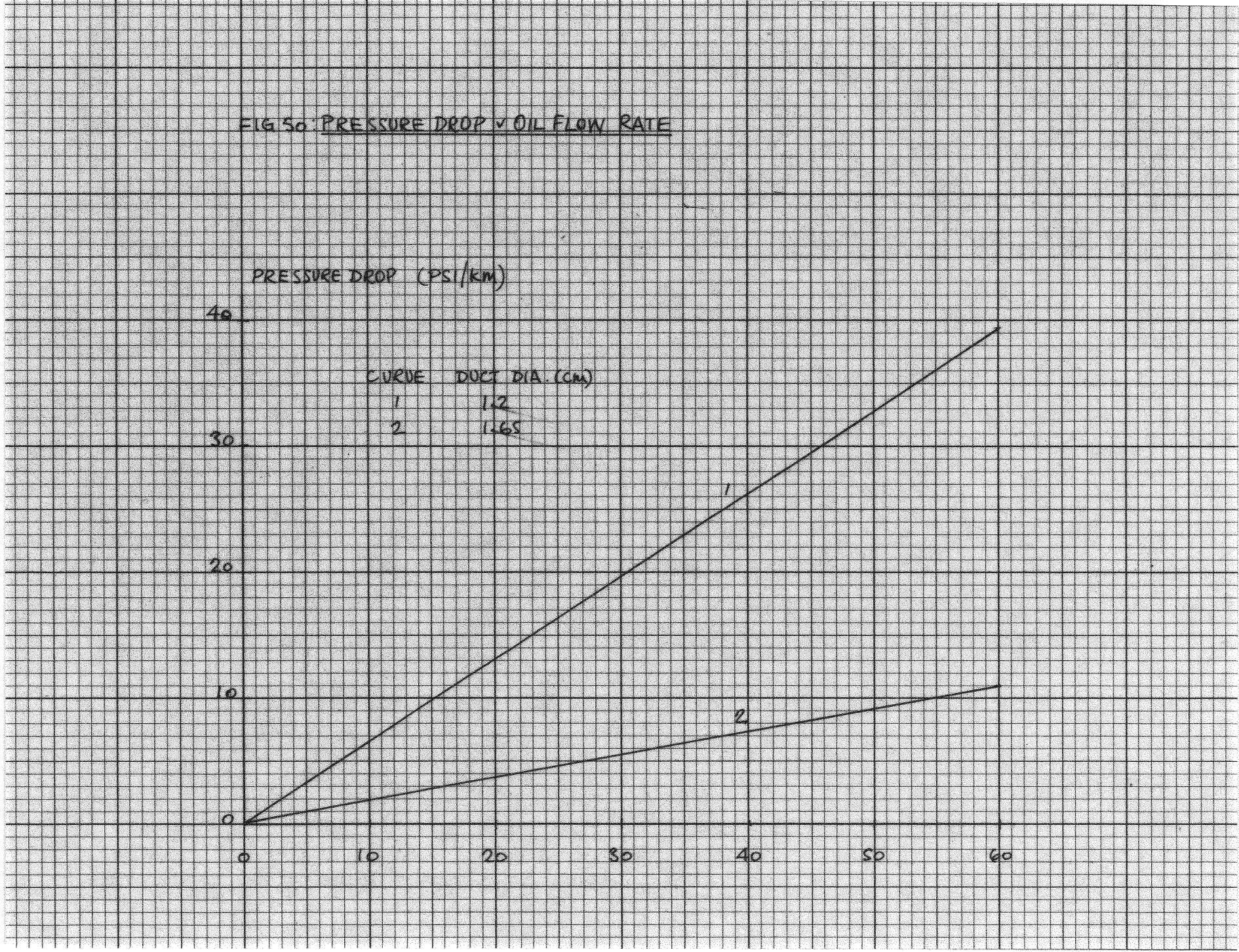

APPENDIX 8

The Frohlich Equation

The Frohlich Equation is frequently used to fit magnetization curves and it may be used, in general, to fit any curve characterized by a sharp 'knee'.

An examination of the equation and its first derivative yields some interesting results.

$$y = x/(\alpha + \beta x)$$

$$\frac{dy}{dx} = \alpha/(\alpha + \beta x)^2$$

The value of y tends to a maximum as x increases. So taking the limit of y as x tends to infinity, we find:

$$\lim_{x\to\infty} (x/(\alpha + \beta x)) = 1/\beta \quad \text{since} \quad \beta x >> \alpha \quad \text{for large x.}$$

i.e. the maximum value of y is $1/\beta$.

Taking the limit of $\frac{dy}{dx}$ as x approaches zero, we obtain the expression

$$\lim_{x\to o} \left(\frac{dy}{dx} \right) = \lim_{x\to o} (\alpha/(\alpha + \beta x)^2)$$

$$= 1/\alpha$$

i.e. the initial gradient of the curve is $1/\alpha$.

APPENDIX 9

Program for transient thermal response of EHV joint and cable

The program description can be conveniently divided into 3 sections:

(1) calculation of transient temperature rise,

(2) calculation of initial temperature distribution,

(3) calculation of parameters (including thermal resistances and capacitances, copper and dielectric losses).

1. Calculation of transient temperature rise

Consider a node n having thermal capacitance C_n, the rate of heat generation at the node is Q_n and the thermal conductance between n and an adjacent node m is H_{mn}. During the transient, the temperature at node n changes from θ_n to θ_n' over the time step Δt, so that the heat balance may be written

$$(\theta_n' - \theta_n) \frac{C_n}{\Delta t} = \sum_m \theta_m H_{mn} + Q_n$$

where m denotes nodes adjacent to n and node n itself. H_{nn} is the self admittance of the node and

$$H_{nn} = - \sum_m H_{mn} , \qquad \text{where } m \neq n.$$

To determine successive values of the temperature θ_n' for all the nodes, we use the equation

$$\theta_n' = \theta_n + \frac{\Delta t}{C_n} \left(\sum_m H_{mn} \theta_m + Q_n \right)$$

2. Calculation of initial temperature distribution

The initial temperature distribution in the mesh is obtained using an S.O.R. technique. If at node n the temperature calculated on the i^{th} iteration is θ_{old} and the temperature on the present iteration $(i+1)^{th}$ is θ_{new}, then we obtain this value from the equation

$$\theta_{new} = \alpha(\theta'_{new} - \theta_{old}) + \theta_{old}$$

where α is an accelerating factor, the value of which is dependent on the mesh size, and θ'_{new} is a temperature obtained at an intermediate step in the calculation from the equation

$$\theta'_{new} = \frac{\sum_{m} \theta_m H_{mn}}{\sum_{m} H_{mn}}, \qquad m \neq n$$

where H_{mn} is the thermal conductance between nodes m and n and θ_m is the temperature at node m. The difference $(\theta_{new} - \theta_{old})$ is the error, and the calculation proceeds until the error at each node in the mesh is less than a previously defined limit.

3. Calculation of parameters

For a node (i,j) in the mesh, we define the following:

$A_{i,j}$ = cross-sectional area of nodal element, axially.

ℓ_j = axial length of nodal element.

r_i = radius at (i,j)

x_j = axial distance between nodes (i,j) and (i,j+1).

$(= \frac{1}{2}(\ell_j + \ell_{j+1}))$

Thermal resistance and capacitance

Radial resistance between nodes (i,j) and (i+1,j)

$$R_r = \frac{g}{2\pi \ell_j} \ln \frac{r_{i+1}}{r_i}$$

Horizontal resistance between nodes (i,j) and (i,j+1)

$$R_n = \frac{g\, x_j}{A_{i,j}}$$

Capacitance at node (i,j)

$$C = C_p A_{i,j} \ell_j$$

Copper and dielectric losses

Copper losses in a nodal section, length ℓ_j, are obtained from the expression

$$Q_j = I^2 (\rho_e \ell_j) (1 + \alpha T)$$

where ρ_e is the a.c. resistance of the conductor per unit length at 85^oC, α is the temperature coefficient of resistance of copper and T is the difference between the actual node temperature and the 85^oC datum.

The dielectric loss in a cable is

$$Q_{d\ell} = \omega C_e V^2 \tan \delta$$

where C_e is the electrical capacitance of the cable defined by

$$\frac{2\pi \epsilon_o \epsilon_r}{\ln \left(\frac{r_o}{r_c} \right)} L$$

(L is the cable length, r_o and r_c are the insulation and conductor outer radii) and δ is the dielectric loss angle.

To calculate the loss in the individual radial sections it is necessary to know the capacitance of these sections and the stress distribution in them. The capacitance of a section of the dielectric with radii r_1 and r_2 ($r_2 > r_1$) is

$$\frac{2\pi\varepsilon_o\varepsilon_r}{\ln \frac{r_2}{r_1}} \text{ F/m}$$

and the electric stress at a distance y from the centre of the conductor is

$$\frac{V}{y \ln \frac{r_o}{r_c}}$$

Considering the node (i,j) situated on the radius r_i, the capacitance lumped at the node is

$$\frac{2\pi\varepsilon_o\varepsilon_r}{\ell_j \ln \frac{b}{a}} ,$$

$b = \frac{1}{2}(r_i + r_{i+1})$, $a = \frac{1}{2}(r_{i-1} + r_i)$, and the dielectric loss is

$$Q_{i,j} = (V_{i,j})^2 \omega \frac{2\pi\varepsilon_o\varepsilon_r}{\ell_j \ln \frac{b}{a}} \tan\delta$$

where $V_{i,j}$ is the voltage across the section and is equal to

$$\int_a^b E\, dy = \int_a^b \frac{V\, dy}{y \ln \frac{r_o}{r_c}}$$

$$= \frac{V \ln \frac{b}{a}}{V \ln \frac{r_o}{r_c}}$$

Thus, the dielectric loss lumped at node (i,j) is

$$Q_{i,j} = \left(\frac{V \ln \frac{b}{a}}{\ln \frac{r_o}{r_c}} \right)^2 \omega \frac{2\pi\varepsilon_o\varepsilon_r}{\ell_j \ln \frac{b}{a}} \tan \delta$$

The value of tan δ is, however, dependent on both temperature and stress. The temperature dependence is allowed for using the formula quoted in Chapter 6. Barnes and Sutton[35] discuss the variation of power factor with stress in modern power cables; over the range of deviation considered here, the variation is small and the relationship almost linear. For the purposes of this investigation the slope of the power factor-stress curve is taken as 4.04×10^{-6} cm/kV.

The overall power factor of the cable is assumed to be 0.003 so that the power factor at node (i,j), where the average stress over the section is $E_{i,j}$, is

$$0.003 + 4.04 \times 10^{-6} (E_{av} - E_{i,j})$$

where E_{av} is the average stress over the whole dielectric.

REFERENCES

1. EMANUELI, L.: 'High Voltage Cables', (Chapman and Hall, 1926).

2. OUDIN, J. M. et al: 'French research and development in the field of high voltage and extra high voltage cables', C.I.G.R.E., 1964, paper 230.

3. BARNES, C. C. et al: 'Progress with underground cable engineering in Great Britain', I.E.E.E. Trans., 1967, PAS-87, pp. 93-101.

4. GOOSSENS, R. F.: 'Report on the work of Study Committee No. 2 (H.V. Cables)', C.I.G.R.E., 1964, paper 233.

5. WATSON, E. P. C. et al: 'Canals as cable routes', Proc. I.E.E. 1967, 114, pp. 510-518.

6. BARNES, C. C.: Discussion contribution to Ref. 3.

7. MIRANDA, F. J. et al: 'Development of 400 kV cable in Great Britain', I.E.E.E. Trans, 1967, PAS-87, pp. 604-611.

8. KOZAK, S.: Discussion contribution to Ref. 3.

9. RALSTON, P. and WEST, G. H.: 'The artificial cooling by water of underground cables', C.I.G.R.E., 1960, paper 215.

10. GIARO, J. A.: 'Temperature rise of power cables in a gallery with forced ventilations', C.I.G.R.E., 1960, paper 213.

11. WEST, G. H. and BALJET, A. F.: 'Water cooling of power cables', Ontario Hydro Research Review, 1962, 14, p. 23.

12. WEBB-WARE, B. and BARTON, A. H.: '400 kV crossing of Southampton Water', Elect. Rev., 1964, 174, p. 659.

13. CLARK, F. M.: 'Chemical changes affecting the stability of cellulose insulation', Trans. Electrochem. Soc., (London), 1943, 83, pp. 143-159.

14. MURPHY, E. J.: 'Gas evolved by thermal decomposition of paper', Trans. Electrochem. Soc., (London), 1943, 83, pp. 161-173.

15. WEEDY, B. M. and PERKINS, J. P.: 'Steady state thermal analysis of a 400 kV cable through joint', Proc. I.E.E., 1967, 114, pp. 109-115.

16. BEALE, H. K. et al: 'The application of intensive cooling techniques to oil-filled cables and accessories for heavy duty transmission circuits', C.I.G.R.E., 1968, paper 21-09.

17. PASQUALINI, G.: 'High power long distance cable cooling', C.I.G.R.E., 1968, paper 21-08.

18. KITAGAWA, K.: 'Forced cooling of power cables in Japan. Its studies and performance.', C.I.G.R.E., 1964, paper 213.

19. WHITEHEAD, S.: 'Dielectric breakdown of solids', (Clarendon Press, Oxford, 1953).

20. PERKINS, J. P.: 'Transient thermal analysis of a 400 kV cable and joint', M.Phil. Thesis, (University of Southampton, 1968).

21. SALVADORI, M. G. and SCHWARZ, R. J.: 'Differential equations in engineering problems', (Prentice-Hall Inc., 1954).

22. CARSLAW, H. S. and JAEGER, J. C.: 'Conduction of heat in solids', (Oxford University Press, 1947).

23. PASCHKIS, V. and BAKER, H. D.: 'A method for determining the unsteady-state heat-transfer by means of an electrical network', Trans. A.S.M.E., 1942, 64, pp. 105-112.

24. WEEDY, B. M.: 'Thermal transients in a high voltage cable system with natural and artificial cooling', Proc. I.E.E., 1962, 109, pp. 461-470.

25. LIS, J. and THELWELL, M. J.: 'Analogue investigation of water cooling of EHV cables', Proc.I.E.E., 1965, 112, pp. 335-341.

26. DUSINBERRE, G. M.: 'Heat transfer calculations by finite differences', (International Text Book Co., Inc., 1955).

27. SIEDER, E. N. and TATE, G. E.: 'Heat transfer and pressure drop of liquids in tubes', Ind. Eng. Chem., 1936, 28, pp. 1429-1435.

28. WEEDY, B. M.: 'Analysis of conductor duct cooling with turbulent and laminar flow of oil', Conference on Progress in Overhead Lines and Cables for 220 kV and above, I.E.E., 1968.

29. NATIONAL ENGINEERING LABORATORY: Private communication.

30. PIRELLI GENERAL CABLE CO. LTD.: Private communication.

31. VAN WORMER, F. C.: 'An improved approximate technique for calculating cable temperature transients', Trans. A.I.E.E., 1955, 74, Pt. 3, pp. 277-280.

32. BARNES, C. C.: 'Power cables', (Chapman and Hall, 1966).

33. PALMIERI, N. and BALL, E. H.: 'Some recent developments in oil filled cable accessory design', Conference on Progress in Overhead Lines and Cables for 220 kV and above', I.E.E., 1968.

34. BARNES, C. C. and SUTTON, C. T. W.: 'Engineering trends in high-voltage cable techniques in Great Britain', Trans. A.I.E.E., 1961, 80, Pt. 3, pp. 647-659.